

UNCLASSIFIED

AD NUMBER

ADB016229

LIMITATION CHANGES

TO:

Approved for public release; distribution is unlimited.

FROM:

Distribution authorized to U.S. Gov't. agencies only; Test and Evaluation; OCT 1976. Other requests shall be referred to Air Force Weapons Laboratory, Kirtland AFB, NM 87117.

AUTHORITY

AFWL ltr, 7 Nov 1986

THIS PAGE IS UNCLASSIFIED

AD Bo 16229

AUTHORITY:

AFWL etc,

7NOV86



AD No. 1
DDC FILE COPY

ADBO 16229

AFWL-TR-76-154 ✓

AFWL-TR-
76-154

AFWL HULL CALCULATIONS OF AIR BLAST OVER A DAM SLOPE

October 1976

Final Report

COPY AVAILABLE TO DDC BOES NOT
PERMIT FULLY LEGIBLE PRODUCTION

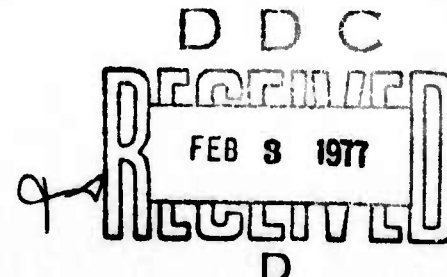


Distribution limited to US Government agencies only because test and evaluation information concerning military systems is discussed in the report (Oct 76). Other requests for this document must be referred to AFWL (DYT), Kirtland AFB, NM 87117.

This research was sponsored by the Defense Nuclear Agency under Subtask SG601, Work Unit 02, Work Unit Title "Structure Interaction".

Prepared for
Director
DEFENSE NUCLEAR AGENCY
Washington, DC 20305

AIR FORCE WEAPONS LABORATORY
Air Force Systems Command
Kirtland Air Force Base, NM 87117



0197

This final report was prepared by the Air Force Weapons Laboratory, Kirtland Air Force Base, New Mexico, under Job Order WDNB4402. Captain Fry (DYT) was the Laboratory Project Officer-in-Charge.

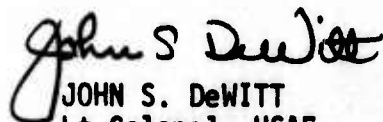
When US Government drawings, specifications, or other data are used for any purpose other than a definitely related Government procurement operation, the Government thereby incurs no responsibility nor any obligation whatsoever, and the fact that the Government may have formulated, furnished, or in any way supplied the said drawings, specifications, or other data is not to be regarded by implication or otherwise as in any manner licensing the holder or any other person or corporation or conveying any rights or permission to manufacture, use, or sell any patented invention that may in any way be related thereto.

This technical report has been reviewed and is approved for publication.



MARK A. FRY
Captain, USAF
Project Officer

FOR THE COMMANDER


DONALD B. MITCHELL
Lt Colonel, USAF
Chief, Theoretical Branch
JOHN S. DeWITT
Lt Colonel, USAF
Chief, Technology Division

DO NOT RETURN THIS COPY. RETAIN OR DESTROY.



UNCLASSIFIED

SECURITY CLASSIFICATION OF THIS PAGE (When Data Entered)

REPORT DOCUMENTATION PAGE		READ INSTRUCTIONS BEFORE COMPLETING FORM
1. REPORT NUMBER AFWL-TR-76-154	2. GOVT ACCESSION NO.	3. RECIPIENT'S CATALOG NUMBER
4. TITLE (and Subtitle) AFWL HULL CALCULATIONS OF AIR BLAST OVER A DAM SLOPE.		5. TYPE OF REPORT & PERIOD COVERED Final Report,
6. PERFORMING ORG. REPORT NUMBER		
7. AUTHOR(s) Mark A. Fry, Capt, USAF, Charles E. Needham, Mitch Stucker, Capt, USAF, Burton S. Chambers, III Gary P. Ganong, Maj, USAF		8. CONTRACT OR GRANT NUMBER(s)
9. PERFORMING ORGANIZATION NAME AND ADDRESS Air Force Weapons Laboratory (DYT) Kirtland AFB, NM 87117		10. PROGRAM ELEMENT, PROJECT, TASK AREA & WORK UNIT NUMBERS 62704H WDNB4402
11. CONTROLLING OFFICE NAME AND ADDRESS Director Defense Nuclear Agency Washington, D.C. 20305		12. REPORT DATE October 1976
13. MONITORING AGENCY NAME & ADDRESS (if different from Controlling Office) Air Force Weapons Laboratory Kirtland AFB, NM 87117		14. SECURITY CLASS. (of this report) UNCLASSIFIED
		15. DECLASSIFICATION/OWNGRADING SCHEDULE
16. DISTRIBUTION STATEMENT (of this Report) Distribution limited to US Government agencies only because test and evaluation information concerning military systems is discussed in the report (Oct 76). Other requests for this document must be referred to AFWL (DT), Kirtland AFB, NM 87117.		
17. DISTRIBUTION STATEMENT (of the abstract entered in Block 20, if different from Report)		
18. SUPPLEMENTARY NOTES This research was sponsored by the Defense Nuclear Agency under Subtask SG601, Work Unit 02, Work Unit Title "Structure Interaction".		
19. KEY WORDS (Continue on reverse side if necessary and identify by block number) Shock Interaction Structure Dam and Blockhouse Overpressures Dynamic Pressures		
20. ABSTRACT (Continue on reverse side if necessary and identify by block number) The Air Force Weapons Laboratory (AFWL) performed Hydrodynamics Unlimited (HULL) calculations of the air blast over a dam for two yields and two pressure regions. A fifth calculation included a rigid blockhouse at the foot of the dam. Although the shielding effect of the dam reduced the incident overpressure, of the incident blast wave, the reflection of the shock from the valley floor raised the peak overpressure up to at least 40% of the free air value. In almost every case, the overpressure impulses near the foot of the dam were greater than or equal to the free air values. The rigid		

DD FORM 1 JAN 73 EDITION OF 1 NOV 65 IS OBSOLETE

UNCLASSIFIED

(cont on p 1473 B)

SECURITY CLASSIFICATION OF THIS PAGE (When Data Entered)

013150 AB

UNCLASSIFIED

SECURITY CLASSIFICATION OF THIS PAGE(When Data Entered)

(B1k 20, cont'd)
Pr P1473 A)

blockhouse experienced the most severe overpressure environments. The assumption of a 50 psi (3.45×10^6 dynes/sp cm) hard blockhouse is reasonable. During the collapse of the blockhouse, it appears to be rigid to the air flow, since it responds slowly to the rapid air blast. Although there may be other reasons to detonate the weapon on the surface of the reservoir, the best way to destroy the blockhouse and any related structures with air blast, probably would be to detonate the device downstream of the blockhouse.

A

1473A

UNCLASSIFIED

SECURITY CLASSIFICATION OF THIS PAGE(When Data Entered)

PREFACE

The authors are indebted to many people at the Air Force Weapons Laboratory (AFWL) for their help with these calculations. In particular, we would like to thank Dr. Reginald Clemens of Science Applications, Incorporated (SAI) and Mrs. Susan Check of AFWL. Partial financial support was supplied by the Defense Nuclear Agency (DNA).

DISPOSITION for	
DIS	White Section <input type="checkbox"/>
DIS	Buff Section <input checked="" type="checkbox"/>
CONTINUOUS	
SPECIFICATION.....	
S2	
CONSTRUCTION/AVAILABILITY CODES	
AVAIL. and/or SPECIAL	
B	

D D C
RECORDED
FEB 8 1977
RECORDED
D

CONTENTS

<u>Section</u>	<u>Page</u>
I INTRODUCTION	5
II COMPUTATIONAL TECHNIQUES	7
Hull Code	7
Phase I	9
Phase II	12
Lamb Code	15
III PROCEDURE	16
Mesh Size	16
Boundary Conditions	16
Stations	17
IV RESULTS	19
APPENDIXES	
A SNAPSHOTS IN TIME	29
B STATION PLOTS	56

SECTION I

INTRODUCTION

A series of theoretical calculations of nuclear weapon air blasts propagating over a dam structure has been completed. The bursts were located over water behind the dam at such distances to give free field peak overpressures of 3.45×10^6 and 6.89×10^5 dynes/sq cm (50 and 10 psi) just beyond the dam. Figure 1 illustrates the problem configuration. These calculations were done with weapon yields of 50 and 1000 KT (209.15 and 4183.0 terajoules).

The AFWL HULL 2-D Cartesian hydrodynamics code (ref. 1) was used to perform the calculations. For computational convenience and cost-effectiveness, the calculations were simplified by specifying a problem mesh to include only the area around the dam and using a left boundary condition that replicates a blast wave entering from the left. In one of the calculations a perfectly rigid structure was inserted to investigate the loading of the blast wave.

1. Fry, M.A., et al., The Hull Hydrodynamics Computer Code, AFWL-TR-76-183, Air Force Weapons Laboratory, September 1976.

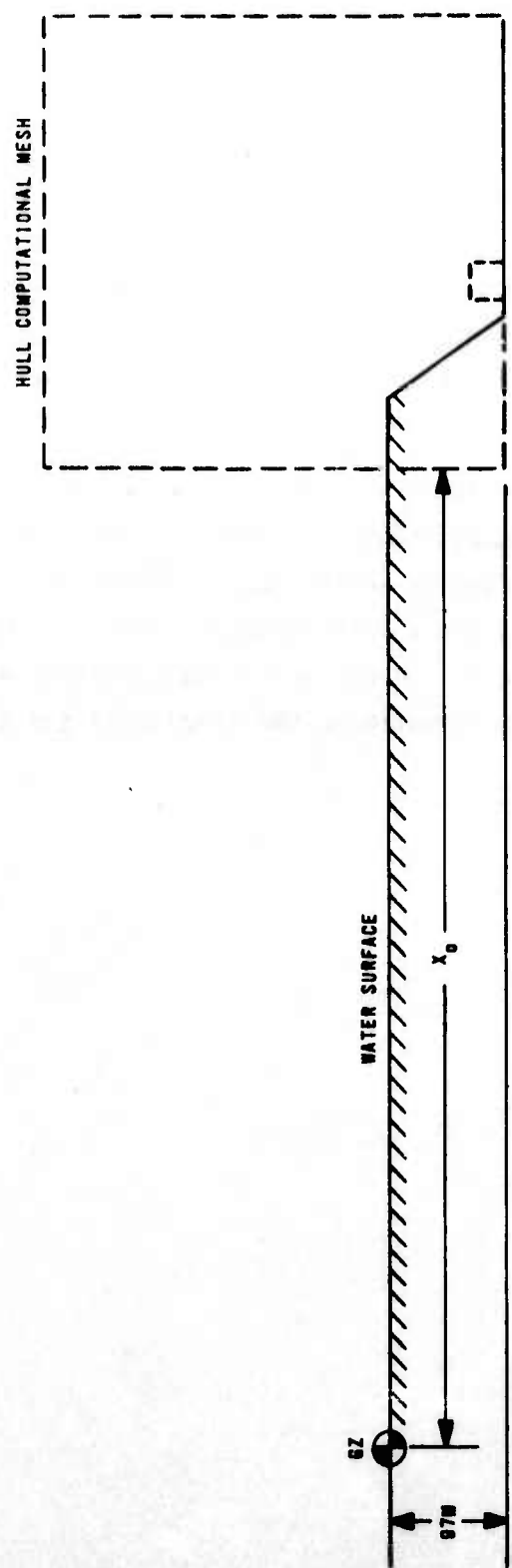


Figure 1. Dimensions for Dam Calculations

SECTION II

COMPUTATIONAL TECHNIQUES

Two computer codes were combined in these theoretical calculations. The Air Force Weapons Laboratory (AFWL) HULL (Hydrodynamics Unlimited) and the LAMB (Low Altitude Multiburst) codes were used. Both codes were developed at the AFWL during the last 5 years. The HULL code is a hydrodynamics code that solves the hyperbolic equations by a two-step finite difference technique. On the other hand, LAMB is a system code that models nuclear phenomenology.

1. HULL CODE

The HULL two-dimensional version was used to predict the hydrodynamic motion of the air blast waves in these problems. Basically the code solves the following equations.

Conservation of Mass

$$\frac{dp}{dt} + \rho \vec{\nabla} \cdot \vec{U} = 0 \quad (1)$$

Conservation of Momentum

$$\rho \frac{d\vec{U}}{dt} + \vec{\nabla} P = -\rho \vec{g} \quad (2)$$

Conservation of Energy

$$\rho \frac{dE}{dt} + \vec{\nabla} \cdot (\rho \vec{U}) = -\rho \vec{U} \cdot \vec{g} \quad (3)$$

Equation of State

$$P = P(\rho, E) \quad (4)$$

where

P = pressure in dynes/cm²

E = total energy in ergs/gm

\vec{U} = fluid velocity in cm/sec

\vec{g} = acceleration of gravity in cm/sec²

ρ = material density in g/cm³

t, T = time in seconds

The first three equations are approximated by a finite difference technique developed by Matuska*. There are two phases in the solution; phase 1 solves equations (2) and (3) and phase 2 solves equation (1) by fluxing mass across cell boundaries.

For the case of a two-dimensional problem, Cartesian coordinates may be used. The first three equations are then rewritten as

$$\frac{d\rho}{dt} + \rho \left(\frac{\partial u}{\partial R} + \frac{\partial v}{\partial Z} \right) = 0 \quad (5)$$

$$\rho \frac{du}{dt} + \frac{\partial P}{\partial R} = 0 \quad (6)$$

$$\rho \frac{dv}{dt} + \frac{\partial P}{\partial Z} = -\rho g \quad (7)$$

$$\rho \frac{dE}{dt} + \frac{\partial Pu}{\partial R} + \frac{\partial Pv}{\partial Z} = -\rho Vg \quad (8)$$

where

R = horizontal coordinate

z = vertical coordinate

u = component of velocity in radial direction

v = component of velocity in vertical direction

To establish the finite difference analogs to equations (5) through (8), we consider a discrete subset of F(R,Z,T) by defining

$$F(I,J,N) = F(R(I),Z(J),T(N))$$

where R(I), Z(J), and T(N) are particular values of R, Z, and T, respectively, and the I, J, and N assume integer values in the range 1 to IMAX for I, 1 to JMAX for J, and 0 to NMAX for N. The R(I) and Z(J) are defined in terms of a given set of DR(I) and DZ(J) such that

*Matuska, Dan, Private Communication, 1975.

$$R(I)=R(0)+(\text{SUM}, K=1, I-1, (DR(K)))+DR(I)/2 \quad \text{FOR } I=2, \dots, I\text{MAX}$$

$$R(1)=R(0)+DR(1)/2$$

$$Z(J)=Z(0)+(\text{SUM}, K=1, J-1, (DZ(K)))+DZ(J)/2 \quad \text{FOR } J=2, \dots, J\text{MAX}$$

$$Z(1)=Z(0)+DZ(1)/2$$

where $R(0)$ and $Z(0)$ have some specified values.

The hydrodynamic variables ρ (material density, ρ), U , V , and E are defined for each set of coordinates (I, J) at a particular time $T(N)$. The pressure $P(I, J, N)$ is defined at each point by the equation of state (equation 4).

Interpolated values of the hydrodynamic variables of the form $F(I+1/2, J, N)$, $F(I, J+1/2, N)$, or $F(I, J, N+1/2)$, or similar forms, are defined in terms of the $F(I, J, N)$. In general

$$F(I+1/2, J, N) = (F(I+1, J, N)+F(I, J, N))/2$$

and

$$F(I, J+1/2, N) = (F(I, J+1, N)+F(I, J, N))/2.$$

This definition will apply except where explicitly noted.

a. Phase I

Using the above convention, we can write the finite difference analogs to equations (6) through (8) as

$$\begin{aligned} U(I, J, N+1) &= U(I, J, N) - DT * (P(I+1/2, J, N+1/2) - P(I-1/2, J, N+1/2)) \\ &\quad / (\rho(I, J, N) * DR(I)) \end{aligned} \quad (9)$$

$$\begin{aligned} V(I, J, N+1) &= V(I, J, N) - DT * (P(I, J+1/2, N+1/2) - P(I, J-1/2, N+1/2)) \\ &\quad / (\rho(I, J, N) * DZ(J)) - DT * G(J) \end{aligned} \quad (10)$$

$$\begin{aligned} E(I, J, N+1) &= E(I, J, N) - DT / \rho(I, J, N) * ((P(I+1/2, J, N+1/2) \\ &\quad * U(I+1/2, J, N+1/2) - P(I-1/2, J, N+1/2) \\ &\quad * U(I-1/2, J, N+1/2)) / DR(I) + (P(I, J+1/2, N+1/2) \\ &\quad * V(I, J+1/2, N+1/2) - P(I, J-1/2, N+1/2) * V(I, J-1/2, N+1/2)) \\ &\quad / DZ(J) - DT * V(I, J, N+1) * G(J)) \end{aligned} \quad (11)$$

where

$DR(I)$ = horizontal dimension of the I th column.
 $DZ(J)$ = vertical dimension of the J th row.
 $DT = T(N+1) - T(N)$
 $R(I+1/2) = R(I) + DR(I)/2$
 $R(I-1/2) = R(I) - 1/2DR(I)$
 $Z(J+1/2) = Z(J) + DZ(J)/2$
 $Z(J-1/2) = Z(J) - 1/2DZ(J)$
 $G(J)$ = value of the gravitational constant at $Z(J)$.

All the values appearing in equations (9) through (11) are immediately known except the time advanced $(N+1/2)$ values for pressure and velocity. These time advanced values are used so that the approximations to the partial derivatives appearing in equations (6) through (8) may be centered in time and space. In the case where

$DR(I) = \text{constant}$ for $I = 1, \dots, IMAX$

and

$DZ(J) = \text{constant}$ for $J = 1, \dots, JMAX$,

this produces a fully second order accurate difference method. In a region where the $DR(I)$ and $DZ(J)$ are not constant the second order accuracy is lost. This adversely affects the stability of the first phase calculation. The amount of instability which may be obtained is related to the magnitude of the incremental changes in $DR(I)$ and $DZ(J)$.

Most of the computations in the first phase are expended in obtaining the time advanced values for pressure and velocity. The time advanced velocities are obtained by differencing equations (6) and (7) as

$$\begin{aligned}
 U(I+1/2, J, N+1/2) &= U(I+1/2, J, N) - DT / (2 * RHO(I+1/2, J, N+1/2)) \\
 &\quad * ((P(I+1, J, N) - P(I, J, N)) / (R(I+1) - R(I))) \quad (12)
 \end{aligned}$$

$$\begin{aligned}
 V(I, J+1/2, N+1/2) &= V(I, J+1/2, N) - DT / (2 * RHO(I, J+1/2, N+1/2)) \\
 &\quad * ((P(I, J+1, N) - P(I, J, N)) / (Z(J+1) - Z(J))) \\
 &\quad - G(J+1/2) * DT / 2 \quad (13)
 \end{aligned}$$

where

$$G(J+1/2) = (G(U)+G(J+1))/2.$$

The time advanced densities appearing in equations (12) and (13) are obtained by differencing equation (5) as

$$\begin{aligned} \text{RHO}(I+1/2, J, N+1/2) &= \text{RHO}(I+1/2, J, N) * (1 - DT/(2 * R(I+1/2)) * (R(I+1) \\ &\quad * U(I+1, J, N) - R(I) * U(I, J, N)) / (R(I+1) - R(I))) \end{aligned} \quad (14)$$

$$\begin{aligned} \text{RHO}(I, J+1/2, N+1/2) &= \text{RHO}(I, J+1/2, N) * (1 - DT/2 * (V(I, J+1, N) - V(I, J, N)) \\ &\quad / (Z(J+1) - Z(J))) \end{aligned} \quad (15)$$

where

$$\begin{aligned} \text{RHO}(I+1/2, J, N) &= (M(I, J, N) + N(I+1, J, N)) / (\text{PI} * (R(I+3/2) ** 2 \\ &\quad - R(I-1/2) ** 2) * DZ(J)) \end{aligned}$$

$$\begin{aligned} \text{RHO}(I, J+1/2, N) &= (M(I, J, N) + N(I, J+1, N)) / (\text{PI} * (R(I+1/2) ** 2 \\ &\quad - R(I-1/2) ** 2) * (DZ(J) + DZ(J+1))) \end{aligned}$$

and the mass associated with a point (I, J, N) is defined by

$$M(I, J, N) = \text{RHO}(I, J, N) * (\text{PI} * (R(I+1/2) ** 2 - R(I-1/2) ** 2) * DZ(J))$$

where

$$\text{PI} = 3.14159\ldots \text{ and } R(I+3/2) = R((I+1)+1/2).$$

The time advanced pressure appearing in equations (9) through (11) requires a little more effort. First an alternative energy equation can be obtained from equations (2) and (3) as

$$\rho \frac{dI}{dt} + P(\nabla \cdot \vec{U}) = 0 \quad (16)$$

An effective γ can be defined by

$$\gamma = 1 + \frac{P}{\rho I} \quad (17)$$

We will assume for the purposes of calculating a half time step advanced pressure, which in turn is used in approximating the partial derivatives in equations (9) through (11), that the Lagrangian derivative with respect to time of gamma is small and can be ignored. In application, it is only required that the change in gamma at a particular point be small over a time of DT/2.

Taking the Lagrangian derivative with respect to time in equation (17) and using equations (1) and (16), we can write

$$\frac{dP}{dt} + (\text{GAMMA})(P)(\vec{\nabla} \cdot \vec{U}) = 0 \quad (18)$$

Equation (18) is used to obtain time advanced pressures given by

$$\begin{aligned} P(I+1/2, J, N+1/2) &= P(I+1/2, J, N) * (1 - DT * \text{GAMMA}(I+1/2, J, N) * (R(I+1) \\ &\quad * U(I+1, J, N) - R(I) * U(I, J, N)) / (2 * R(I+1/2) * (R(I+1) \\ &\quad - R(I)))) \\ P(I, J+1/2, N+1/2) &= P(I, J+1/2, N) * (1 - DT * \text{GAMMA}(I, J+1/2, N) \\ &\quad * (V(I, J+1, N) - V(I, J, N)) / (2 * (Z(J+1) - Z(J)))) \end{aligned}$$

where gamma is obtained from equation (17) as

$$\text{GAMMA}(I+1/2, J, N) = 1 + P(I+1/2, J, N) / (\text{RHO}(I+1/2, J, N) * I(I+1/2, J, N))$$

$$\text{GAMMA}(I, J+1/2, N) = 1 + P(I, J+1/2, N) / (\text{RHO}(I, J+1/2, N) * I(I, J+1/2, N)).$$

All quantities needed to solve equations (9), (10), and (11) are now defined. Solution of these equations will complete a second order accurate Lagrangian calculation. The next step would normally be that of transporting mesh vertices. Instead we choose to flux the hydrodynamic quantities to retain the original mesh configuration. This calculation is done in Phase II.

b. Phase II

Changes in density are computed in phase II by calculating a mass flux between mesh points and then transporting the appropriate amount of mass from point to point. The transported mass carries with it a proportionate amount of internal energy and momentum. The velocities and specific internal energy are

then redefined at each mesh point by conserving momentum and total energy at that point.

The mass flux between mesh points is defined as the product of the interpolate velocity, the density as defined by solution of equation (1), the intermediate cross sectional area, and the time step.

$$\begin{aligned} MF(I+1/2, J, N+1) = & U(I+1/2, J, N+1) * RHO(I+1/2, J, N+1) * 2 * PI * R(I+1/2) \\ & * DZ(J) * DT \end{aligned}$$

$$\begin{aligned} MF(I, J+1/2, N+1) = & V(I, J+1/2, N+1) * RHO(I, J+1/2, N+1) * 2 * PI * R(I) * DR(I) \\ & * DT \end{aligned}$$

where the time advanced densities are obtained by differencing equation (5) as

$$\begin{aligned} RHO(I+1/2, J, N+1) = & RHO(ID, J, N) * (1 - DT/R(I+1/2)) * (R(I+1) \\ & * U(I+1, J, N+1) - R(I) * U(I, J, N+1)) / (R(I+1) - R(I))) \end{aligned}$$

$$\begin{aligned} RHO(I, J+1/2, N+1) = & RHO(I, JD, N) * (1 - DT * (V(I, J+1, N+1) - V(I, J, N+1)) \\ & / (Z(J+1) - Z(J))) \end{aligned}$$

where

$$\begin{aligned} ID = I & \text{ IF } U(I+1/2, J, N+1) \text{ GT } 0 \\ & = I+1 \text{ IF } U(I+1/2, J, N+1) \text{ LT } 0 \end{aligned}$$

$$\begin{aligned} JD = J & \text{ IF } V(I, J+1/2, N+1) \text{ GT } 0 \\ & = J+1 \text{ IF } V(I, J+1/2, N+1) \text{ LT } 0. \end{aligned}$$

This is the classical donor cell differencing technique. The most obvious advantages of this technique are its rigid numerical conservation and its stability. This scheme also insures that more material can not be removed from a point than is present.

HULL has a continuous rezone capability. When this is employed, the interpolated velocities appearing in the mass flux equations are replaced by

$$\begin{aligned} & U(I+1/2, J, N+1) - UR(I+1/2, J, N+1) \\ & V(I, J+1/2, N+1) - VR(I, J+1/2, N+1) \end{aligned}$$

where UR and VR are the interpolated grid velocities (determined arbitrarily by how fast one wishes to transport the coordinate grid).

The corresponding momentum fluxes are

$$UF(I+1/2, J, N+1) = MF(I+1/2, J, N+1)*U(ID, J, N+1)$$

$$VF(I+1/2, J, N+1) = MF(I+1/2, J, N+1)*V(ID, J, N+1)$$

$$UF(I, J+1/2, N+1) = MF(I, J+1/2, N+1)*U(I, JD, N+1)$$

$$VF(I, J+1/2, N+1) = MF(I, J+1/2, N+1)*V(I, JD, N+1)$$

and the energy fluxes are

$$EF(I+1/2, J, N+1) = MF(I+1/2, J, N+1)*E(ID, J, N+1)$$

$$EF(I, J, 1/2, N+1) = MF(I, J, 1/2, N+1)*E(I, JD, N+1)$$

When these quantities are fluxed, final values for mass, density, velocity, and energy are computed by

$$M(I, J) = M(I, J, N) + MF(I-1/2, J, N+1) + MF(I, J-1/2, N+1) - MF(I+1/2, J, N+1) - MF(I, J+1/2, N+1)$$

$$\rho(I, J) = M(I, J) / (\pi * (R(I+1/2)**2 - R(I-1/2)**2) * dz(J))$$

$$U(I, J) = (U(I, J, N+1) * M(I, J, N) + UF(I-1/2, J, N+1) + UF(I, J-1/2, N+1) - UF(I+1/2, J, N+1) - UF(I, J+1/2, N+1)) / M(I, J)$$

$$V(I, J) = (V(I, J, N+1) * M(I, J, N) + VF(I-1/2, J, N+1) + VF(I, J-1/2, N+1) - VF(I, J+1/2, N+1) - VF(I+1/2, J, N+1)) / M(I, J)$$

$$I(I, J) = (E(I, J, N+1) * M(I, J, N) + EF(I-1/2, J, N+1) + EF(I, J-1/2, N+1) - EF(I+1/2, J, N+1) - EF(I, J+1/2, N+1) - (U(I, J)**2 + V(I, J)**2) * M(I, J) / 2) / M(I, J)$$

$$E(I, J) = I(I, J) + (U(I, J)**2 + V(I, J)**2) / 2$$

where the lack of a time specification indicates final values for this time step.

2. LAMB CODE

The LAMB code is a three-dimensional system code. It is basically a model based upon two and three-dimensional HULL calculations (ref. 2). The phenomenology that LAMB can predict includes shock-shock, shock-fireball, fireball-fireball, shock-ground and fireball-ground interactions. Since it is a model, it can quickly predict a complete hydrodynamic description for a freefield environment at a point in space and time.

2. Needham, C., Matuska, D., Bauer, B., and Whitaker, W., Air Force Weapons Laboratory LAMB Model, AFWL Technical Note, 1972.

SECTION III

PROCEDURE

The computational method that has been employed in these calculations is a hybrid of the normal hydrodynamic calculations with the LAMB model. Since the LAMB code predicts only the free field environment, the hydrodynamics code HULL must be used to predict the fluid flow over or around objects. The configuration of the problem is a blast wave running off the top of a man-made dam. It is a two-dimensional problem that can be solved in slab geometry; that is, two-dimensional Cartesian coordinates. Initial conditions assume a standard temperate atmosphere at sea level with respect to the base of the dam.

1. MESH SIZE

In order to sharply define the dam and the structure used for the computations, the size of the rectangular mesh chosen was 200 columns and 130 rows. The area covered by the mesh is indicated in figure 1. In addition, the area from the left boundary to the right of the structure was finely zoned with cells being equal to 1 meter in the horizontal and vertical directions. Beyond the structure, the cell sizes were incrementally increased 10 percent in the horizontal direction.

2. BOUNDARY CONDITIONS

There are two types of boundary conditions normally used in the HULL code. A reflective boundary is utilized at the center of symmetry or whenever a perfectly reflecting surface is used. The transmissive boundary utilized is simply a set of mesh points constrained to be ambient. It is perhaps better termed an observer of a boundary.

For these problems we have used reflective boundaries at the top and bottom and transmissive at the right. At the left boundary the time dependent hydrodynamic values were preset from LAMB at each time step. The AFWL LAMB code was used to obtain the correct variables for the specified weapon yield as a function of time for the boundary. A good representation for the air blast waveform can be obtained in this manner.

In order to represent the dam as well as the structure within the problem mesh, the island construct of the HULL code was used. Islands are simply a name

for an algorithm which inserts reflecting boundaries for any geometry within the mesh. As a result, the dam and structure below the dam are outlined with reflecting boundaries and the cells within these boundaries become inactive.

3. STATIONS

In an effort to monitor the loading on the structure and the physical parameters of the shock as a function of time, stations were placed at various points in the mesh. The hydrodynamic variables of these points are recorded for every time step and stored on a separate data tape. Figure 2 indicates the location of the stations in the mesh.

From the station data one can compute the arrival time of the shock front, the peak overpressure and its impulse, the dynamic pressure and the dynamic pressure impulse.

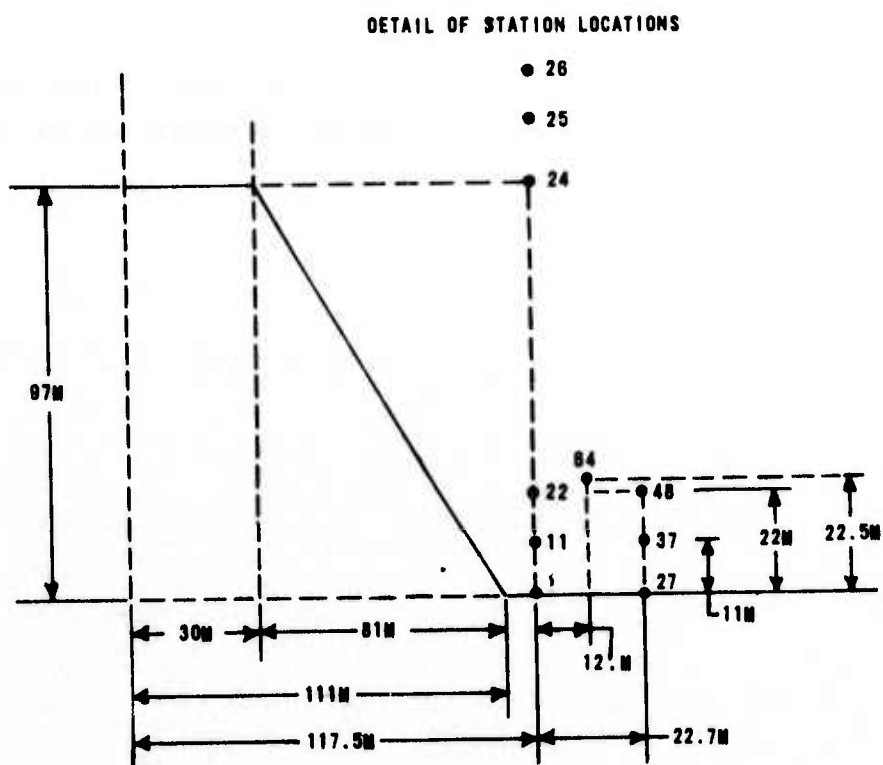


Figure 2. Detail of Station Locations

SECTION IV
RESULTS

This study of air blast loading included four combinations of yield and range. They were 1 megaton and 50 kilotons (4183.0 and 209.15 terajoules) at the 50 psi and 10 psi (3.45×10^6 and 6.89×10^5 dynes/sq cm) ranges. In addition, a fifth problem, 50.017, included a perfectly rigid blockhouse structure at the foot of the front face of the dam. Table 1 summarizes the calculations.

Table 1
SUMMARY OF PROBLEMS

<u>HULL PROBLEM NUMBER</u>	<u>YIELD (KT)</u>	<u>BURST POSITION X_0 (M)</u>	<u>HEIGHT OF BURST ABOVE WATER</u>	<u>NOMINAL FREE FIELD OVERPRESSURE dynes/sq cm</u>
51.013	1000	1360.9	0	3.45×10^6 (50 psi)
51.014	1000	3098.9	0	6.89×10^5 (10 psi)
51.015	50	427.0	0	3.45×10^6 (50 psi)
51.016	50	1063.1	0	6.89×10^5 (10 psi)
51.017*	50	427.0	0	3.45×10^6 (50 psi)

*This problem includes the structure at the foot of the dam.

To understand the overall phenomenology, consider the two-dimensional contour and vector plots in appendix A for problems 51.015 and 51.017, 50 kilotons at the 50 psi range.

For the first 30 meters from the left side of the computational mesh, the blast travels over the top of the dam reservoir, which is assumed to be rigid. When the blast reaches the front of the dam, it expands downward reducing the overpressure.

The reduction in peak pressure is shown by the contour plots of appendix A. At a time of 480 milliseconds for problem 51.0170 the peak pressure near the face of the dam is approximately 2.5 atmospheres while the free air shock is over 3.4 atmospheres. As the shock front expands down the face of the dam, a rarefaction

begins to develop. Examination of values in table 2 indicates this effect. Stations 24, 25, and 26 are at the same ground range but at increasing heights above the top of the dam. The peak overpressure increases with the height above the dam from 2.77×10^6 dynes/sq cm at a point even with the dam top to 3.61×10^6 dynes/sq cm a distance 32 m above the dam. The impulses are similarly affected. The reduction in pressure and impulse above the dam is a result of mass and energy flow down the face of the dam.

From the time the shock enters the left boundary to a time of 480 milliseconds, problems 51.017 and 51.015 (with and without the structure) are identical. As the shock impinges upon the structure, however, the flow is considerably modified.

Consider first the less complex shock reflections as the blast wave traverses the flat surface with no structure (problem 51.015).

In problem 51.015, the blockhouse was composed of air. Trace particles located in the region of the blockhouse moved with local air velocities as the blast swept by. They simulate the debris from a very fragile structure.

The shock reaches the bottom of the dam at a time of just over 0.5 second; at this point the shock is much weaker (about half the strength) than the free air shock above the dam. By a time of 0.53 second the free air shock has passed out of the region of the blockhouse and the shock near the base of the dam has reflected. The peak reflected pressure is greater than the free air pressure, but it must be remembered that the vertical flow is stagnated and therefore there is little dynamic pressure associated with this overpressure.

An interesting side effect is the circulation pattern developing along the face of the dam. This is the same effect that would be seen over the trailing edge of an airplane wing. The flow over the dam creates a partial vacuum along the face of the dam. This flow and reduced pressure have little effect on the peak pressure near the base of the dam, but do reduce the positive duration and impulse near the base.

As the reflecting shock travels away from the base of the dam, the effect of the dam in reducing peak pressure becomes less important. This is seen by the increasing peak pressures between stations 1 and 27 (from 3.6 to 4.1 atmospheres). The reflected pressures at stations 1 and 27 are somewhat greater than in the free air stream as described above; however, as the distance between the shock and the dam base increases, the shock characteristics approach those of the free air

Table 2.
AFWL CALCULATION OF 1 MT EFFECT ON DAM STRUCTURE AT 50 PSI RANGE PROB 51.013

STATION NUMBER	RANGE FROM EDGE OF GRID (CM)	HEIGHT (CM)	ARRIVAL TIME (SEC)	FIRST OVERPRESSURE PEAK (DYNES/SQ.CM.)	MAXIMUM OVERPRESSURE (DYNES/SQ.CM.)	OVERTPRESSURE IMPULSE (DYNES/SQ.CM.SEC.)
1	1.175E+04	1.000E+02	1.175E+00	3.791E+06	3.791E+06	4.769E+05*
11	1.175E+04	1.100E+03	1.154E+00	1.535E+06	2.401E+06	4.276E+05*
22	1.175E+04	2.200E+03	1.137E+00	1.594E+06	1.952E+06	3.842E+05*
24	1.175E+04	9.700E+03	1.053E+00	2.478E+06	2.478E+06	3.454E+05*
25	1.175E+04	1.150E+04	1.045E+00	2.865E+06	2.865E+06	3.603E+05*
26	1.175E+04	1.290E+04	1.042E+00	3.197E+06	3.197E+06	3.672E+05*
27	1.405E+04	1.000E+02	1.202E+00	4.174E+06	4.174E+06	4.652E+05*
37	1.405E+04	1.100E+03	1.183E+00	1.591E+06	3.386E+06	4.364E+05*
48	1.405E+04	2.200E+03	1.167E+00	1.652E+06	2.507E+06	3.987E+05*
64	1.295E+04	2.250E+03	1.152E+00	1.630E+06	2.243E+06	3.983E+05*
CALCULATION OF 1 MT EFFECT AT 10 PSI RANGE PROB 51.014						
1	1.175E+04	1.000E+02	4.665E+00	4.811E+05	4.811E+05	1.572E+05*
11	1.175E+04	1.100E+03	4.640E+00	2.432E+05	4.561E+05	1.551E+05*
22	1.175E+04	2.200E+03	4.618E+00	2.539E+05	4.187E+05	1.531E+05*
24	1.175E+04	9.700E+03	4.518E+00	4.241E+05	4.241E+05	1.505E+05*
25	1.175E+04	1.150E+04	4.510E+00	5.134E+05	5.134E+05	1.488E+05*
26	1.175E+04	1.290E+04	4.508E+00	5.869E+05	5.869E+05	1.494E+05*
27	1.405E+04	1.000E+02	4.705E+00	5.176E+05	5.245E+05	1.483E+05*
37	1.405E+04	1.100E+03	4.683E+00	2.563E+05	5.257E+05	1.473E+05*

*Indicates that positive phase is incomplete

Table 2. (Continued)

STATION NUMBER	RANGE FROM EDGE OF GRID (CM)	HEIGHT (CM)	ARRIVAL TIME (SEC)	FIRST OVER- PRESSURE PEAK (DYNES/SQ.CM)	MAXIMUM OVERPRESSURE (DYNES/SQ.CM)	OVERPRESSURE IMPULSE (DYNES/SQ.CM SEC)
				CALCULATION OF 1 MT EFFECT AT 10 PSI RANGE PROB 51.014		
48	1.405E+04	2.200E+03	4.663E+00	2.674E+05	4.817E+05	1.458E+05*
64	1.295E+04	2.250E+03	4.641E+00	2.624E+05	4.455E+05	1.501E+05*
CALCULATION OF 50 KT EFFECT AT 50 PSI RANGE PROB 51.015						
1	1.175E+04	1.000E+02	5.160E-01	3.615E+06	3.615E+06	3.487E+05*
11	1.175E+04	1.100E+03	4.953E-01	1.495E+06	2.214E+06	3.045E+05*
22	1.175E+04	2.200E+03	4.778E-01	1.559E+06	1.573E+06	2.675E+05*
24	1.175E+04	9.700E+03	3.913E-01	2.774E+06	2.774E+06	2.181E+05
25	1.175E+04	1.150E+04	3.826E-01	3.169E+06	3.169E+06	2.320E+05
26	1.175E+04	1.290E+04	3.795E-01	3.609E+06	3.609E+06	2.413E+05
27	1.405E+04	1.000E+02	5.428E-01	4.077E+06	4.077E+06	3.442E+05*
37	1.405E+04	1.100E+03	5.235E-01	1.562E+06	3.396E+06	3.171E+05*
48	1.405E+04	2.200E+03	5.071E-01	1.629E+06	2.373E+06	2.813E+05*
64	1.295E+04	2.250E+03	4.929E-01	1.608E+06	1.966E+06	2.779E+05*
CALCULATION OF 50 KT EFFECT AT 10 PSI RANGE PROB 51.016						
1	1.175E+04	1.000E+02	1.807E+00	5.027E+05	5.027E+05	1.116E+05*
11	1.175E+04	1.100E+03	1.781E+00	2.551E+05	4.292E+05	1.092E+05*
22	1.175E+04	2.200E+03	1.759E+00	2.683E+05	3.925E+05	1.069E+05*
24	1.175E+04	9.700E+03	1.659E+00	4.571E+05	4.571E+05	1.008E+05*

*Indicates that positive phase is incomplete

Table 2. (Continued)

STATION NUMBER	RANGE FROM EDGE OF GRID (CM)	HEIGHT (CM)	ARRIVAL TIME (SEC)	FIRST OVERPRESSURE PEAK (DYNES/SQ. CM)	MAXIMUM OVERPRESSURE (DYNES/SQ. CM)	OVERTPRESSURE IMPULSE (DYNES/SQ. CM. SEC.)
CALCULATION OF 50 KT EFFECT AT 10 PSI RANGE PROB 51.0116						
25	1.175E+04	1.150E+04	1.651E+00	5.557E+05	5.557E+05	1.032E+05*
26	1.175E+04	1.290E+04	1.649E+00	6.361E+05	6.361E+05	1.046E+05*
27	1.405E+04	1.000E+02	1.846E+00	5.422E+05	5.433E+05	1.057E+05*
37	1.405E+04	1.100E+03	1.824E+00	2.700E+05	5.368E+05	1.041E+05*
48	1.405E+04	2.200E+03	1.804E+00	2.818E+05	4.713E+05	1.021E+05*
64	1.295E+04	2.250E+03	1.782E+00	2.757E+05	4.294E+05	1.051E+05*
CALCULATION OF 50 KT EFFECT AT 50 PSI RANGE PROB 51.0117						
1	1.175E+04	1.000E+02	5.169E-01	8.958E+06	8.958E+06	5.609E+05
11	1.175E+04	1.100E+03	4.952E-01	3.022E+06	5.345E+06	4.779E+05
22	1.175E+04	2.200E+03	4.787E-01	2.460E+06	3.776E+06	3.751E+05
24	1.175E+04	9.700E+03	3.913E-01	2.774E+06	2.774E+06	2.181E+05
25	1.175E+04	1.150E+04	3.826E-01	3.169E+06	3.169E+06	2.320E+05
26	1.175E+04	1.290E+04	3.795E-01	3.609E+06	3.609E+06	2.413E+05
27	1.405E+04	1.000E+02	5.593E-01	2.031E+06	2.031E+06	2.309E+05*
37	1.405E+04	1.100E+03	5.306E-01	7.905E+05	9.748E+05	1.539E+05*
48	1.405E+04	2.200E+03	5.074E-01	3.312E+06	3.312E+06	2.359E+05*
64	1.295E+04	2.250E+03	4.937E-01	4.242E+06	4.242E+06	3.453E+05*

*Indicates that positive phase is incomplete

region. The overall effect of the dam becomes negligible after the shock has traveled approximately four dam heights, in this case 400m.

The above description and effects are modified when the structure at the base of the dam is included. Now consider the two-dimensional contour and vector plots for problem 51.017 (appendix A). The blockhouse is perfectly rigid; the blast is more complicated than in the previous example. In the region between the dam face and the blockhouse, the shock is intensified by the convergence of the two surfaces. The shock strikes the upper corner of the structure at approximately 480 ms. The reflected pressure at the corner is far less than from a planar surface reflection, as expected, and is actually less than the free air shock pressure. The center of the roof and the center of the front face are struck at very nearly the same time. The loading on the roof is considerably greater than the initial shock on the front face (4.2 vs. 3.0 atmospheres). The shock continues down the front face of the structure and is completely stagnated, horizontally and vertically, by the constraints of the dam, the structure, and the ground. This results in a peak overpressure nearly six times that of the incident wave (9.0 vs. 1.6 atmospheres). The reflected shock travels up the front face of the structure and decays to 5.3 atmospheres at the midpoint. Thus, the peak pressure at the midpoint comes from the reflected shock, is about 75 percent greater than the initial shock, and arrives approximately 50 ms after the first.

When the reflected shock reaches the upper corner of the front face, the pressure has dropped to about 150 percent of the first shock, and is less than the free air incident pressure.

On the back of the structure, pressures are significantly reduced, and at the midpoint the peak overpressure is less than 1 atmosphere.

The pressure gradient across the structure tends to translate the structure. In this case the pressure difference is about 4.3 atmospheres.

Tables 2 and 3 list the peak values of the station data. Problem 51.013 is nominally 1 megaton in the 50 psi (3.45×10^6 dynes/sq.cm.) region. From the overpressure at station 26, the station closest to the free air blast, one can see that the overpressure is 7 percent below the nominal value.

The station data show that the effect of the dam is to weaken the incident shock by rapid expansion. The incident overpressure is one half of the free air value (at station 26). However, the reflection of the shock off the ground

Table 3.
AFWL CALCULATIONS OF EFFECTS ON DAM STRUCTURE

STATION NUMBER	PEAK HORIZONTAL DYNAMIC PRESSURE (DYNES/SQ. CM.)	VERTICAL DYNAMIC PRESSURE (DYNES/SQ. CM.)	POSITIVE PHASE DURATION (SEC.)	AFWL CALCULATION OF 1 MT EFFECT ON DAM STRUCTURE AT 50 PSI RANGE PROB 51.013		AFWL CALCULATION OF 1 MT EFFECT ON DAM AT 10 PSI RANGE PROBLEM 51.014
				HORIZONTAL DYNAMIC PRESSURE (DYNES/SQ. CM. SEC.)	VERTICAL DYNAMIC PRESSURE IMPULSE (DYNES/SQ. CM. SEC.)	
1	6.071E+05	-4.413E+05	2.245E-01*	1.110E+04	-2.550E+03	
11	2.590E+05	-4.595E+05	2.452E-01*	2.461E+04	-2.716E+04	
22	2.983E+05	-4.494E+05	2.624E-01*	3.500E+04	-4.645E+04	
24	1.469E+06	-2.258E+05	3.465E-01*	2.867E+05*	-4.810E+04*	
25	2.071E+06	-1.126E+05	3.545E-01*	3.499E+05	-2.036E+04	
26	2.576E+06	-4.440E+04	3.574E-01*	3.816E+05	-6.695E+03	
27	1.418E+06	-3.509E+05	1.979E-01*	6.019E+04	-1.354E+03	
37	7.984E+05	-4.217E+05	2.164E-01*	5.154E+04	-1.504E+04	
48	4.136E+05	-4.174E+05	2.323E-01*	5.192E+04	-3.179E+04	
64	3.409E+05	-4.285E+05	2.470E-01*	4.187E+04	-3.814E+04	
1	1.770E+04	-5.697E+03	4.336E-01*	1.040E+03	-8.230E+01	
11	1.602E+04	-1.828E+04	4.591E-01*	2.706E+03*	-1.716E+03*	
22	1.998E+04	-2.240E+04	4.816E-01*	4.667E+03*	-3.290E+03*	
24	5.812E+04	-1.112E+04	5.802E-01*	2.483E+04	-3.656E+03	
25	8.838E+04	-5.463E+03	5.824E-01*	3.020E+04*	-1.711E+03	
26	1.154E+05	-2.077E+03	5.915E-01*	3.319E+04	-5.990E+02	

* Indicates that positive phase is incomplete

Table 3. (Continued)

STATION NUMBER	PEAK HORIZONTAL DYNAMIC PRESSURE (DYNES/SQ. CM.)	VERTICAL DYNAMIC PRESSURE (DYNES/SQ. CM.)	AFWL	CALCULATION OF 1 MT EFFECT ON DAM AT 10 PSI RANGE PROBLEM 51.014				AFWL	CALCULATION OF 50 KT EFFECT ON DAM AT 50 PSI RANGE PROBLEM 51.015				AFWL	CALCULATION OF 50 KT EFFECT ON DAM AT 10 PSI RANGE PROBLEM 51.016					
				HORIZONTAL DYNAMIC PRESSURE (DYNES/SQ. CM.)	POSITIVE PHASE DURATION (SEC)	HORIZONTAL DYNAMIC PRESSURE IMPULSE (DYNES/SQ. CM. SEC)	VERTICAL DYNAMIC PRESSURE IMPULSE (DYNES/SQ. CM. SEC)		HORIZONTAL DYNAMIC PRESSURE IMPULSE (DYNES/SQ. CM. SEC)	VERTICAL DYNAMIC PRESSURE IMPULSE (DYNES/SQ. CM. SEC)	HORIZONTAL DYNAMIC PRESSURE IMPULSE (DYNES/SQ. CM. SEC)	VERTICAL DYNAMIC PRESSURE IMPULSE (DYNES/SQ. CM. SEC)		HORIZONTAL DYNAMIC PRESSURE IMPULSE (DYNES/SQ. CM. SEC)	VERTICAL DYNAMIC PRESSURE IMPULSE (DYNES/SQ. CM. SEC)	HORIZONTAL DYNAMIC PRESSURE IMPULSE (DYNES/SQ. CM. SEC)	VERTICAL DYNAMIC PRESSURE IMPULSE (DYNES/SQ. CM. SEC)		
27	4.139E+04	-4.266E+03		3.944E-01*	6.025E+03		-3.182E+01												
37	4.133E+04	-1.334E+04		4.162E-01*	6.291E+03*		-6.321E+02												
48	3.536E+04	-1.680E+04		4.358E-01*	6.976E+03		-1.492E+03												
64	2.643E+04	-1.911E+04		4.582E-01*	5.810E+03*		-2.078E+03*												
			AFWL	CALCULATION OF 50 KT EFFECT ON DAM AT 50 PSI RANGE PROBLEM 51.015					CALCULATION OF 50 KT EFFECT ON DAM AT 50 PSI RANGE PROBLEM 51.015						CALCULATION OF 50 KT EFFECT ON DAM AT 10 PSI RANGE PROBLEM 51.016				
1	5.549E+05	-4.176E+05		2.039E-01*	9.948E+03		-2.385E+03												
11	2.279E+05	-4.436E+05		2.247E-01*	1.898E+04		-2.205E+04												
22	2.736E+05	-4.421E+05		2.422E-01*	2.505E+04		-3.432E+04												
24	1.724E+06	-3.107E+05		2.298E-01	1.255E+05		-2.474E+04												
25	2.442E+06	-1.318E+05		1.898E-01	1.705E+05		-1.201E+04												
26	3.145E+06	-4.866E+04		1.861E-91	1.974E+05		-4.266E+03												
27	1.285E+06	-3.320E+05		1.772E-01*	4.548E+04		-1.319E+03												
37	7.578E+05	-4.177E+05		1.964E-01*	3.612E+04		-1.371E+04												
48	3.470E+05	-4.310E+05		2.128E-01*	3.326E+04		-2.585E+04												
64	3.165E+05	-4.412E+05		2.271E-01*	2.809E+04		-2.944E+04												
			AFWL	CALCULATION OF 50 KT EFFECT ON DAM AT 10 PSI RANGE PROBLEM 51.016					CALCULATION OF 50 KT EFFECT ON DAM AT 10 PSI RANGE PROBLEM 51.016						CALCULATION OF 50 KT EFFECT ON DAM AT 10 PSI RANGE PROBLEM 51.016				
1	1.935E+04	-6.492E+03		3.154E-01*	9.147E+02		-7.872E+01												
11	1.614E+04	-1.913E+04		3.393E-01*	2.094E+03		-1.413E+03												

* Indicates that positive phase is incomplete

Table 3. (Continued)

STATION NUMBER	PEAK HORIZONTAL DYNAMIC PRESSURE (DYNES/SQ.CM.)	PEAK VERTICAL DYNAMIC PRESSURE (DYNES/SQ.CM.)	HORIZONTAL DYNAMIC PRESSURE IMPULSE (DYNES/SQ.CM SEC.)	HORIZONTAL DYNAMIC PRESSURE IMPULSE (DYNES/SQ.CM SEC.)	VERTICAL DYNAMIC PRESSURE IMPULSE (DYNES/SQ.CM SEC.)
					AFWL CALCULATION OF 50 KT EFFECT ON DAM AT 10 PSI RANGE PROBLEM 51.016
22	1.778E+04	-2.099E+04	3.617E-01*	3.396E+03	-2.612E+03
24	6.693E+04	-1.119E+04	4.614E-01*	1.458E+04	-2.404E+03
25	1.029E+05	-5.887E+03	4.693E-01*	1.793E+04*	-1.088E+03*
26	1.353E+05	-2.323E+03	4.717E-01*	1.974E+04	-3.658E+02
27	4.495E+04	-4.851E+03	2.763E-01*	4.693E+03	-3.378E+01
37	4.258E+04	-1.409E+04	2.966E-01*	4.621E+03	-6.097E+02
48	3.315E+04	-1.629E+04	3.162E-01*	4.887E+03	-1.363E+03
64	2.407E+04	-1.823E+04	3.385E-01*	4.121E+03	-1.782E+03
					AFWL CALCULATION OF 50 KT EFFECT ON DAM AND STRUCTURE AT 50 PSI RANGE PROBLEM 51.017
1	-3.064E+03	-1.671E+06	2.032E-01	-2.705E+01	-8.746E+03
11	1.602E+04	-1.429E+06	2.249E-01	5.504E+01	-3.048E+04
22	2.527E+05	-4.274E+05	2.414E-01	9.462E+03	2.800E+04*
24	1.724E+06	-3.107E+05	2.298E-01	1.255E+05	-2.473E+04
25	2.442E+06	-1.318E+05	1.898E-01	1.705E+05	-1.201E+04
26	3.145E+06	-4.866E+04	1.861E-01	1.974E+05	-4.266E+03
27	-6.404E+02	-1.456E+05	1.609E-01*	-6.575E+01	-1.040E+03
37	-9.208E+02	4.725E+05	1.896E-01*	-7.860E+01*	4.491E+04*
48	1.687E+06	3.386E+05	2.128E-01*	1.187E+05	-9.316E+03
64	1.425E+06	-1.194E+05	2.265E-01*	4.697E+04	-3.522E+02

* Indicates that positive phase is incomplete

below the dam increases the overpressures on the ground above the free air value.

Overpressure in the reflected shock decreases with increasing altitude, as the shock expands upward. Overpressure increases with increasing range, from the reinforcement of the reflected and incident waves. This reinforcement is not from the Mach stem, which is never more than a meter high in the vicinity of the blockhouse. The reflection opposes the incident flow close to the dam, but strengthens the horizontal portion of the flow away from the dam.

Although the peak overpressure is usually lower near the blockhouse than in the free air above the dam, the overpressure impulse is usually higher near the blockhouse than above the dam.

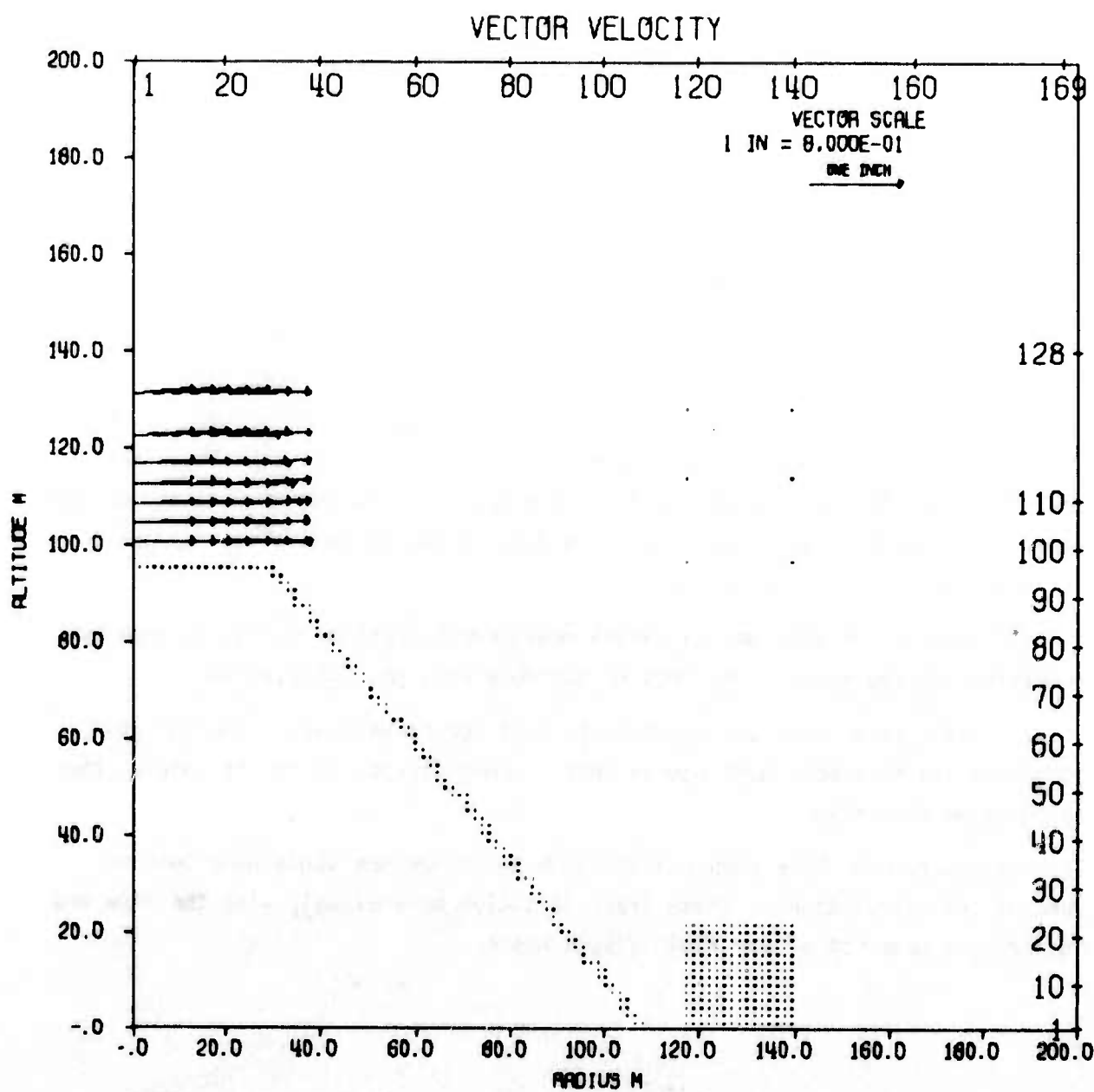
While buildings are vulnerable to overpressure and overpressure impulse, objects such as towers, trucks, cables, and poles are sensitive to the drag from dynamic pressure. The latter is reduced in every case in the region in front of the dam. The dynamic pressure impulses were also reduced in this region. The only enhancement of dynamic pressures occurred in the vertical direction, but these are small compared to the free air horizontal dynamic pressure.

Each of the five problems differed slightly from the nominal blast values of 50 and 10 psi (3.45×10^6 and 6.89×10^5 dynes/sq cm). Considering the differences in the inputs, the calculations showed good agreement. The overall phenomenology was the same for the problems without a rigid blockhouse. However, the dam protected the blockhouse more in the cases of 10 psi than for the cases of 50 psi.

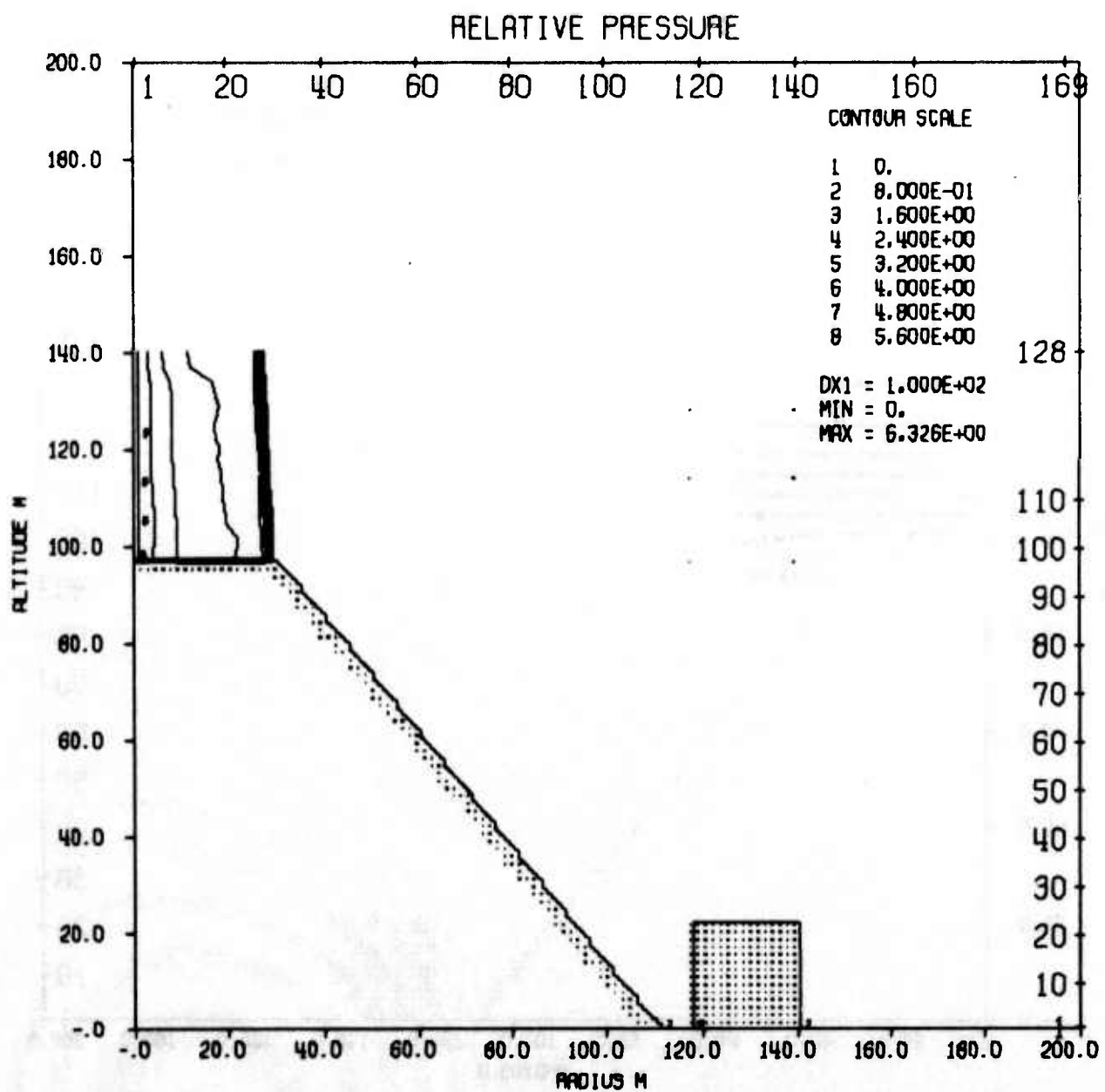
APPENDIX A
SNAPSHOTS IN TIME

The following information will be useful in interpreting the three types of plots that follow.

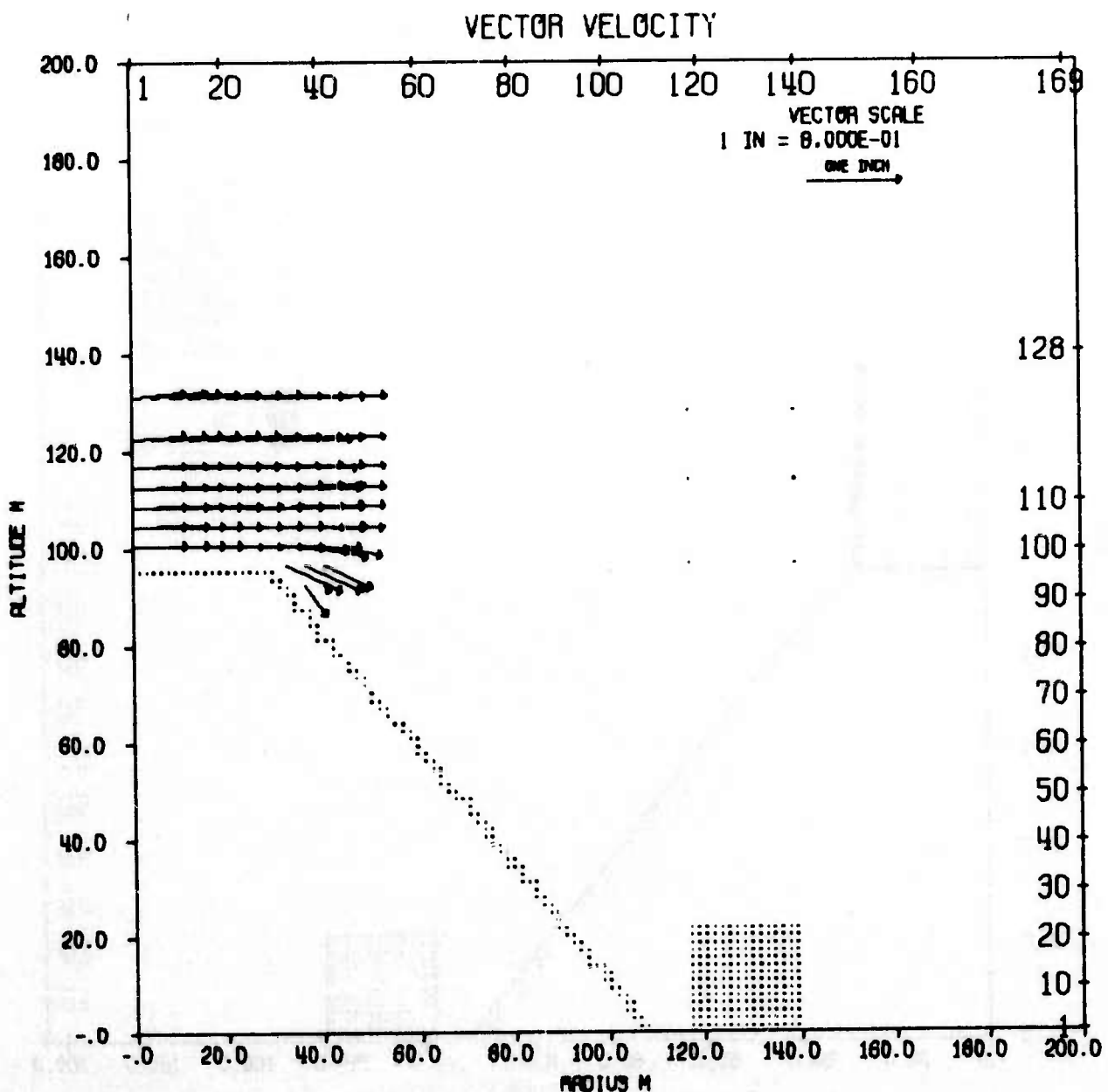
1. Vector Velocity Plots: These plots show only the largest velocities. The scale is in kilometers/second and the magnitude is based on the scale in the upper right hand corner of the plots. The point of each measurement is the beginning (tail) of the arrow.
2. Relative Pressure Contour Plots: Relative pressure is the ratio of the local pressure to the ambient atmospheric pressure. The contour lines connect points of equal relative pressure and are analogous to isobars. The contour values given in the upper right hand corner are dimensionless. D x 1 is the width of the first computational column, and min and max refer to the minimum and maximum relative pressure values. Note that the dots in the various plots represent different things in the same plot.
 - a. Some of the dots merely denote measurement stations as can be seen by referring to figure 2. These dots do not move with the calculation.
 - b. Rigid structures are outlined by dots for convenience. The dam and structure are thus both outlined by dots. These structures do not move as the calculation progresses.
3. Trace particles have been placed where the structure would have been in some of the calculations. These trace particles move exactly with the flow and "trace" the movement of any fluid displacement.



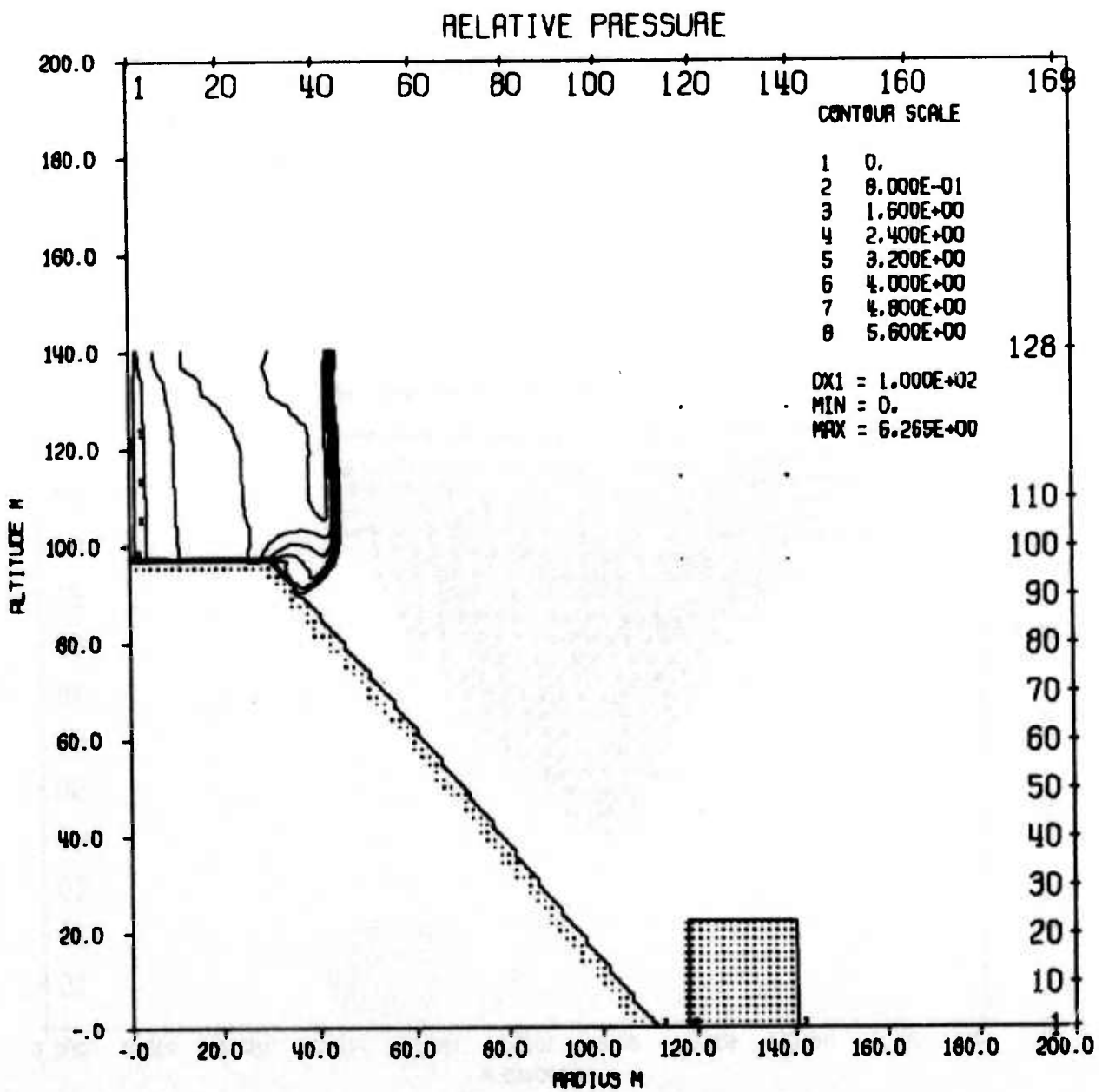
AFWL HULL CAL OF SOFT EFFECT ON DAM AND STRUCTURE AT 50PSI RANGE
TIME 260.000 MSEC CYCLE 47. PROBLEM 51.0170



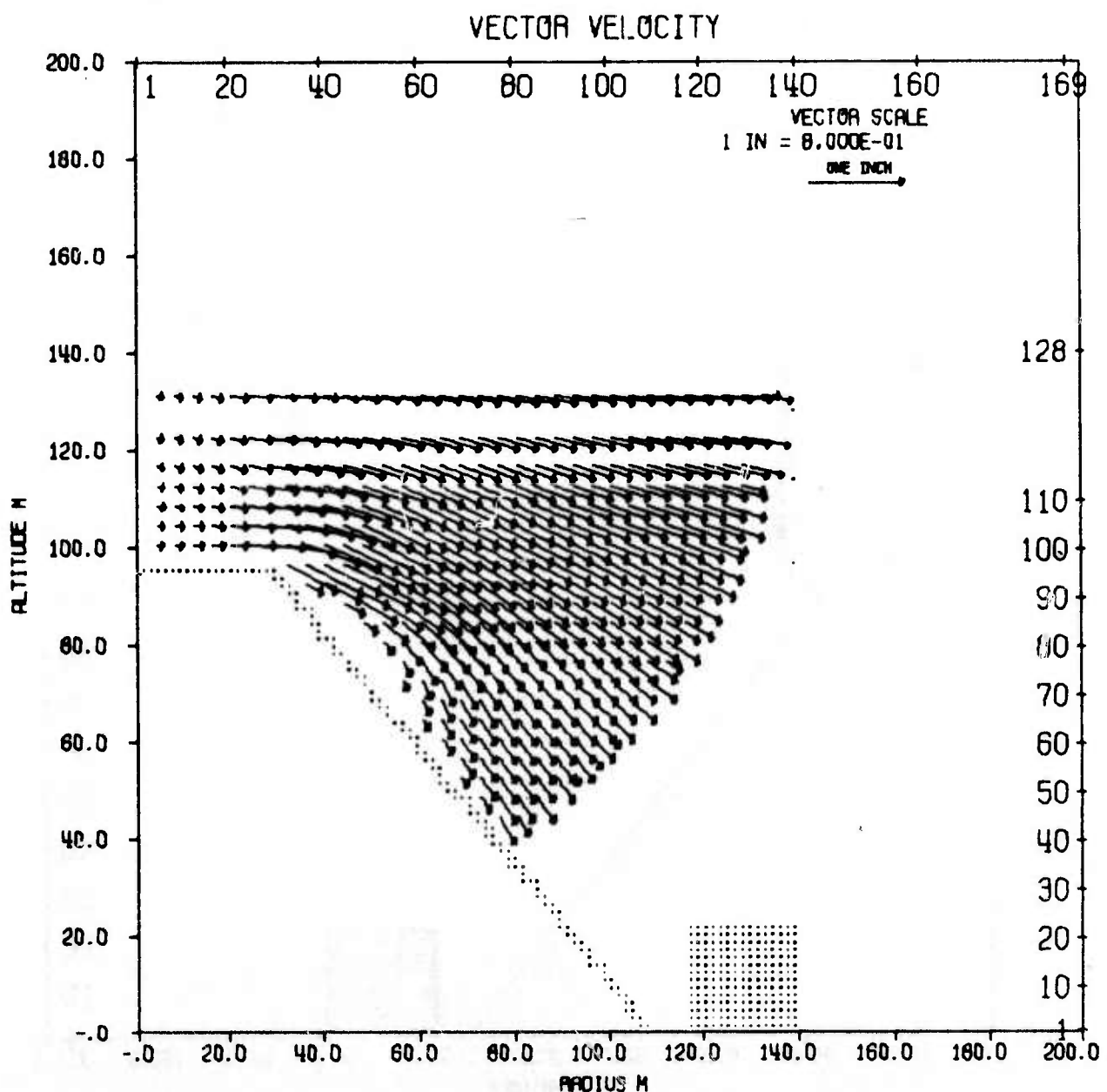
AFWL HULL CAL OF 50KT EFFECT ON DAM AND STRUCTURE AT 50PSI RANGE
TIME 260.000 MSEC CYCLE 47. PROBLEM 51.0170



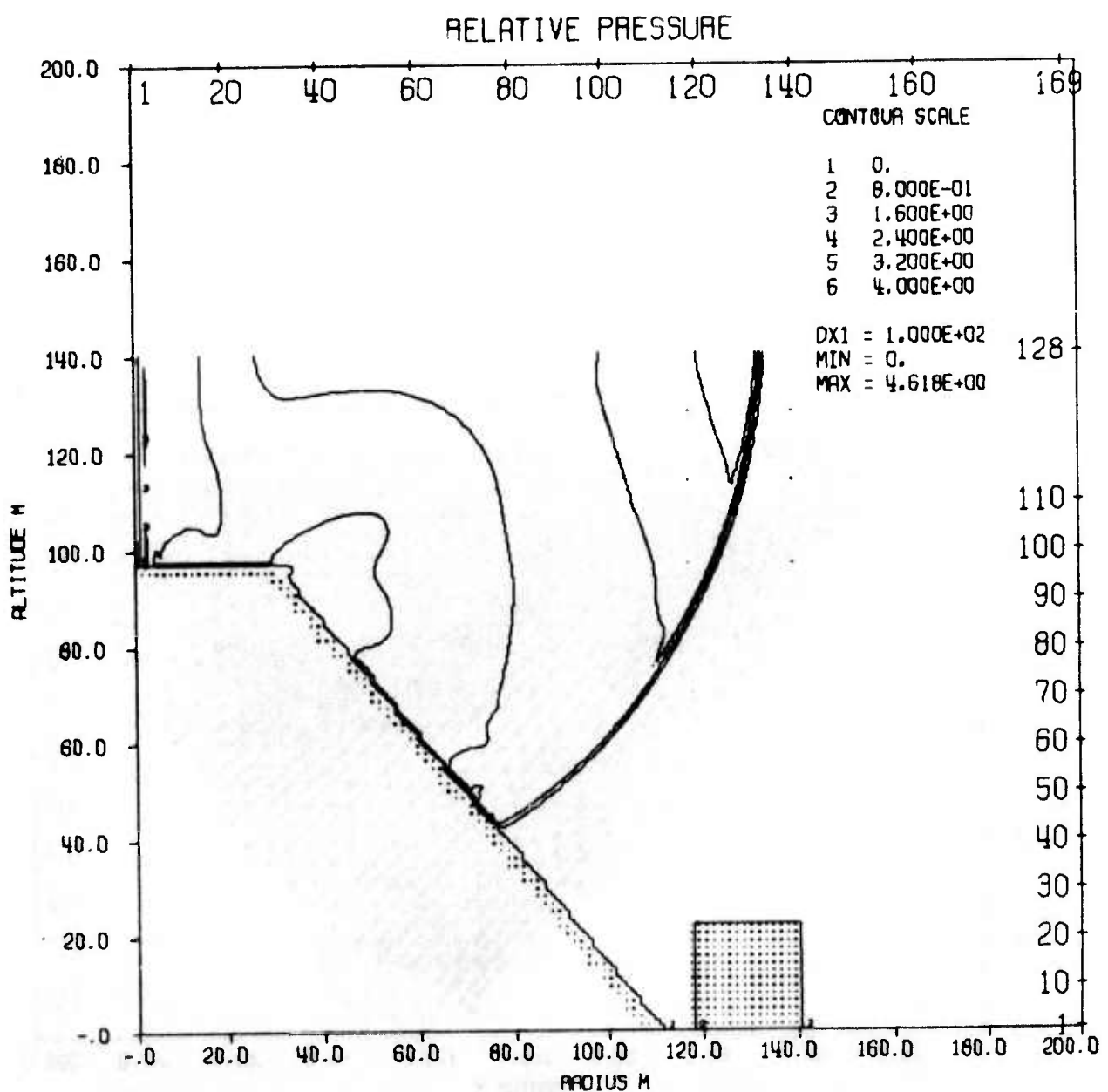
AFWL HULL CAL OF 50KT EFFECT ON DAM AND STRUCTURE AT 50PSI RANGE
TIME 280.000 MSEC CYCLE 71. PROBLEM 51.0170



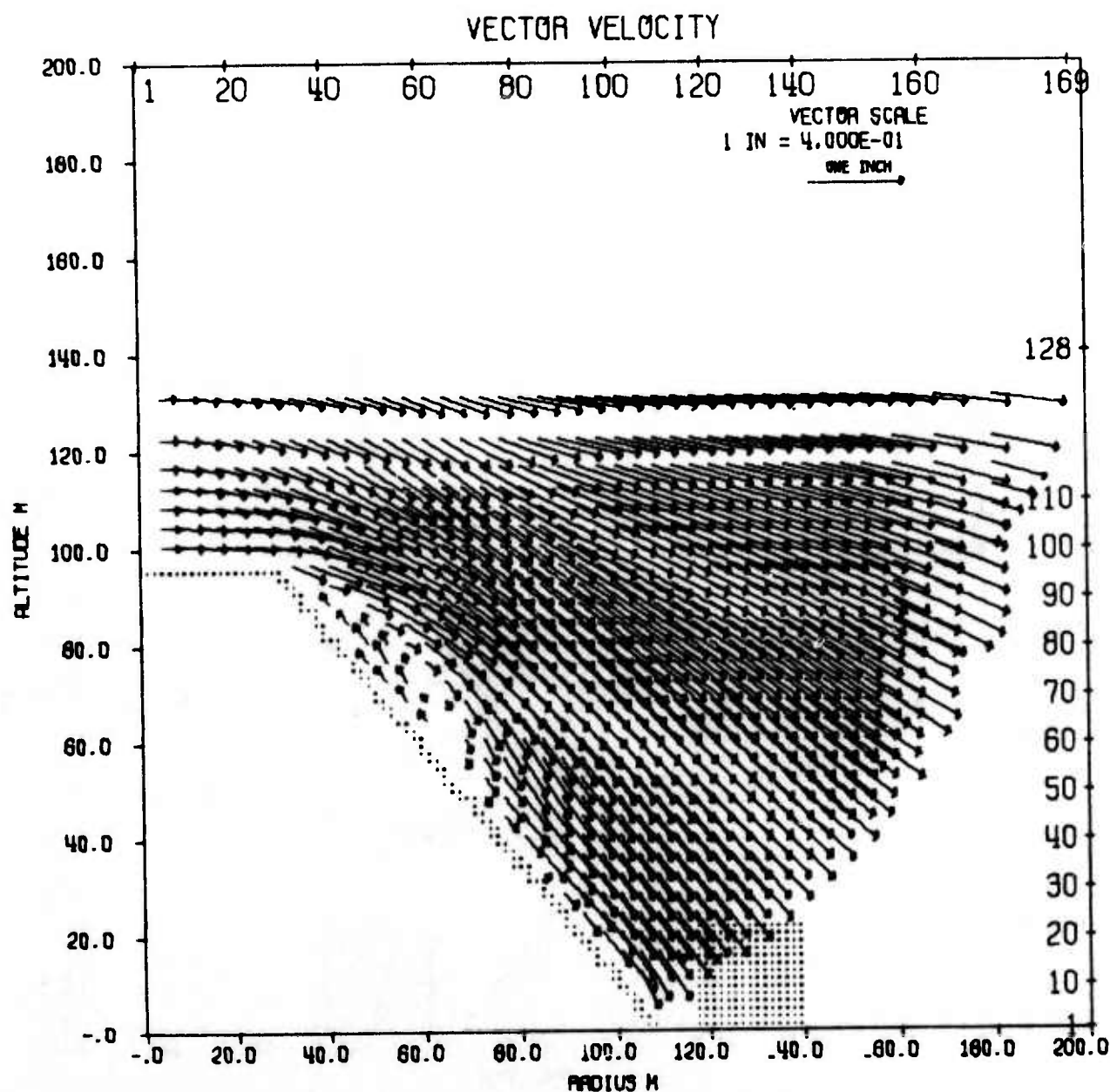
AFWL HULL CAL OF 50KT EFFECT ON DAM AND STRUCTURE AT 50PSI RANGE
TIME 280.000 MSEC CYCLE 71. PROBLEM 51.0170



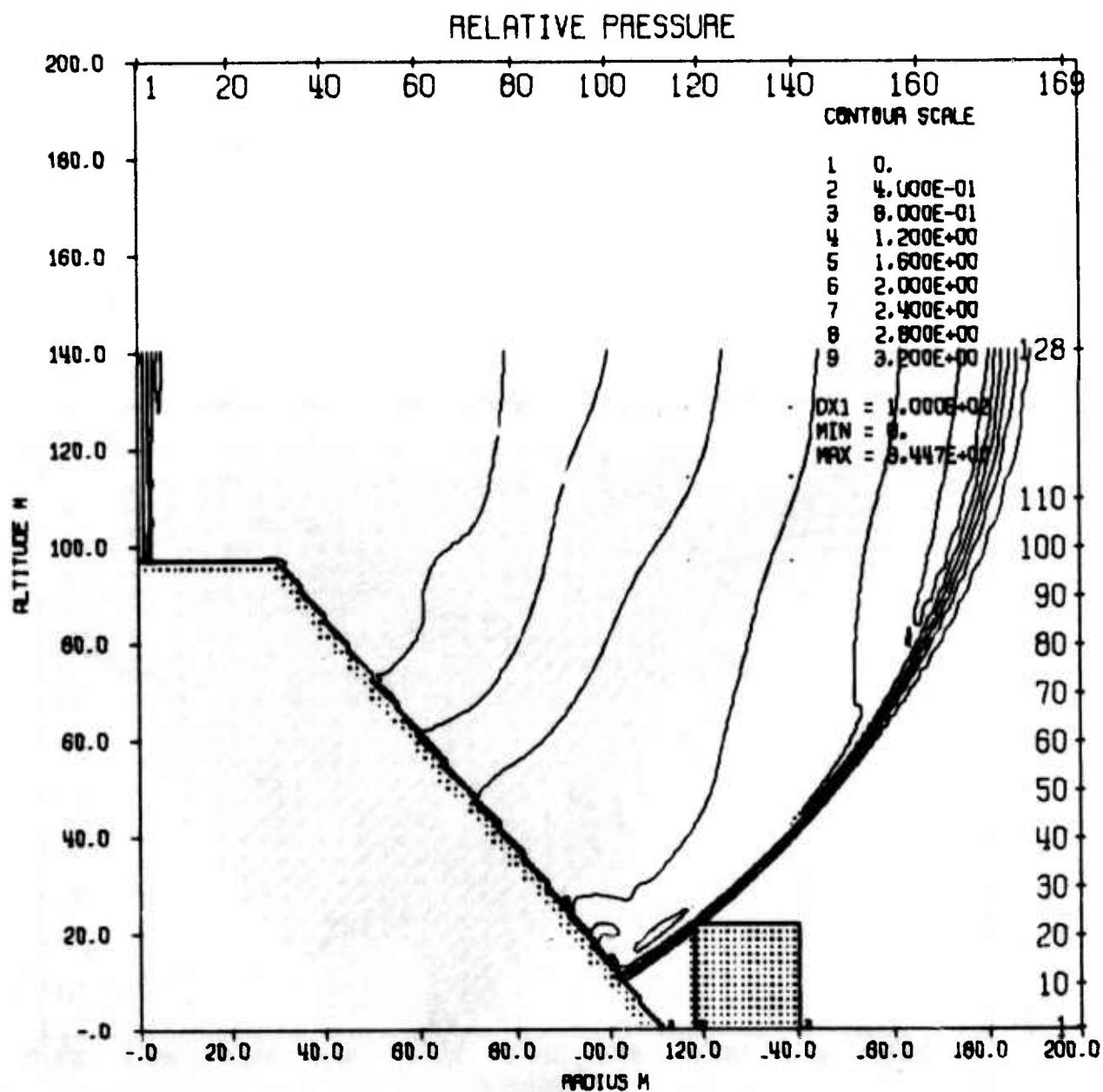
AFWL HULL CAL OF 50KT EFFECT ON DAM AND STRUCTURE AT 50PSI RANGE
TIME 400.000 MSEC CYCLE 208. PROBLEM 51.0170



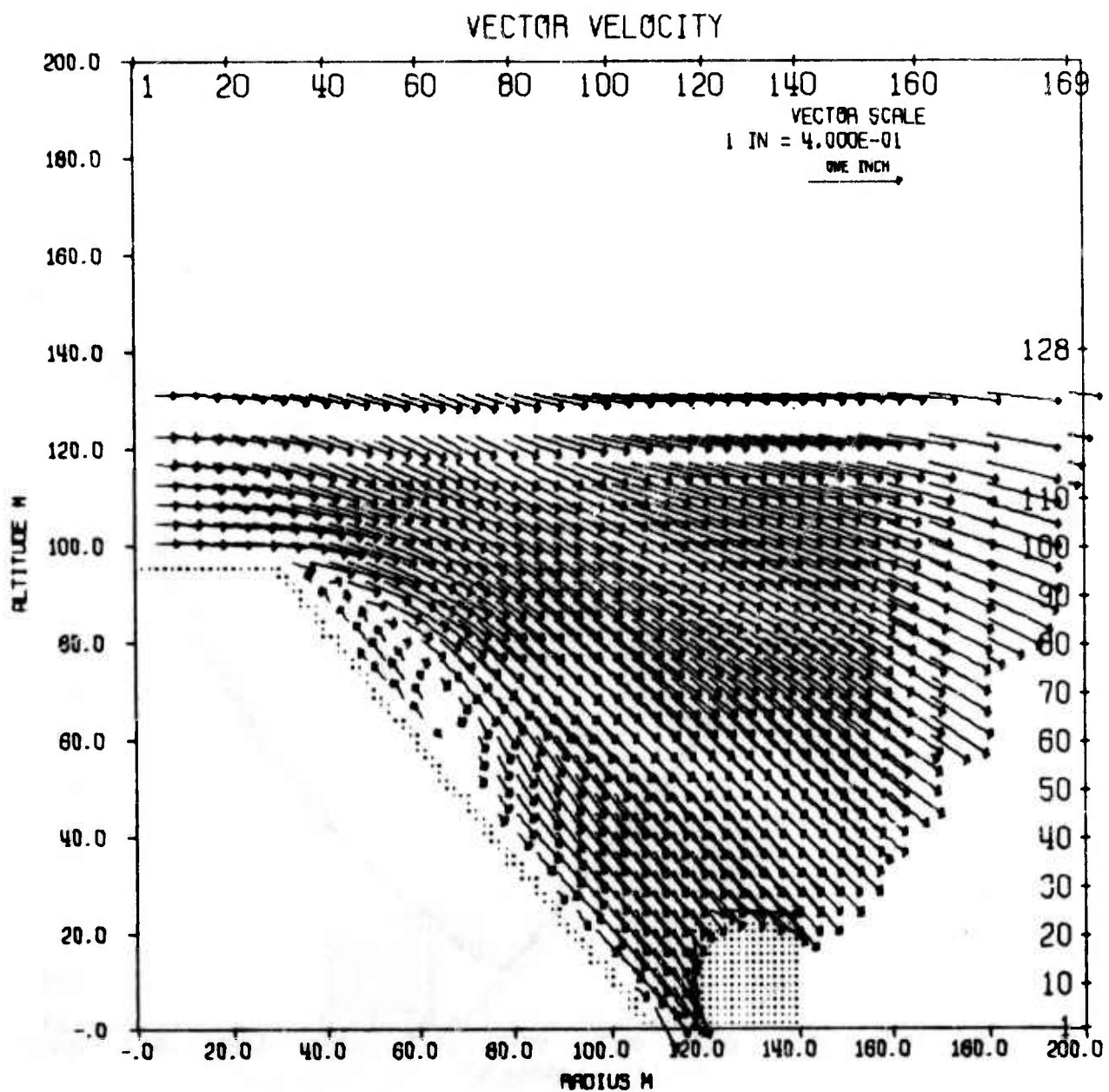
AFWL HULL CAL OF 50KT EFFECT ON DAM AND STRUCTURE AT 50PSI RANGE
TIME 400.000 MSEC CYCLE 208. PROBLEM 51.0170



AFWL HULL CAL OF SOFT EFFECT ON DAM AND STRUCTURE AT 50PSI RANGE
TIME 480.000 MSEC CYCLE 294. PROBLEM 51.0170

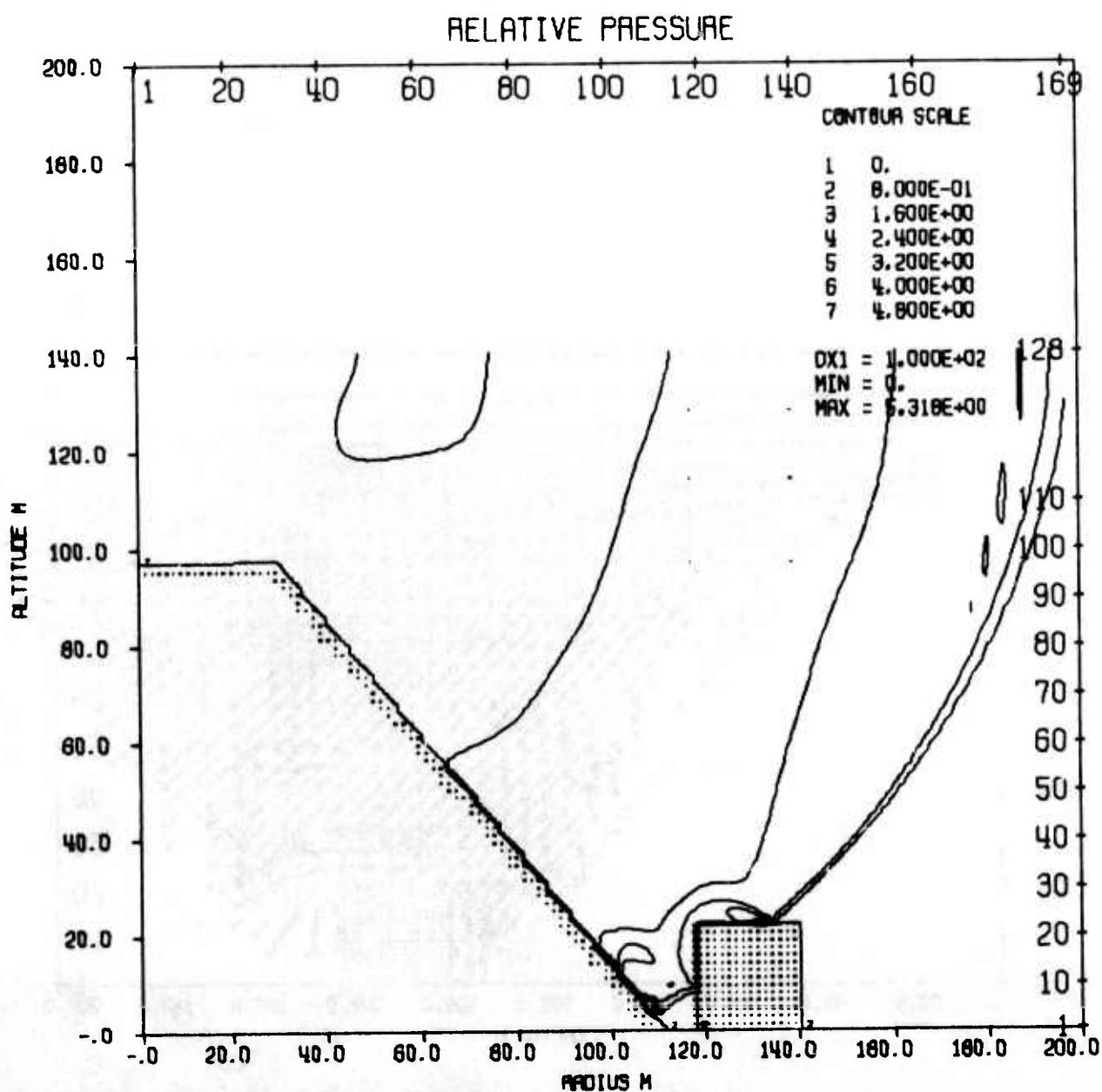


AFWL HULL CAL OF 50KT EFFECT ON DAM AND STRUCTURE AT 50PSI RANGE
TIME 480.000 MSEC CYCLE 294. PROBLEM 51.01.0

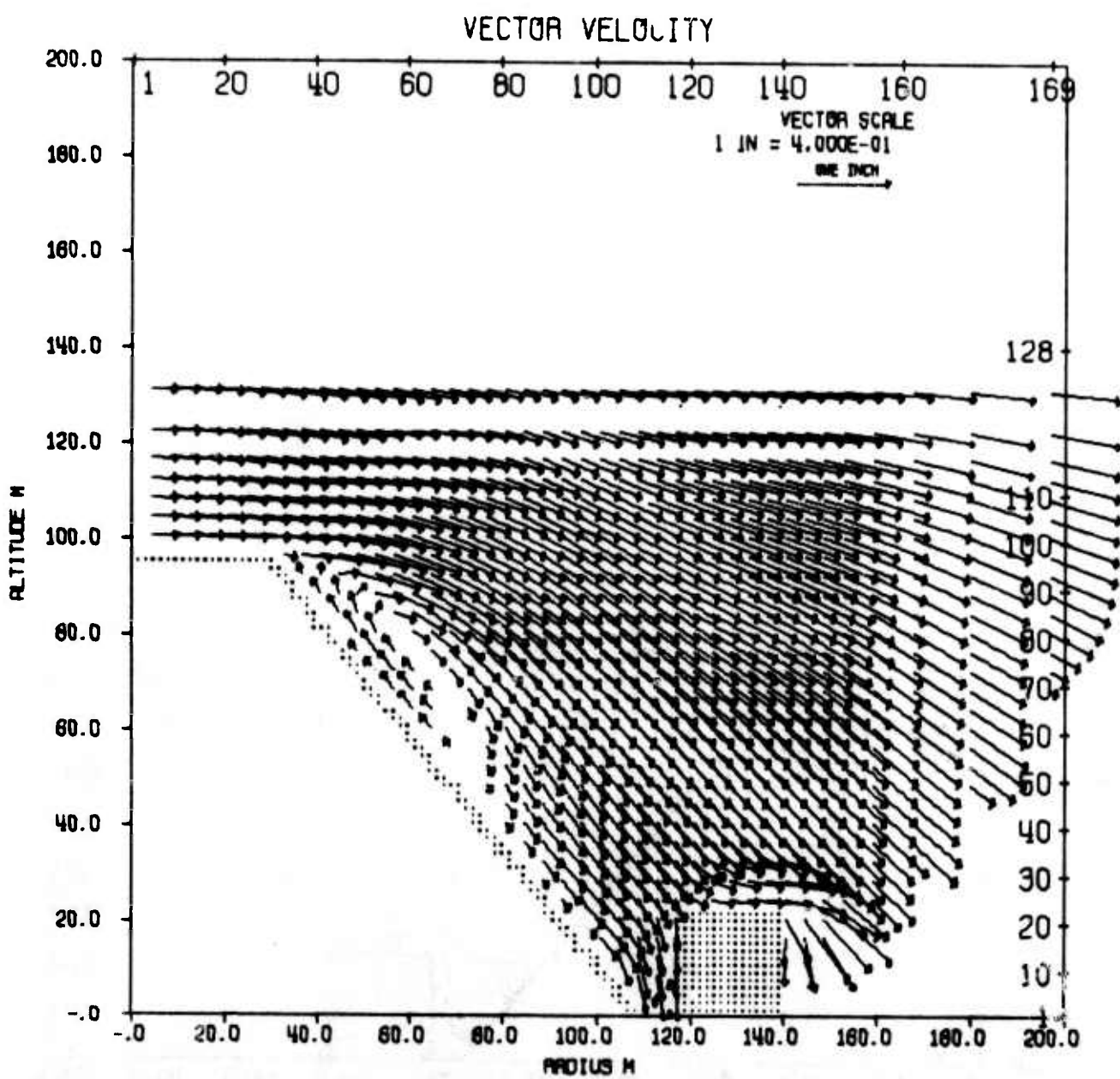


AFWL HULL CAL OF 50KT EFFECT ON DAM AND STRUCTURE AT 50PSI RANGE
TIME 500.000 MSEC CYCLE 315. PROBLEM 51.0170

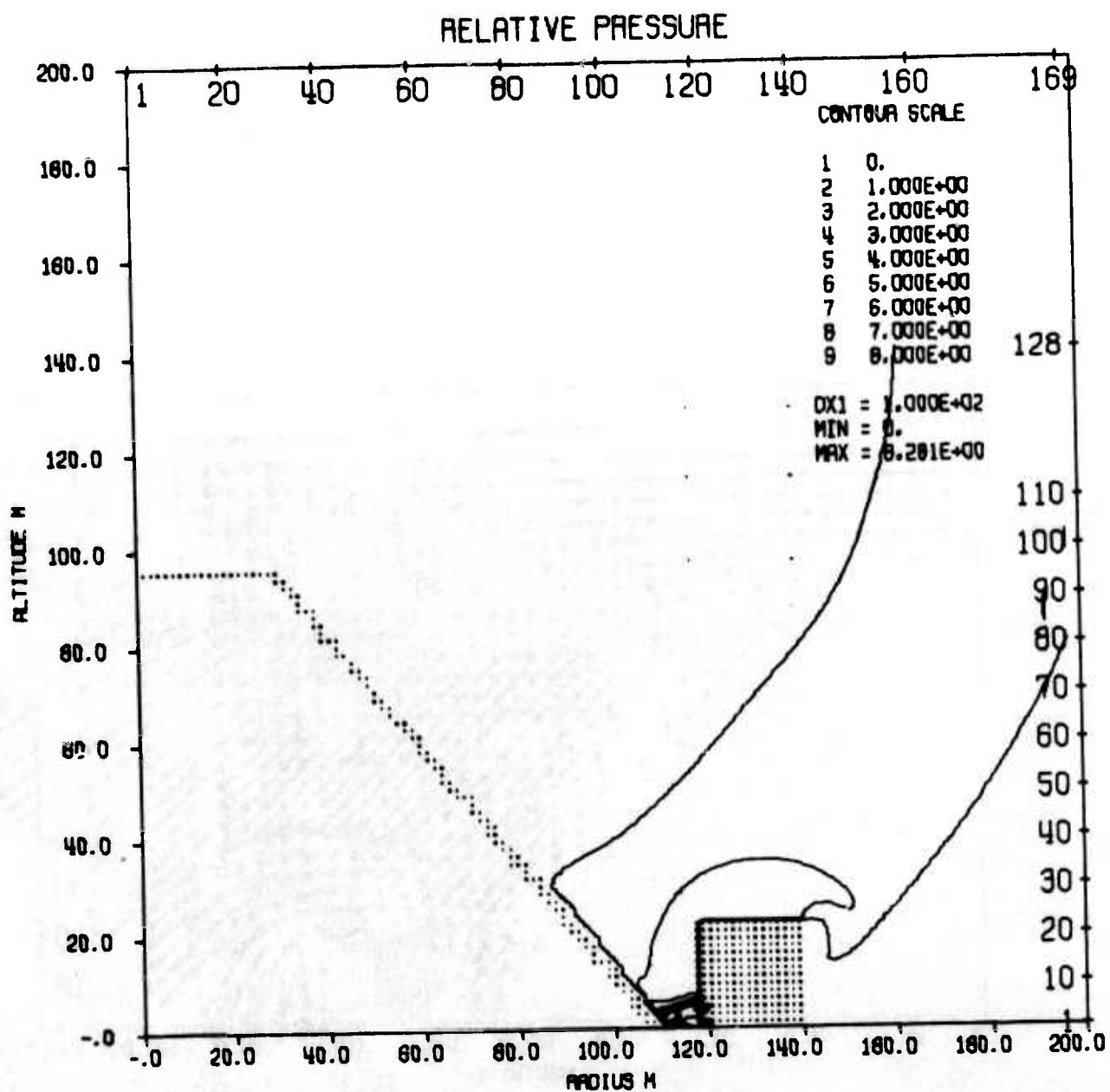
6



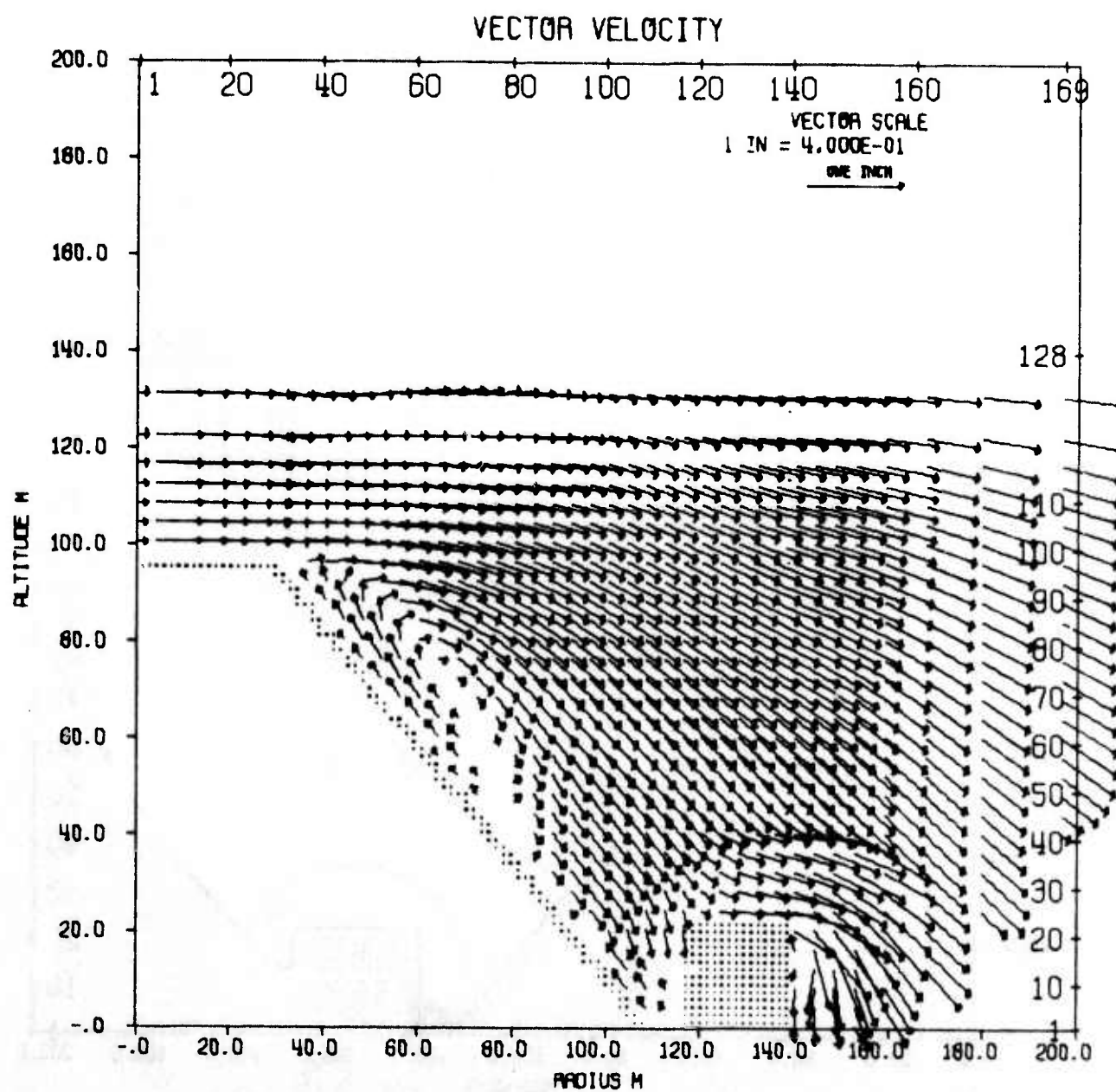
AFWL HULL CAL OF 50KT EFFECT ON DAM AND STRUCTURE AT 50PSI RANGE
TIME 500.000 MSEC CYCLE 315. PROBLEM 51.0170



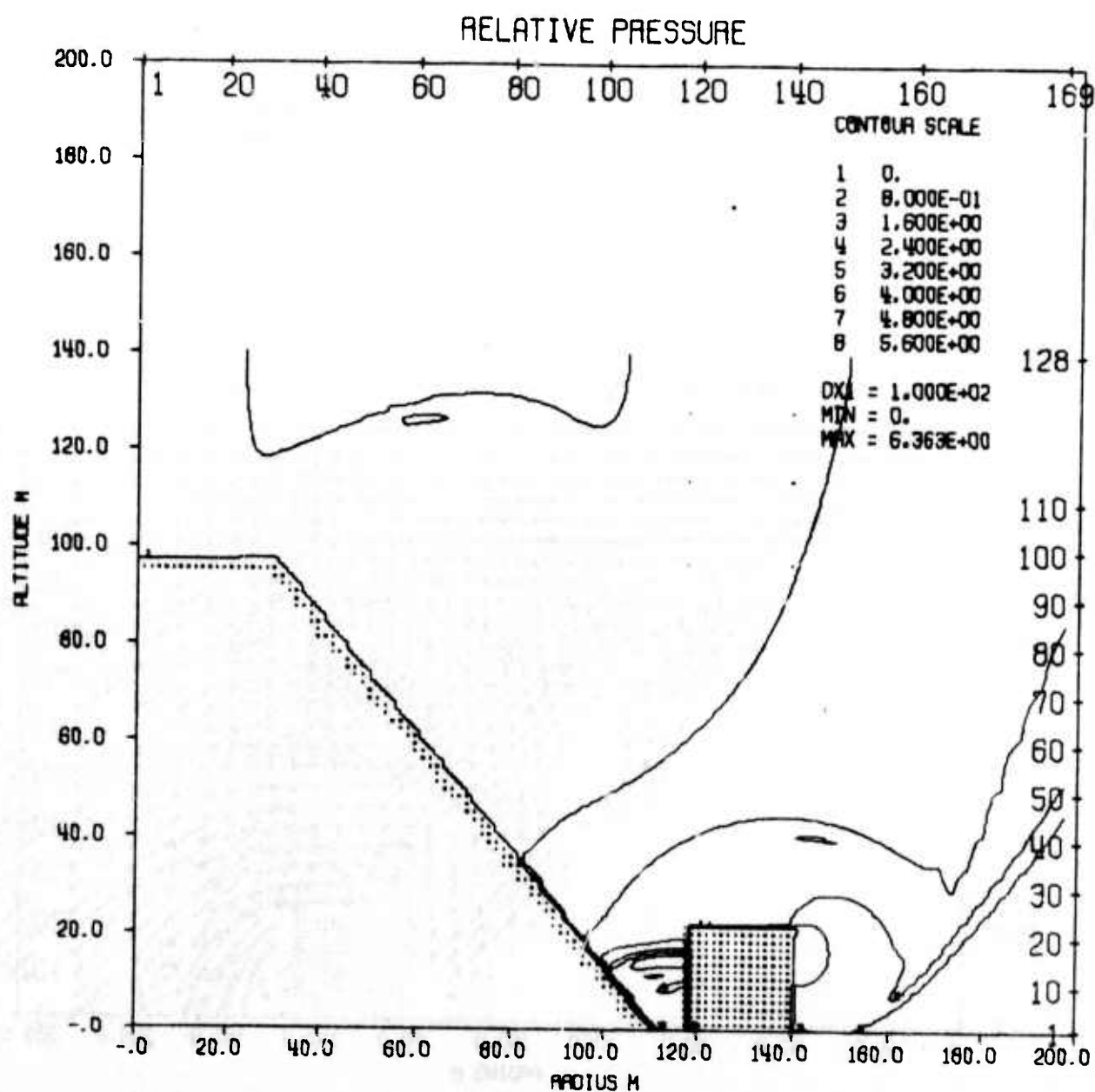
AFWL HULL CAL OF SOKT EFFECT ON DAM AND STRUCTURE AT SOPS1 RANGE
TIME 530.000 MSEC CYCLE 346. PROBLEM 51.0170



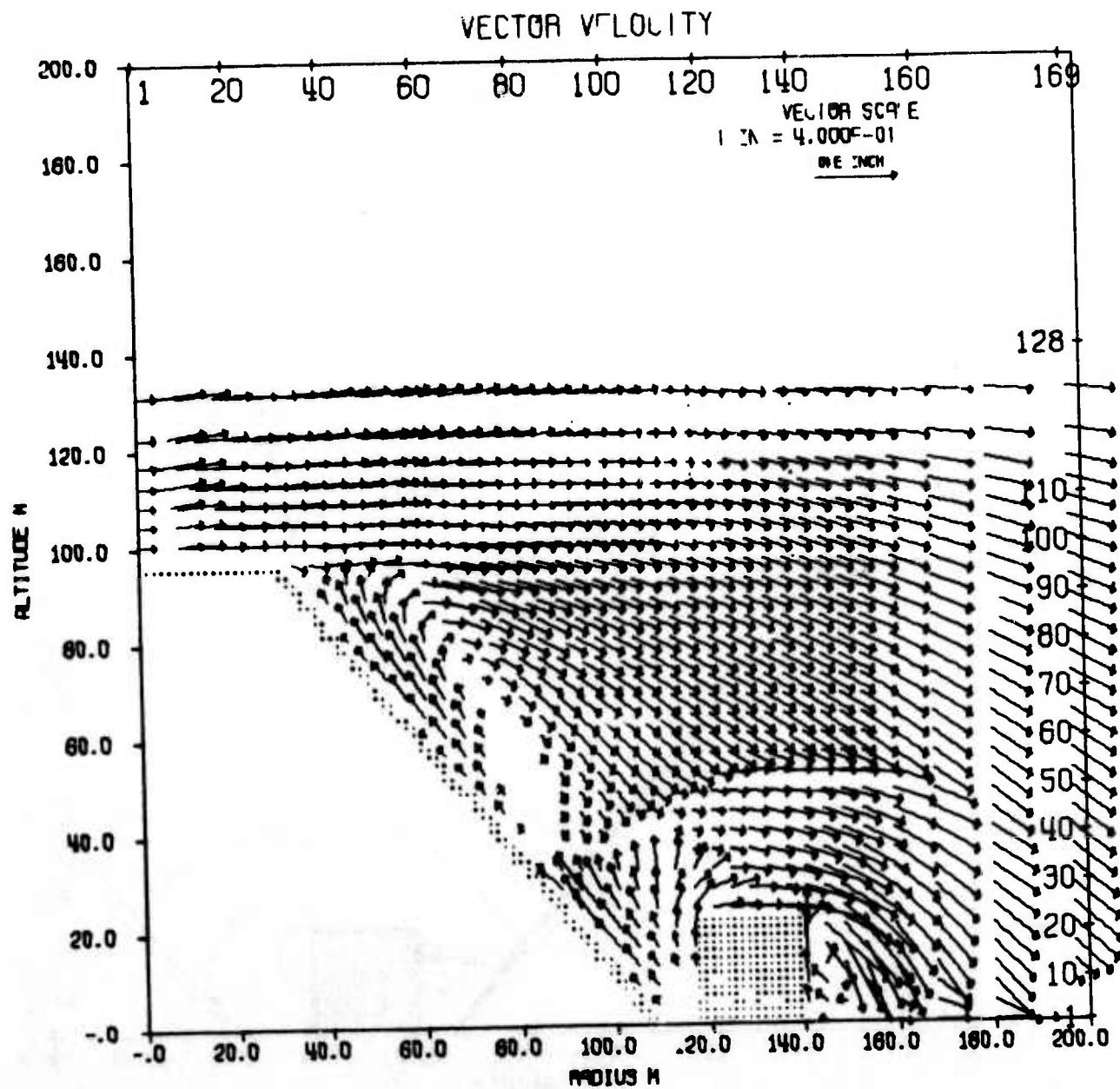
AFWL HULL CAL OF 50KT EFFECT ON DAM AND STRUCTURE AT 50PSI RANGE
TIME 530.000 MSEC CYCLE 346. PROBLEM 51.0170



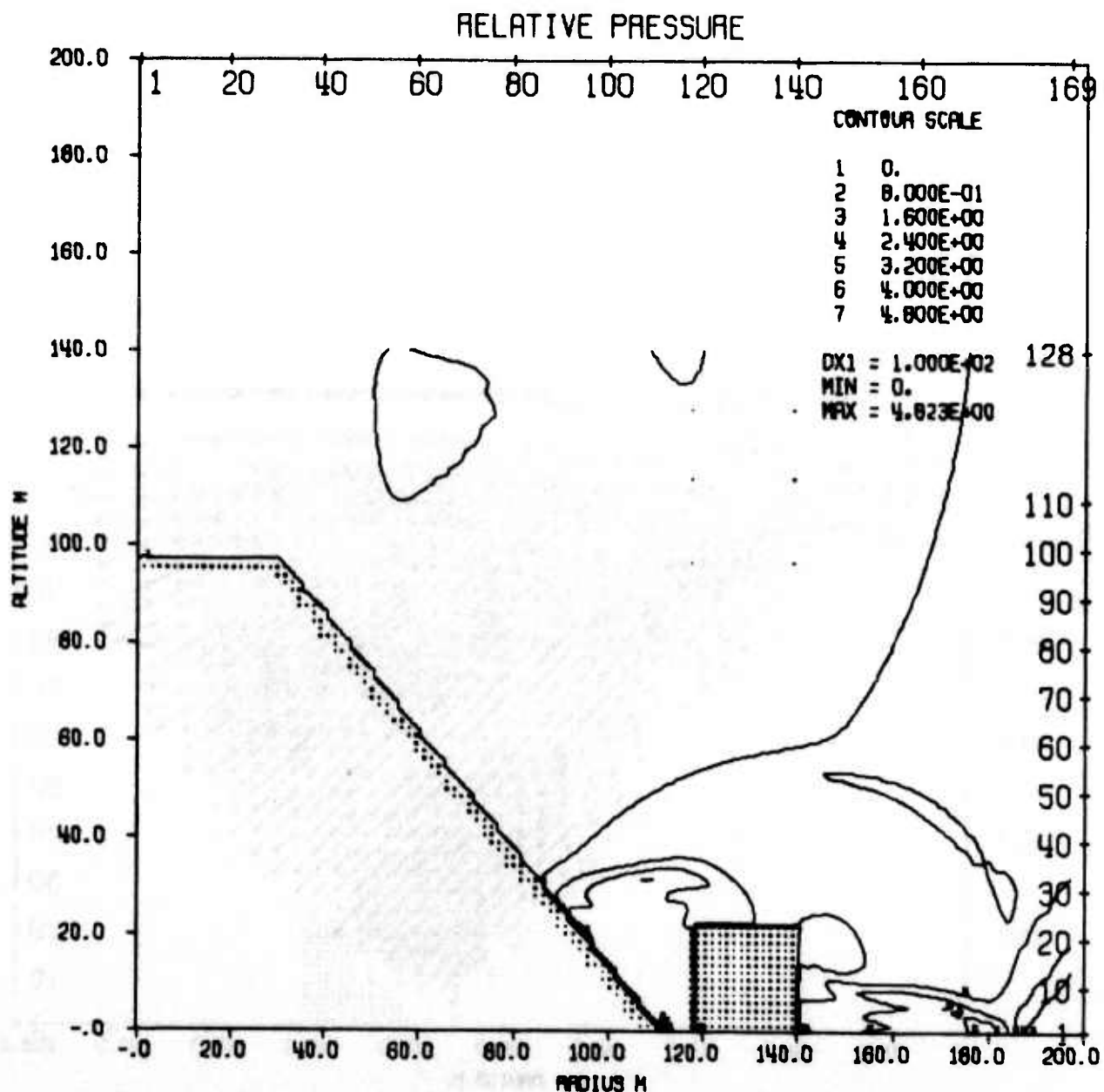
AFWL HULL CAL OF SOFT EFFECT ON DAM AND STRUCTURE AT 50PSI RANGE
TIME 560.000 MSEC CYCLE 491. PROBLEM 51.0170



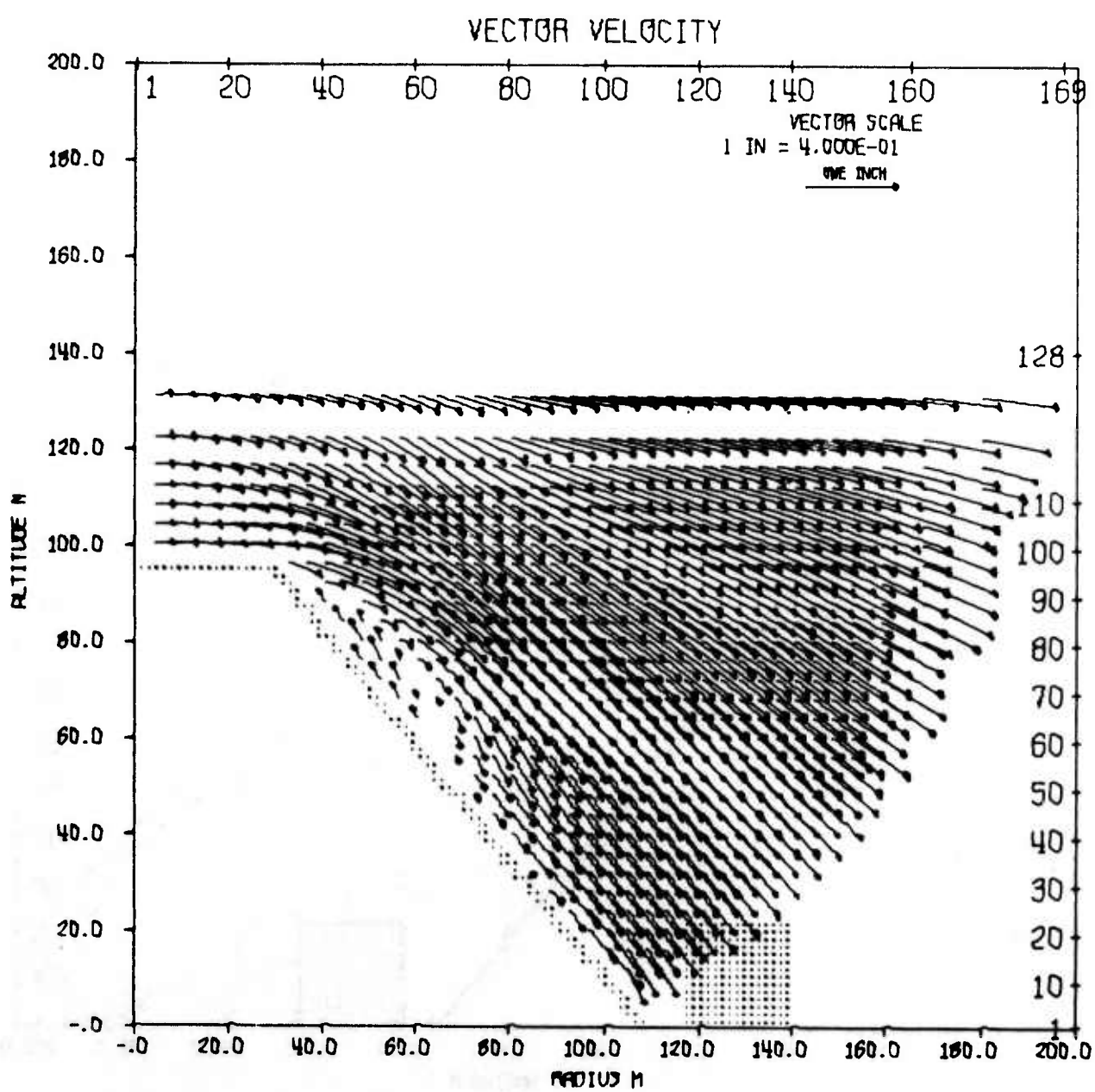
AFWL HULL CAL OF 50KT EFFECT ON DAM AND STRUCTURE AT 50PSI RANGE
TIME 560.000 MSEC CYCLE 491. PROBLEM 51.0170



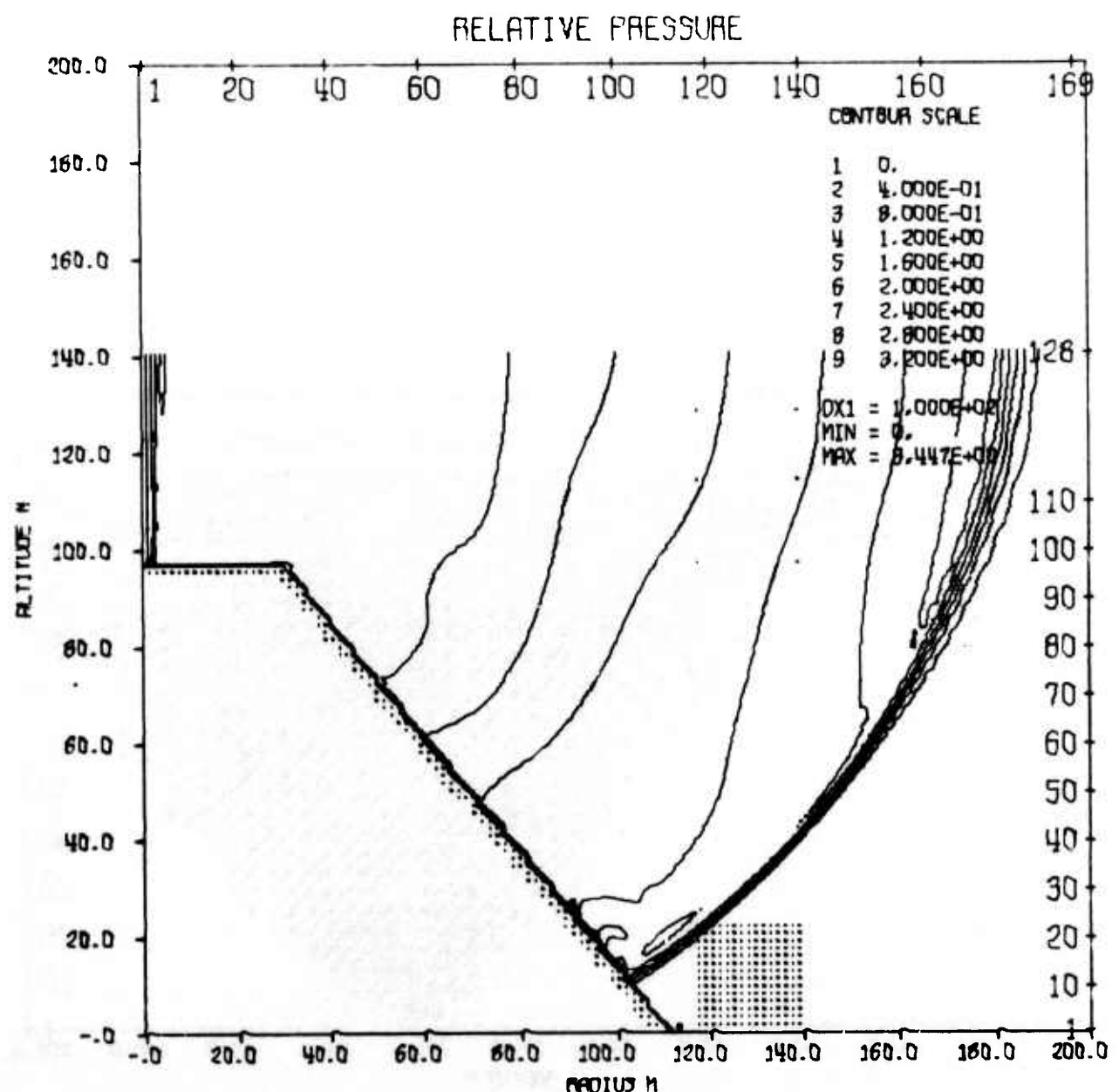
AFWL HULL CAL OF 50KT EFFECT ON DAM AND STRUCTURE AT 50PSI RANGE
TIME 600.000 MSEC CYCLE 703. PROBLEM 51.0170



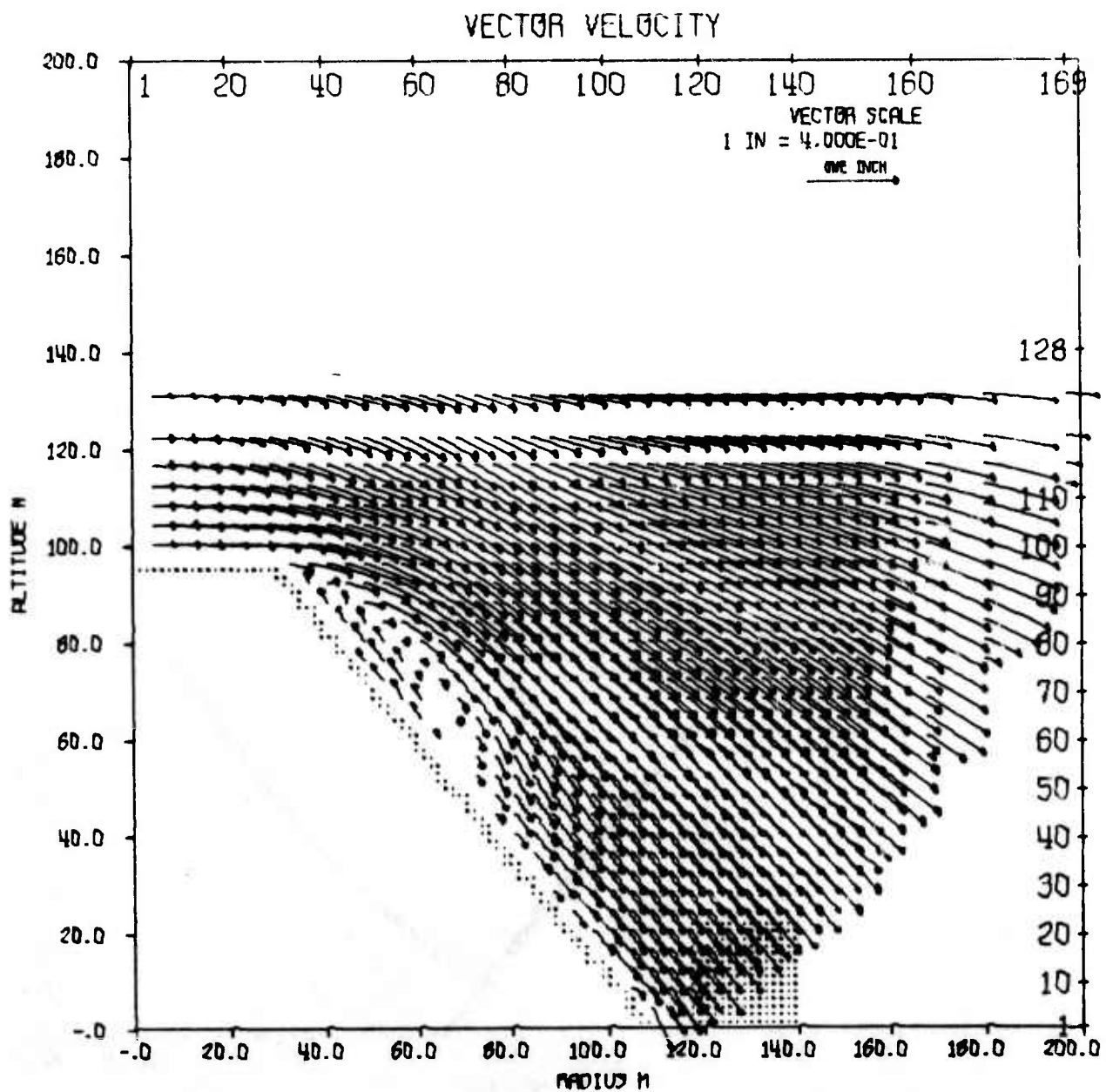
AFWL HULL CAL OF SOKT EFFECT ON DAM AND STRUCTURE AT 50PSI RANGE
TIME 600.000 MSEC CYCLE 703. PROBLEM 51.0170



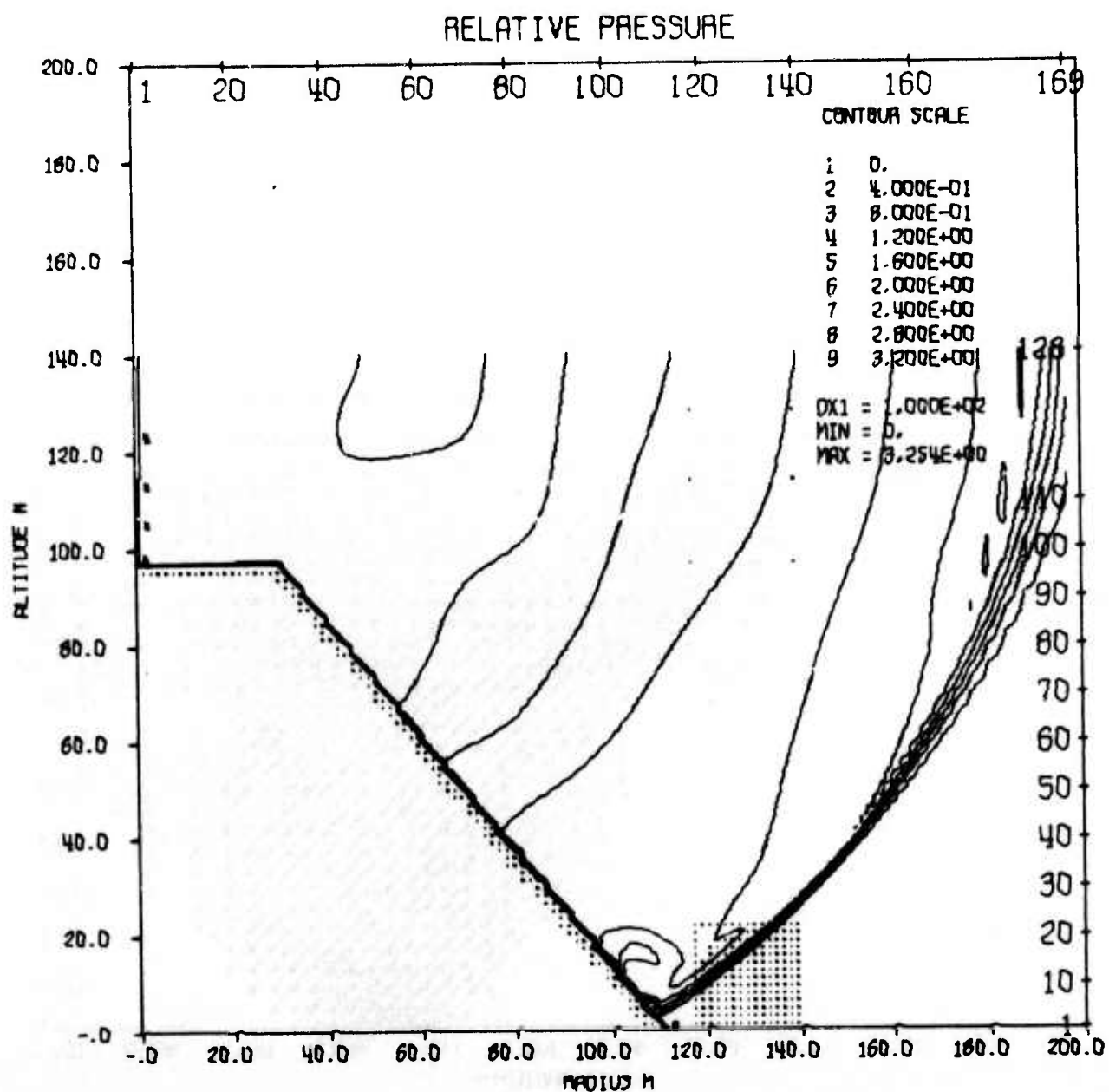
AFWL HULL CAL OF 50KT EFFECT ON DAM AT 50PSI RANGE
TIME 480.000 MSEC CYCLE 294. PROBLEM 51.0150



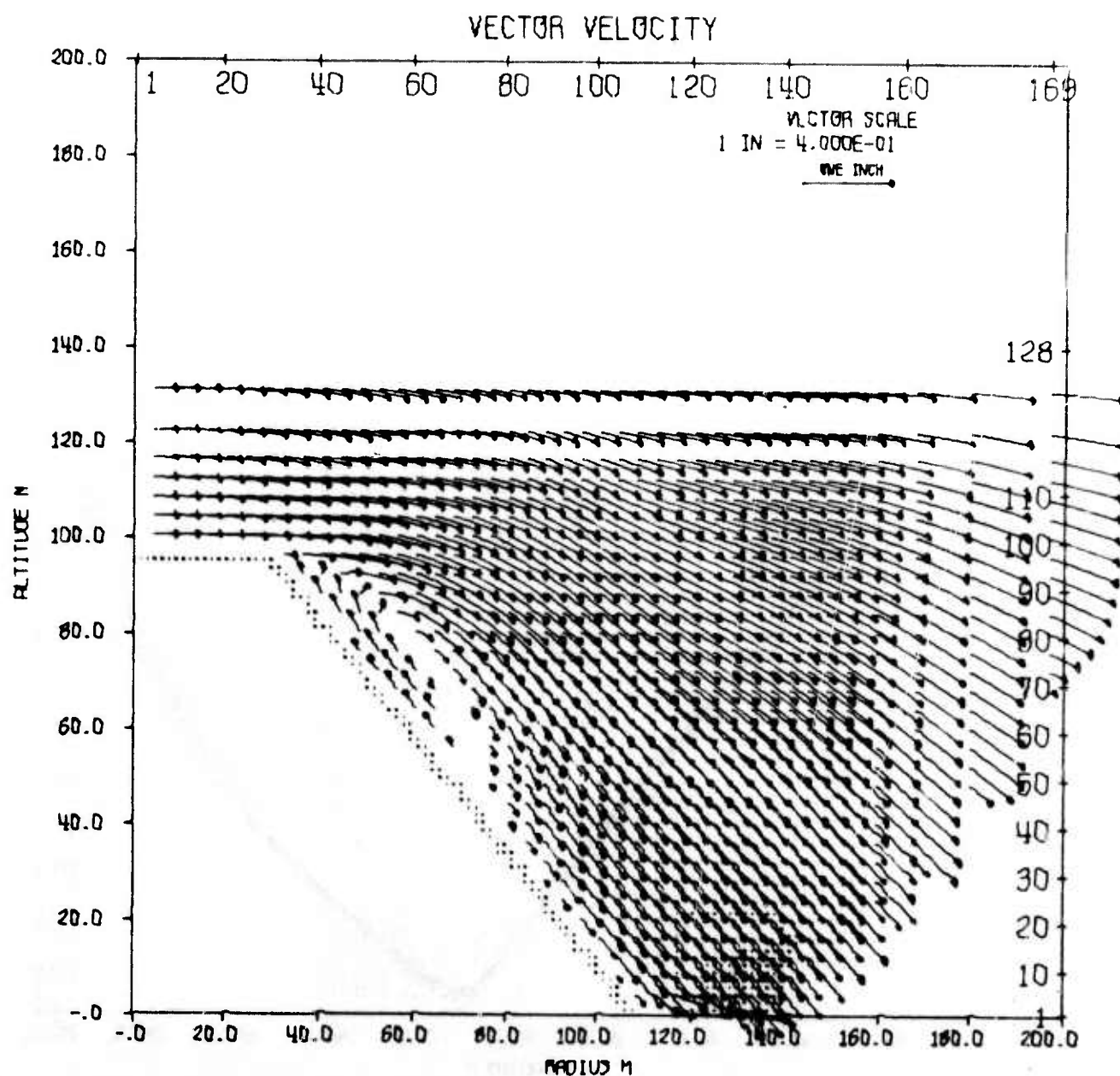
AFWL HULL CAL OF 50KT EFFECT ON DAM AT 50PSI RANGE
TIME 480.000 MSEC CYCLE 294. PROBLEM 51.0150



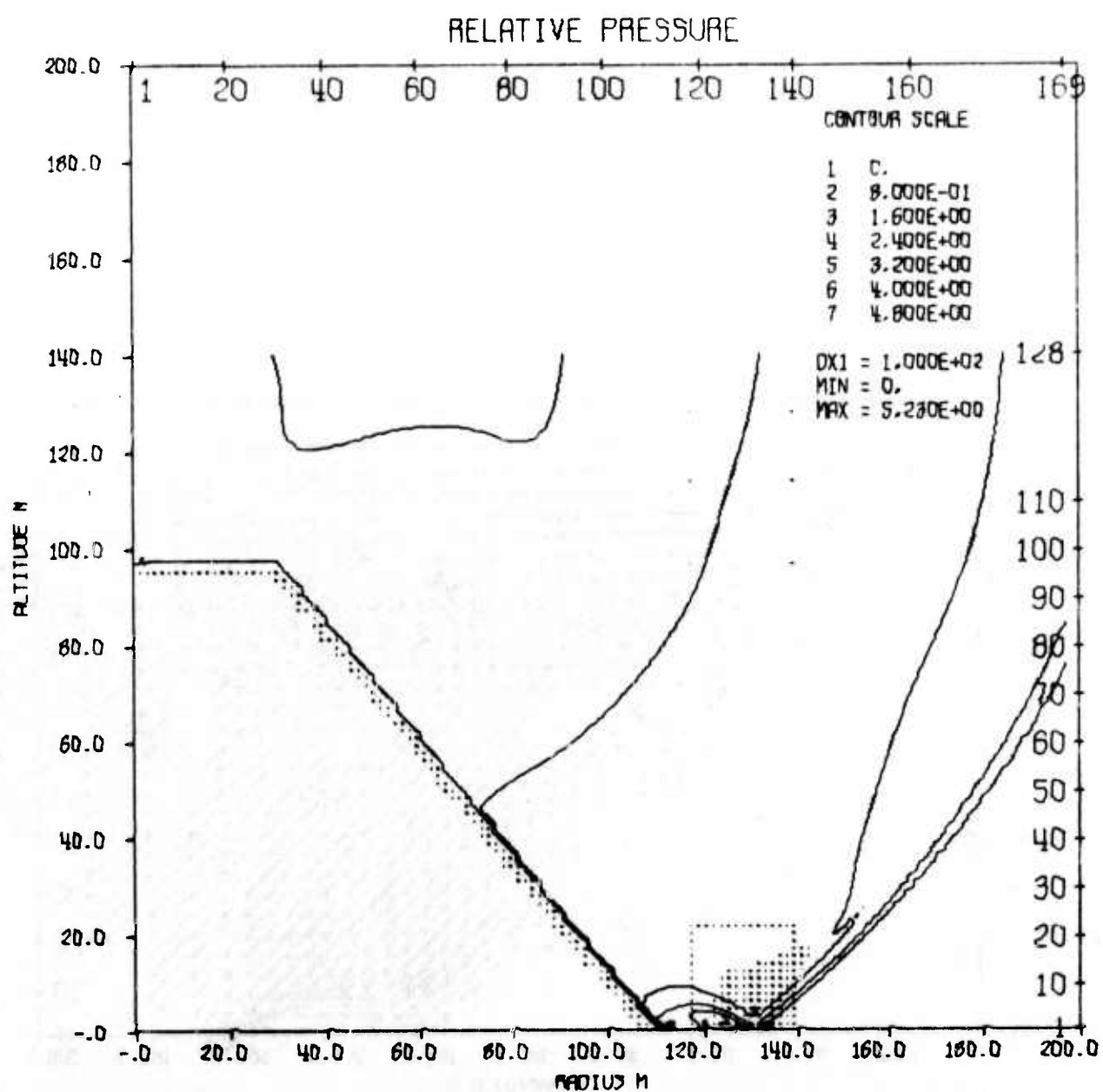
AFWL HULL CAL OF SOFT EFFECT ON DAM AT SOPS1 RANGE
TIME 500.000 MSEC CYCLE 315. PROBLEM 51.0150



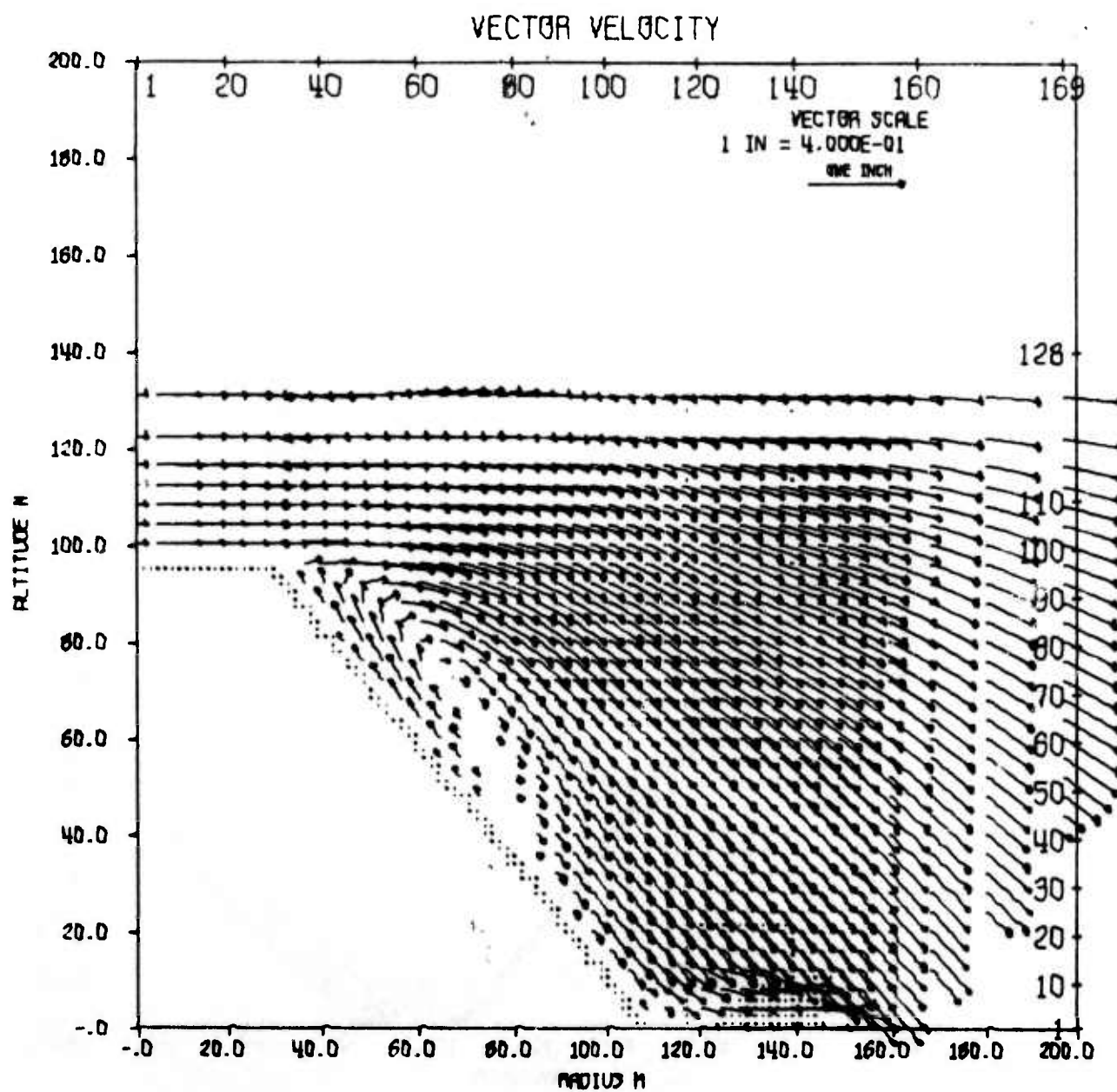
AFWL HULL CAL OF SOFT EFFECT ON DAM AT SOPS1 RANGE
TIME 500.000 MSEC CYCLE 315. PROBLEM 51.0150



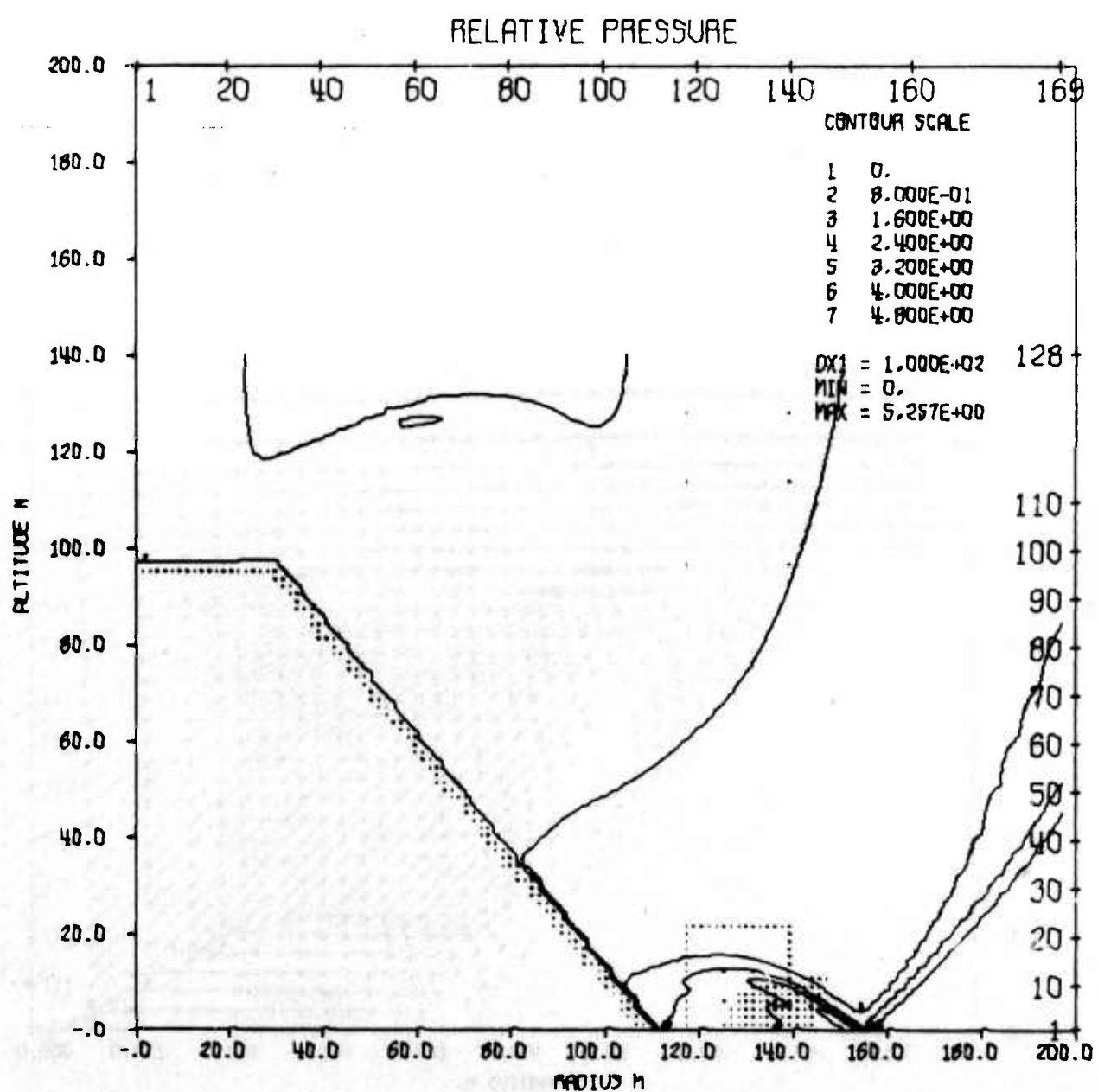
AFWL HULL CAL OF 50KT EFFECT ON DAM AT 50PSI RANGE
TIME 530.000 MSEC CYCLE 346. PROBLEM 51.0150



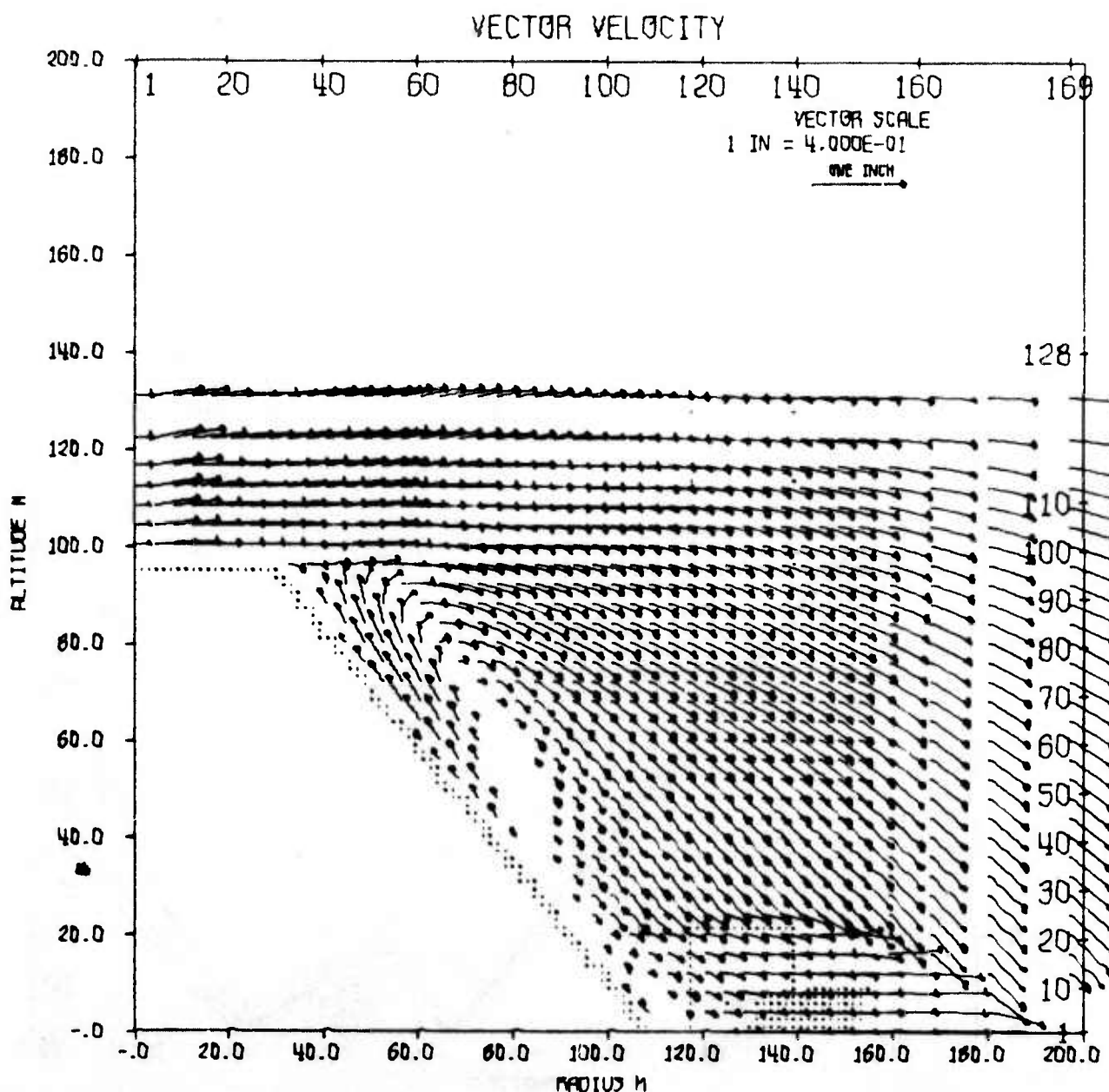
AFWL HULL CAL OF 50KT EFFECT ON DAM AT 50PSI RANGE
TIME 530.000 MSEC CYCLE 346. PROBLEM 51.0150



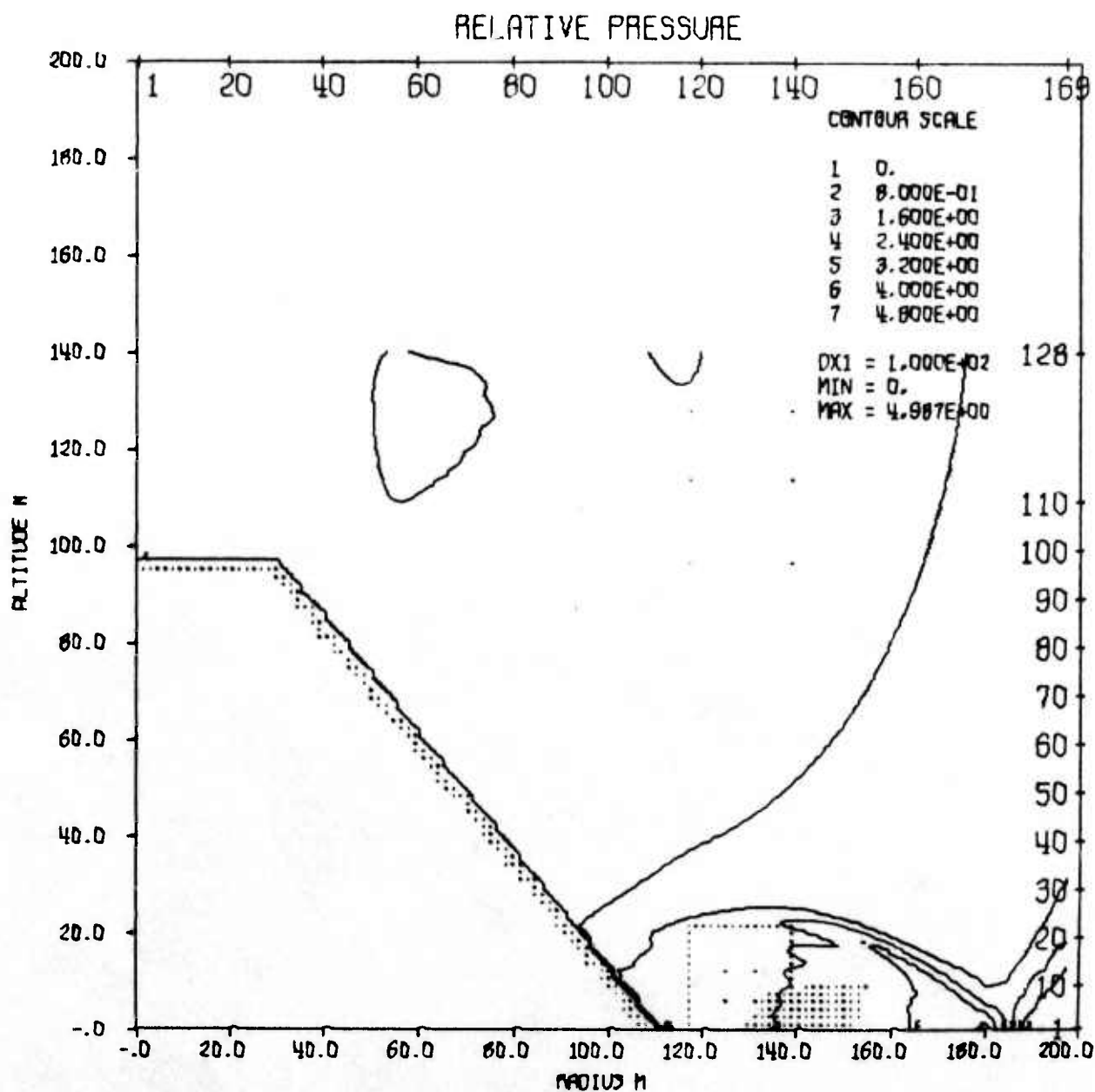
AFWL HULL CAL OF SOFT EFFECT ON DAM AT SOPS1 RANGE
TIME 560.000 MSEC CYCLE 491. PROBLEM 51.0150



AFWL HULL CAL OF SOKT EFFECT ON DAM AT SOPS1 RANGE
TIME 560.000 MSEC CYCLE 491. PROBLEM 51.0150



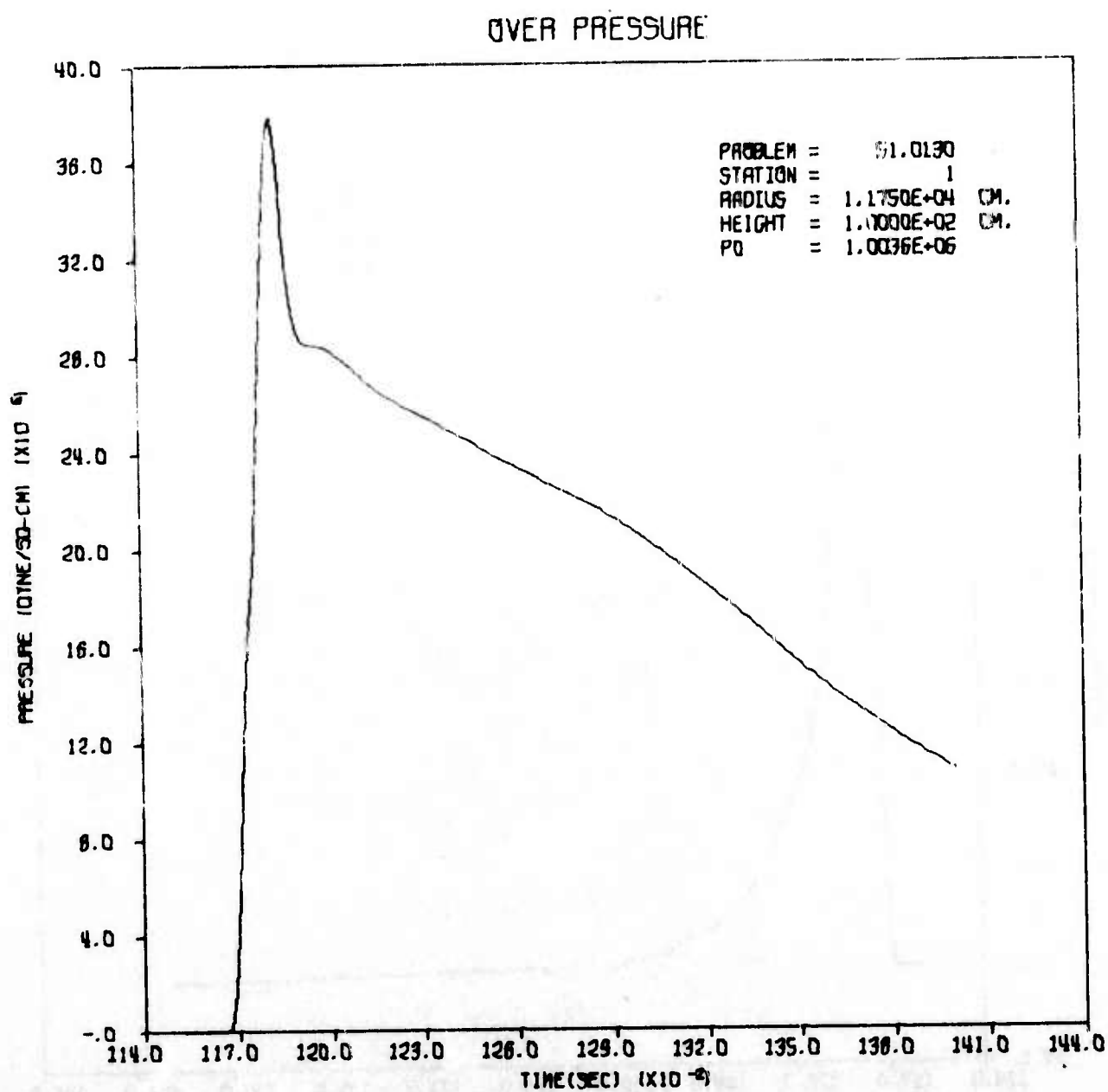
AFWL HULL CAL OF SOFT EFFECT ON DAM AT 50PSI RANGE
TIME 600.000 MSEC CYCLE 703. PROBLEM 51.0150



AFWL HULL CAL OF 50KT EFFECT ON DAM AT 50PSI RANGE
TIME 600.000 MSEC CYCLE 703. PROBLEM 51.0150

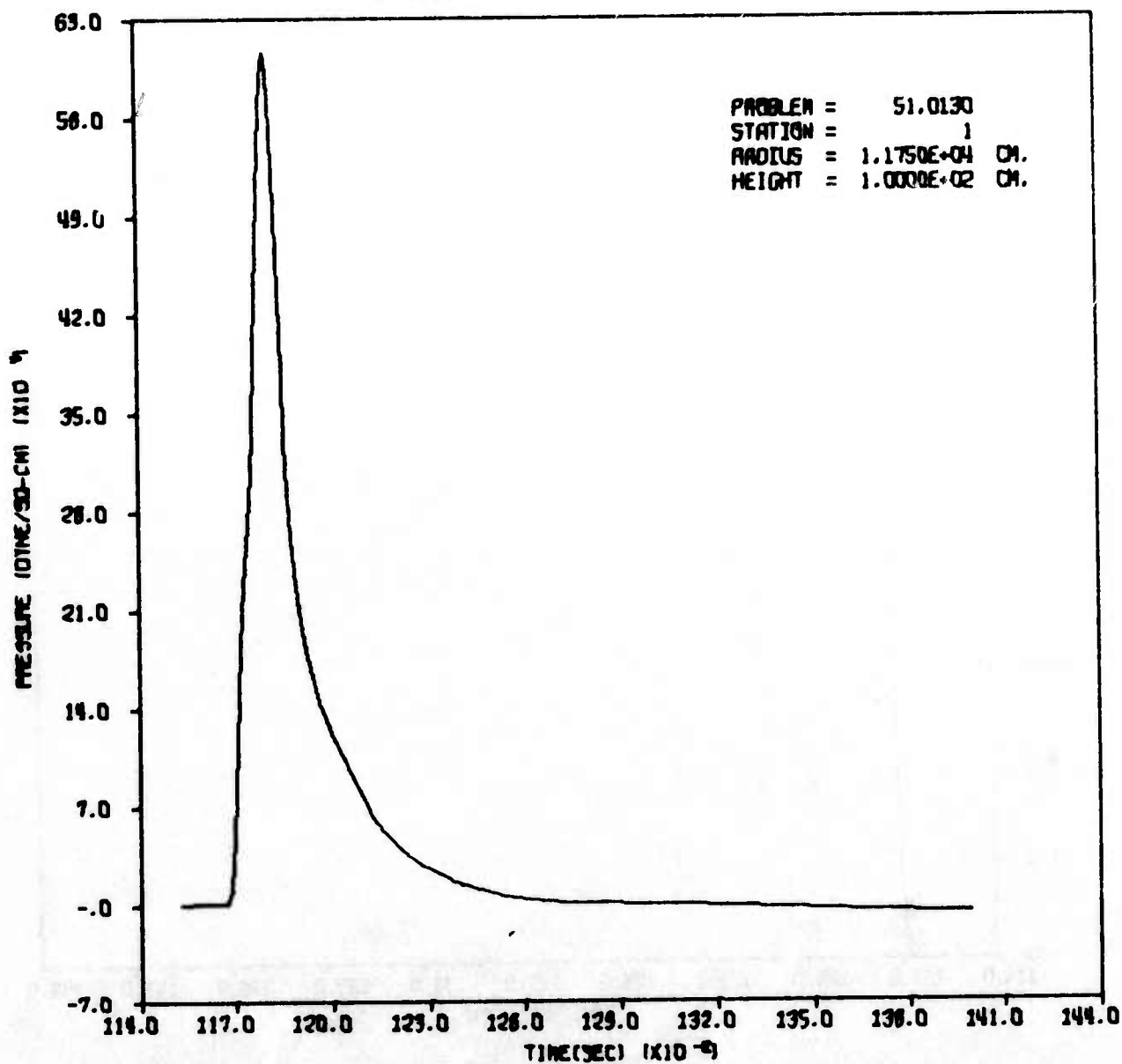
APPENDIX B
STATION PLOTS

Station plots are the calculational equivalents of experimental sensors. At the prescribed station points, all available calculated data are recorded. The plots show the value of the hydrodynamic variables with respect to time. Note that the station number with its location can be determined by referring to figure 2 or by the coordinates given in the upper right hand corner of the plot. The radius is the X coordinate and the height is the Y coordinate with respect to the lower left hand corner of the computational mesh.



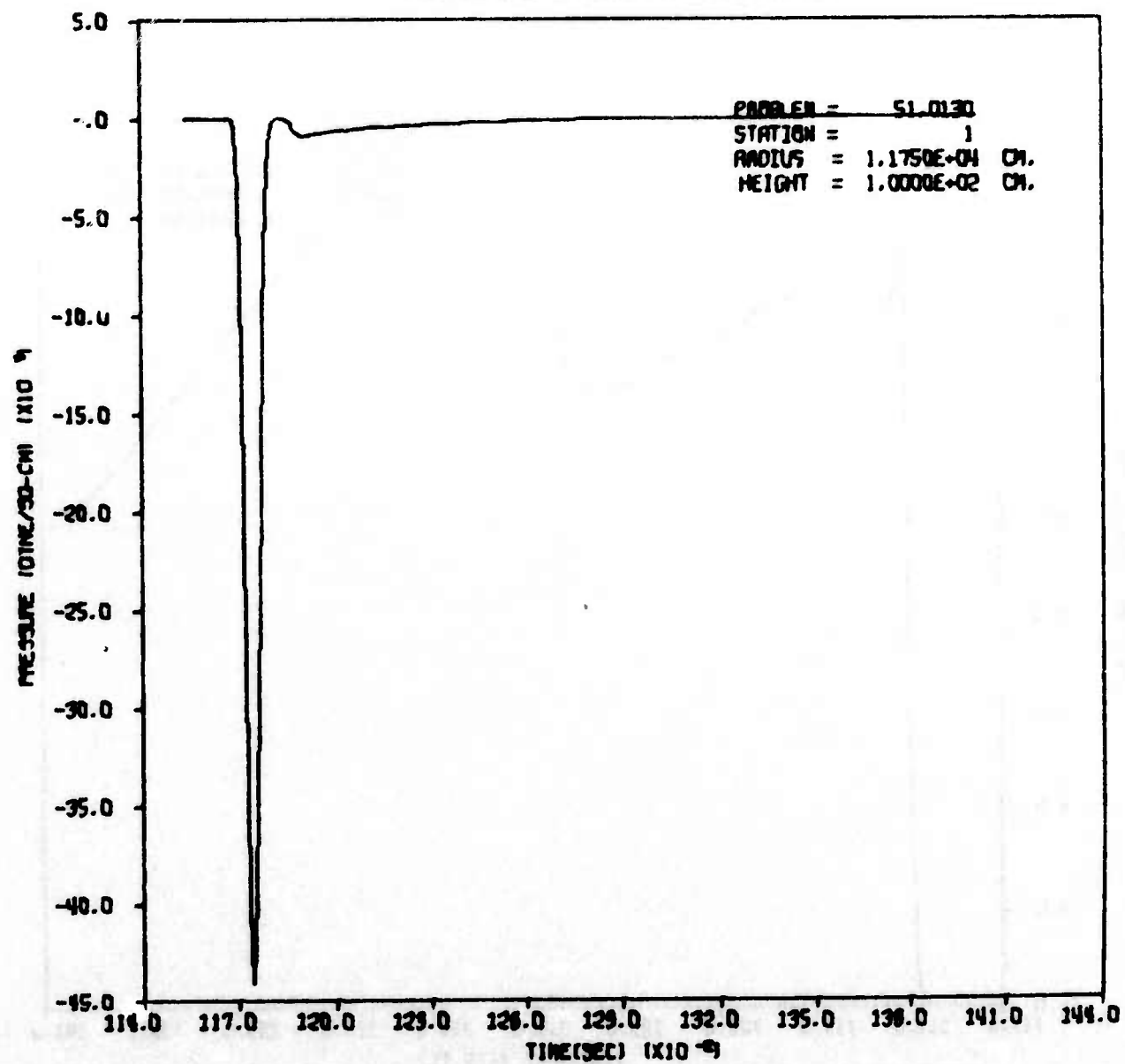
AFWL HULL CAL OF 1MT EFFECT ON DAM STRUCTURE AT 50PSI RANGE

HORIZONTAL DYNAMIC PRESSURE

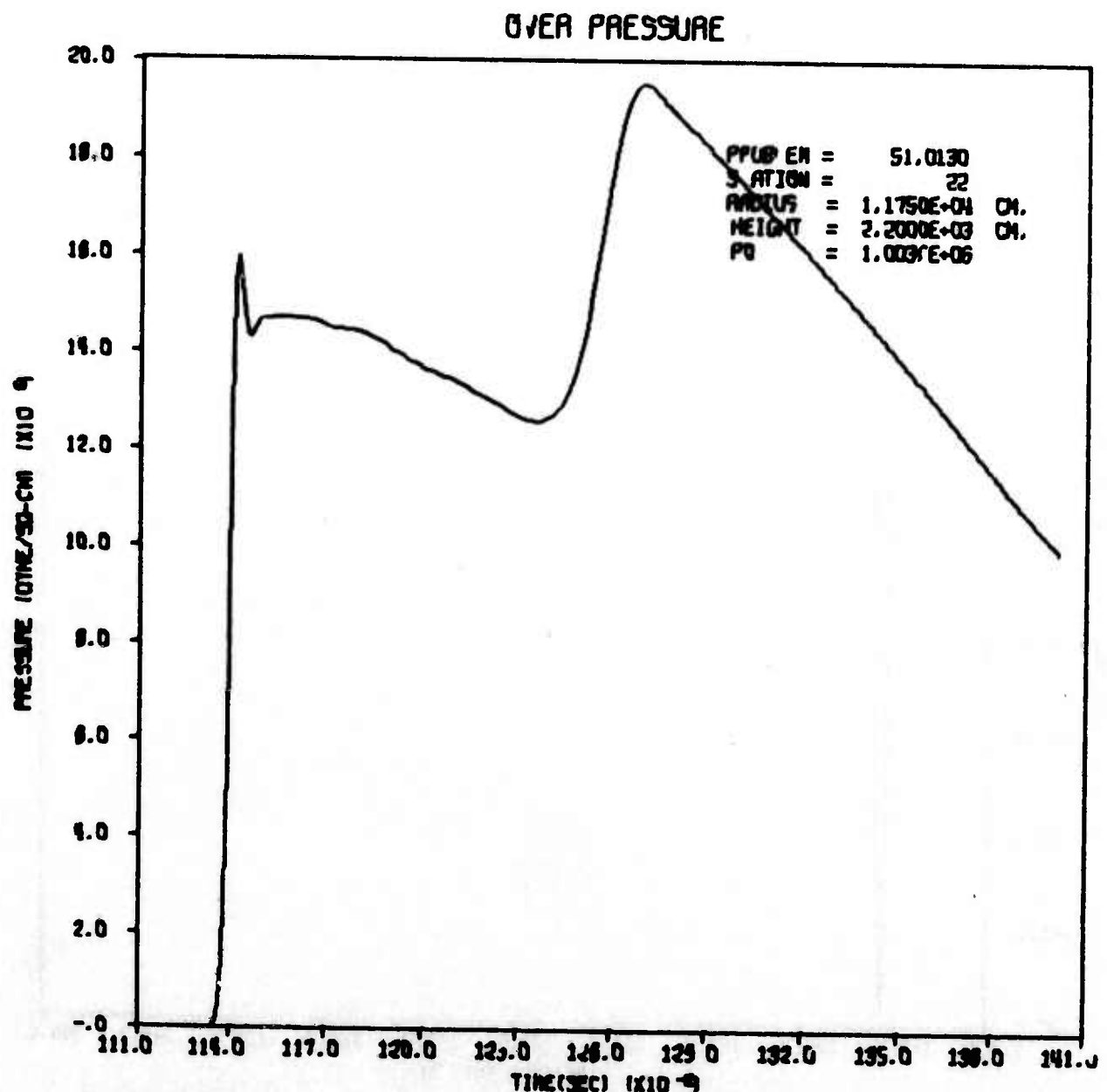


AFWL HULL CAL OF 1MT EFFECT ON DAM STRUCTURE AT 50PSI RANGE

VERTICAL DYNAMIC PRESSURE

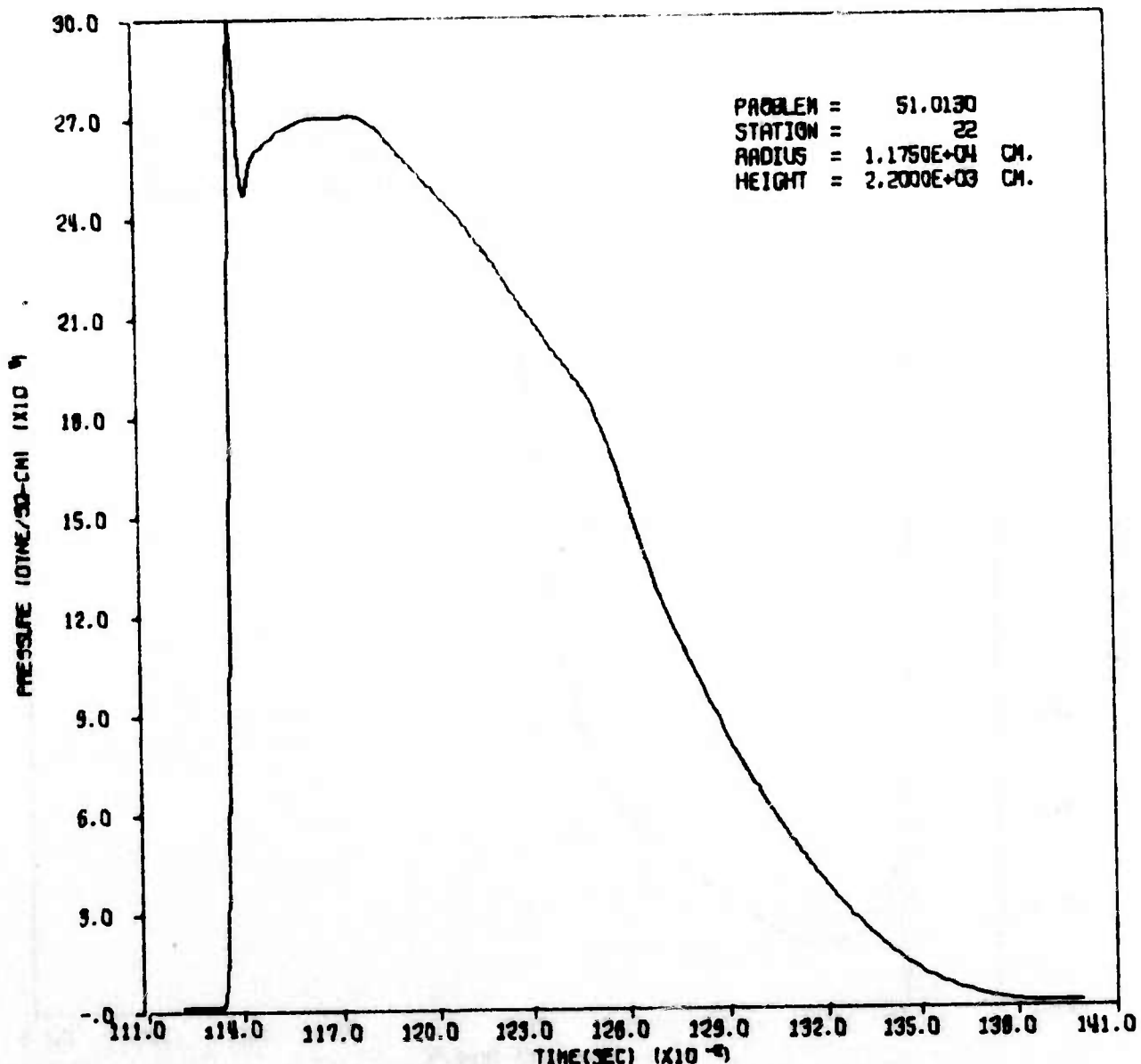


AFWL HULL CAL OF 1MT EFFECT ON DAM STRUCTURE AT 50PSI RANGE



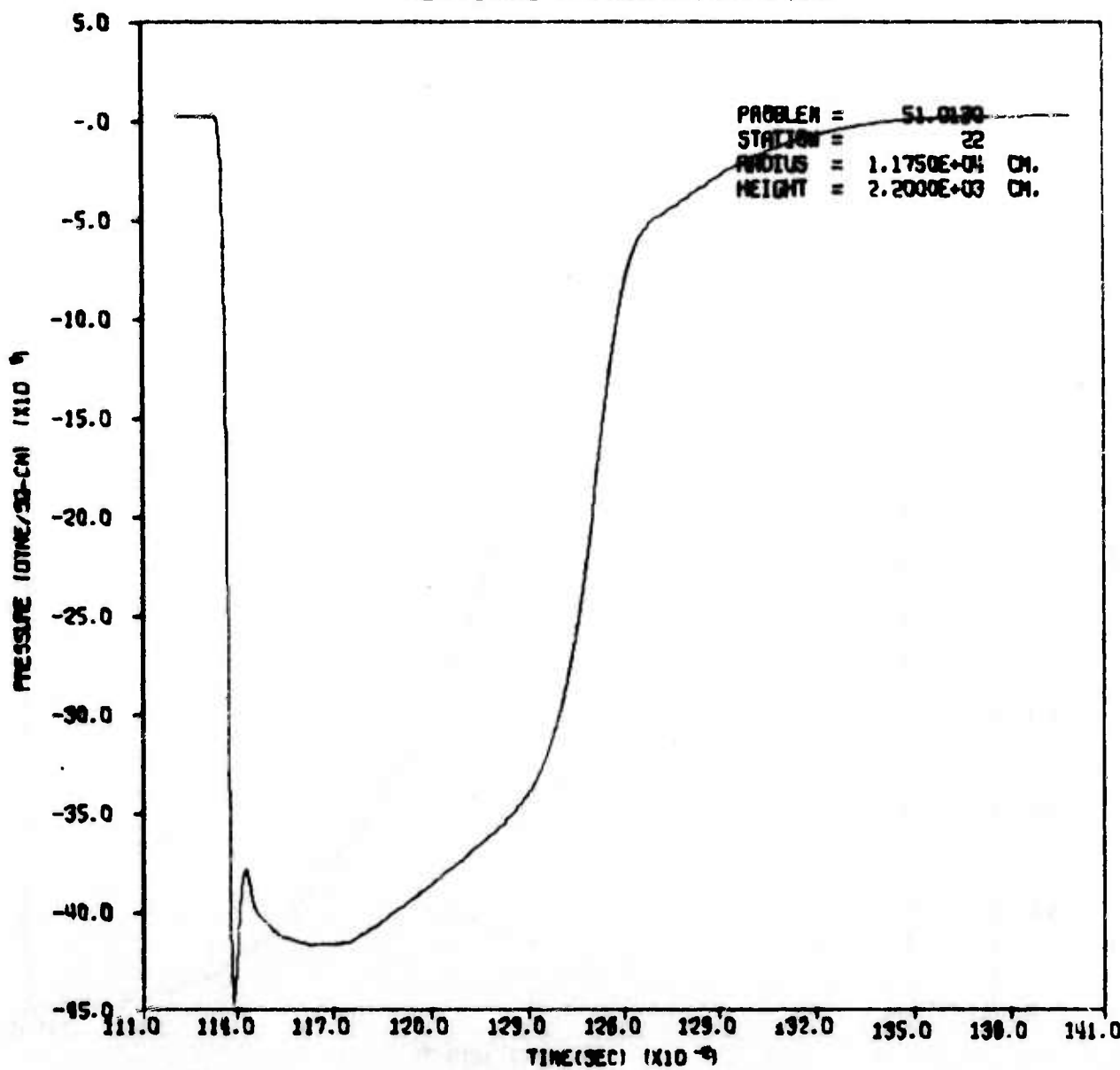
AFWL HULL CAL OF 1MT EFFECT ON DAM STRUCTURE AT 50PSI RANGE

HORIZONTAL DYNAMIC PRESSURE

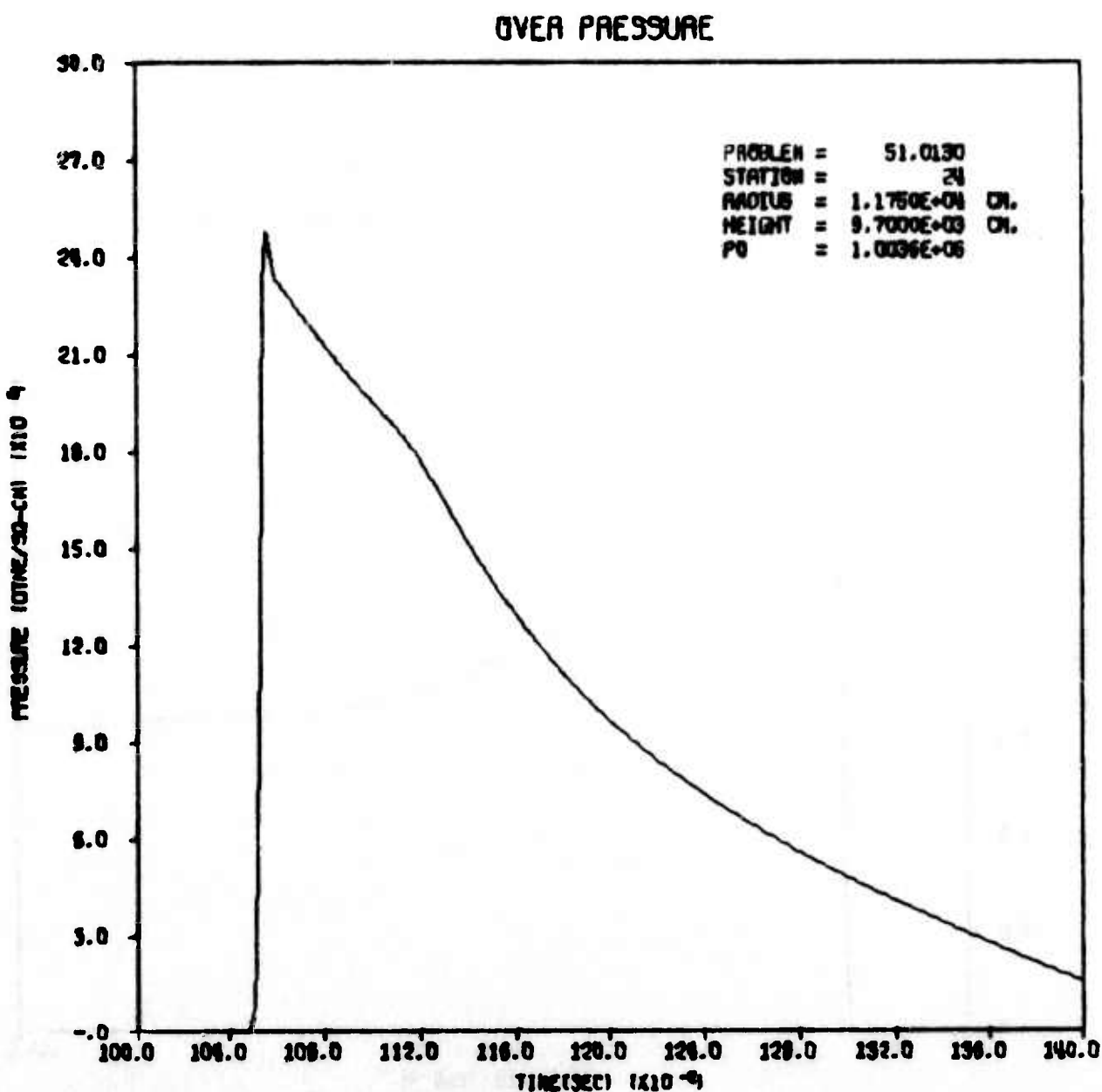


AFWL HULL CAL OF 1MT EFFECT ON DAM STRUCTURE AT 50PSI RANGE

VERTICAL DYNAMIC PRESSURE

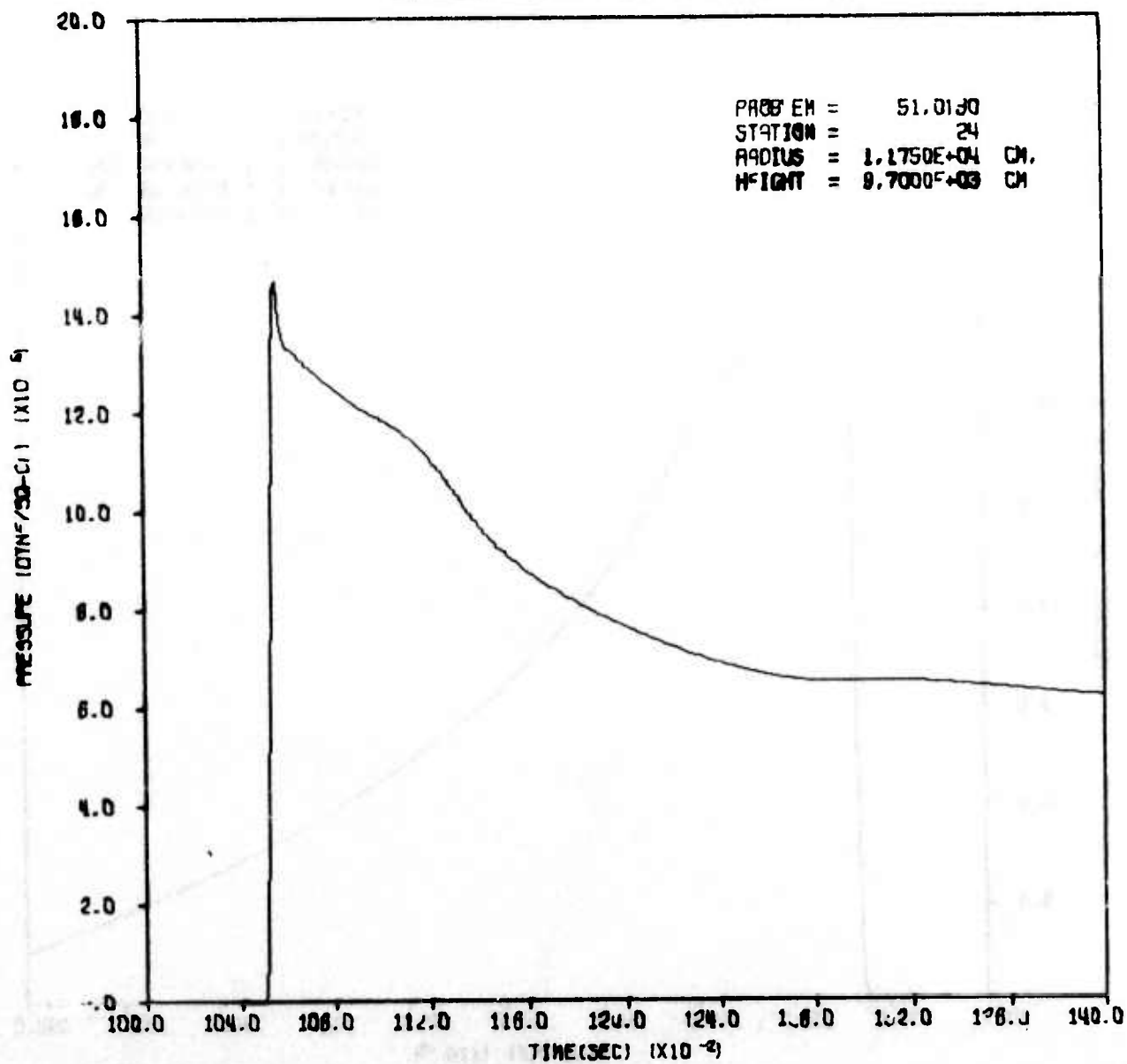


AFWL HULL CAL OF 1MT EFFECT ON DAM STRUCTURE AT 50PSI RANGE



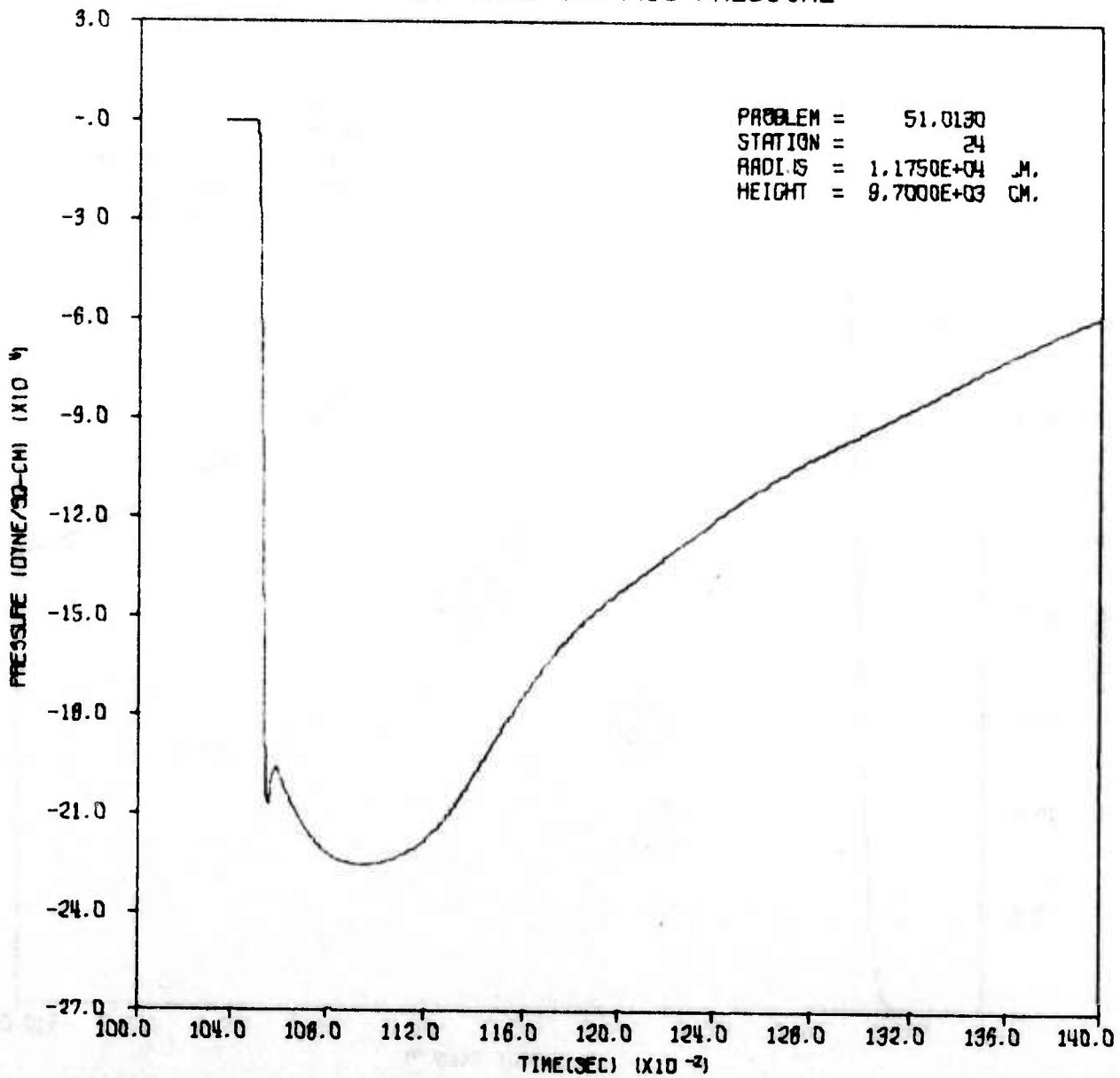
AFWL HULL CAL OF INT EFFECT ON DAM STRUCTURE AT 50PSI RANGE

HORIZONTAL DYNAMIC PRESSURE

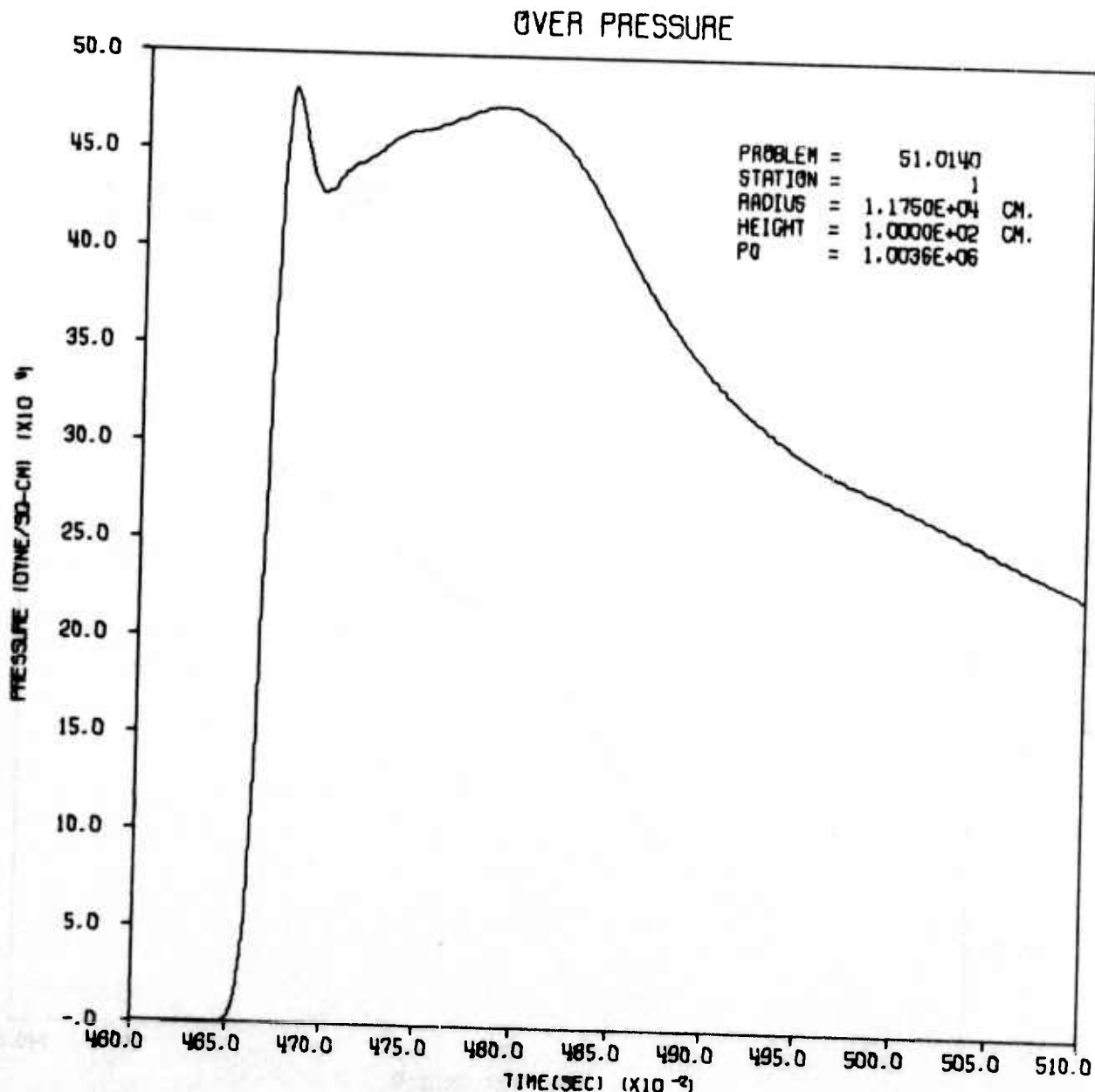


AFWL HULL CAL OF 1MT EFFECT ON DAM STRUCTURE AT 50PSI RANGE

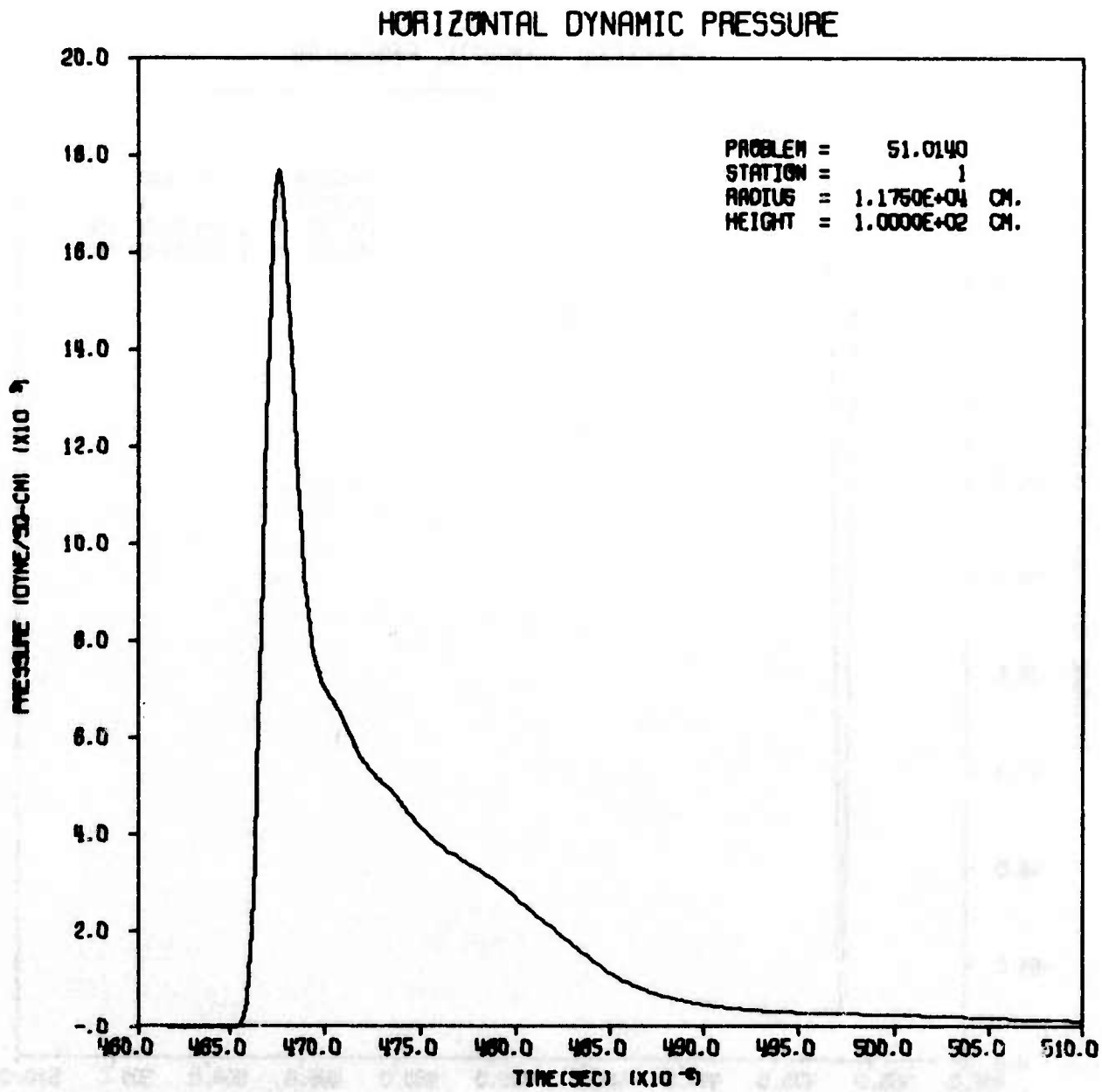
VERTICAL DYNAMIC PRESSURE



AFWL HULL CAL OF 1MT EFFECT ON DAM STRUCTURE AT 50PSI RANGE

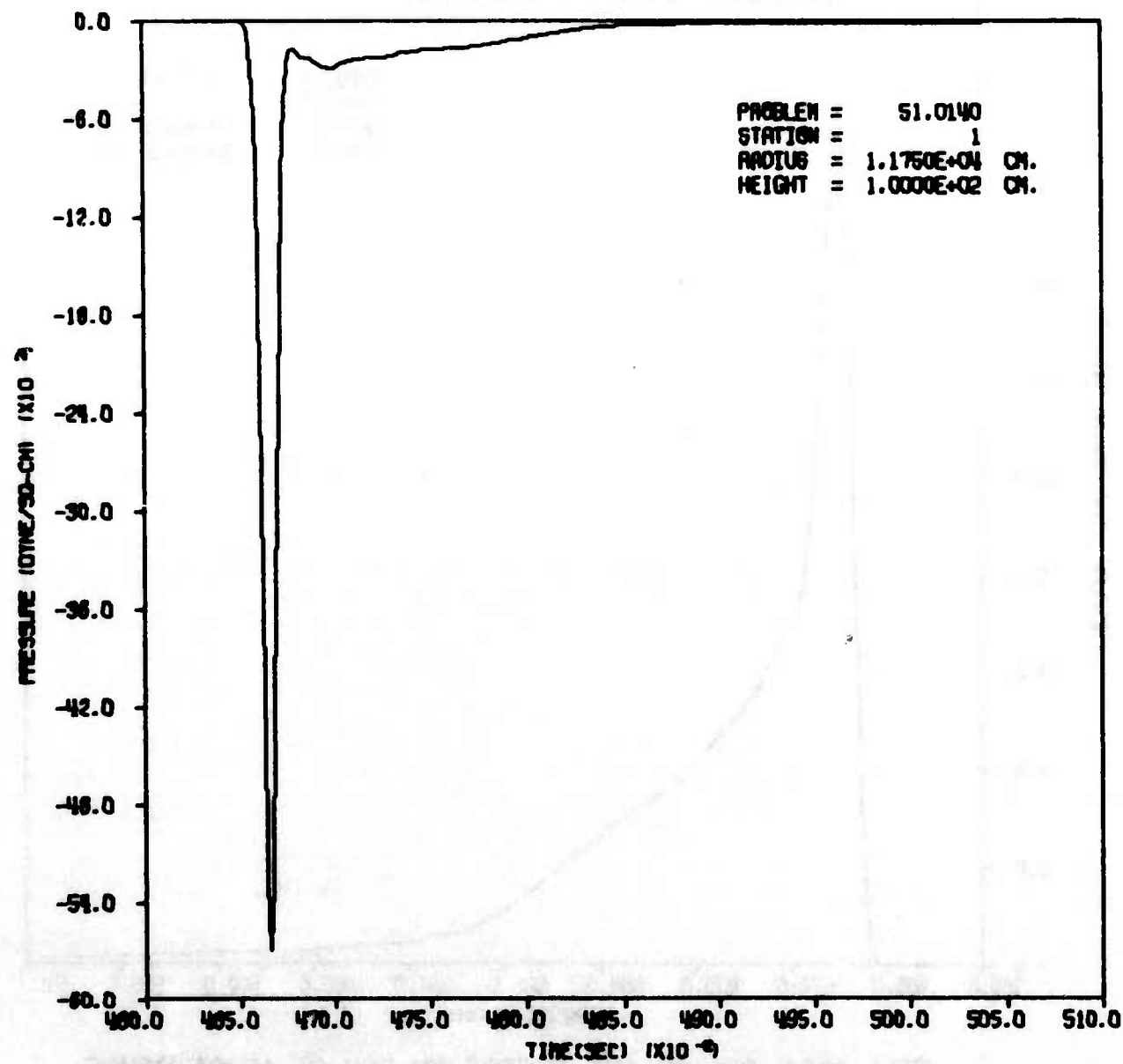


AFWL HULL CAL OF 1MT EFFECT ON DAM AT 10PSI RANGE

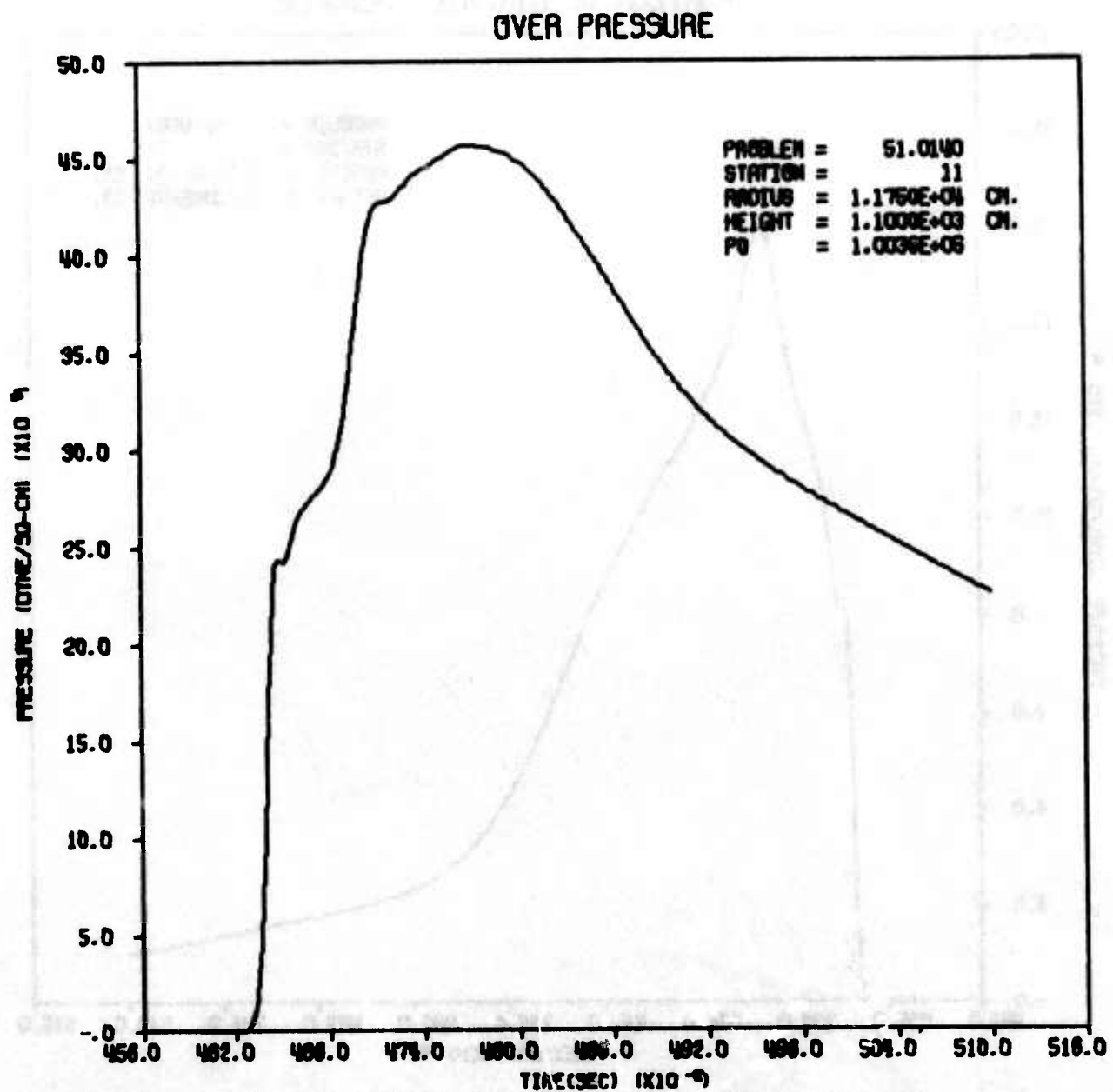


AFWL HULL CAL OF 1MT EFFECT ON DAM AT 10PSI RANGE

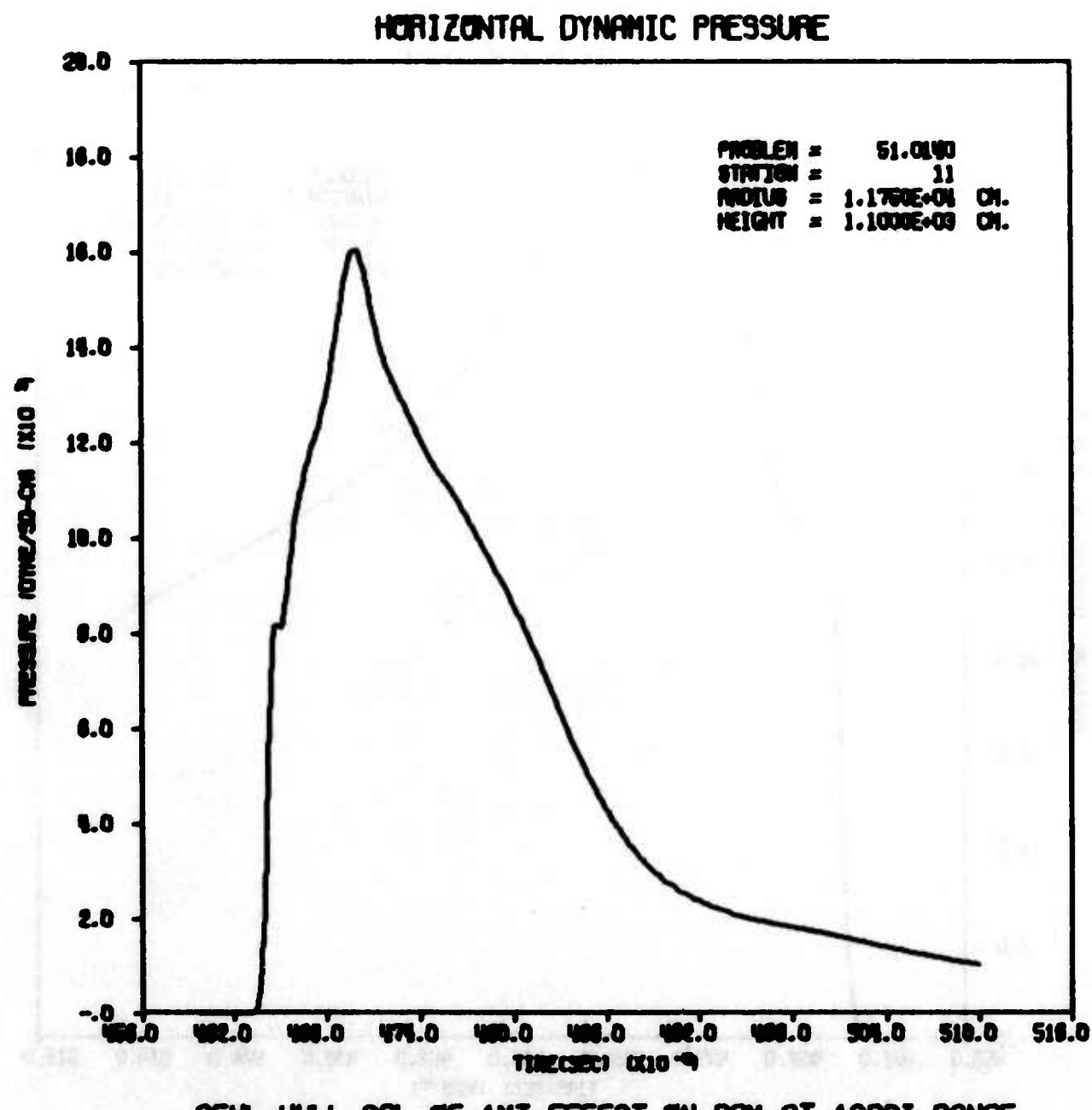
VERTICAL DYNAMIC PRESSURE

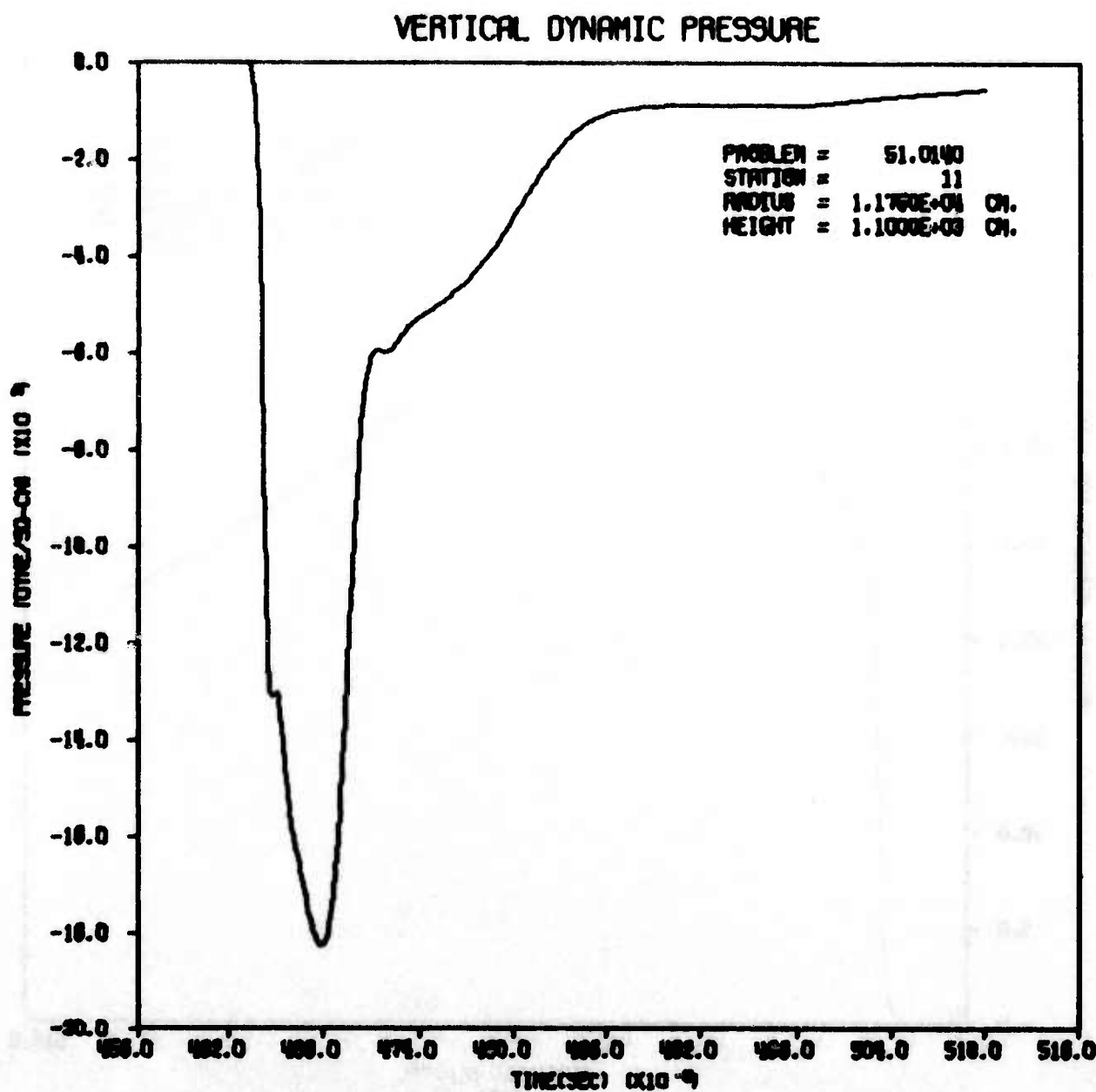


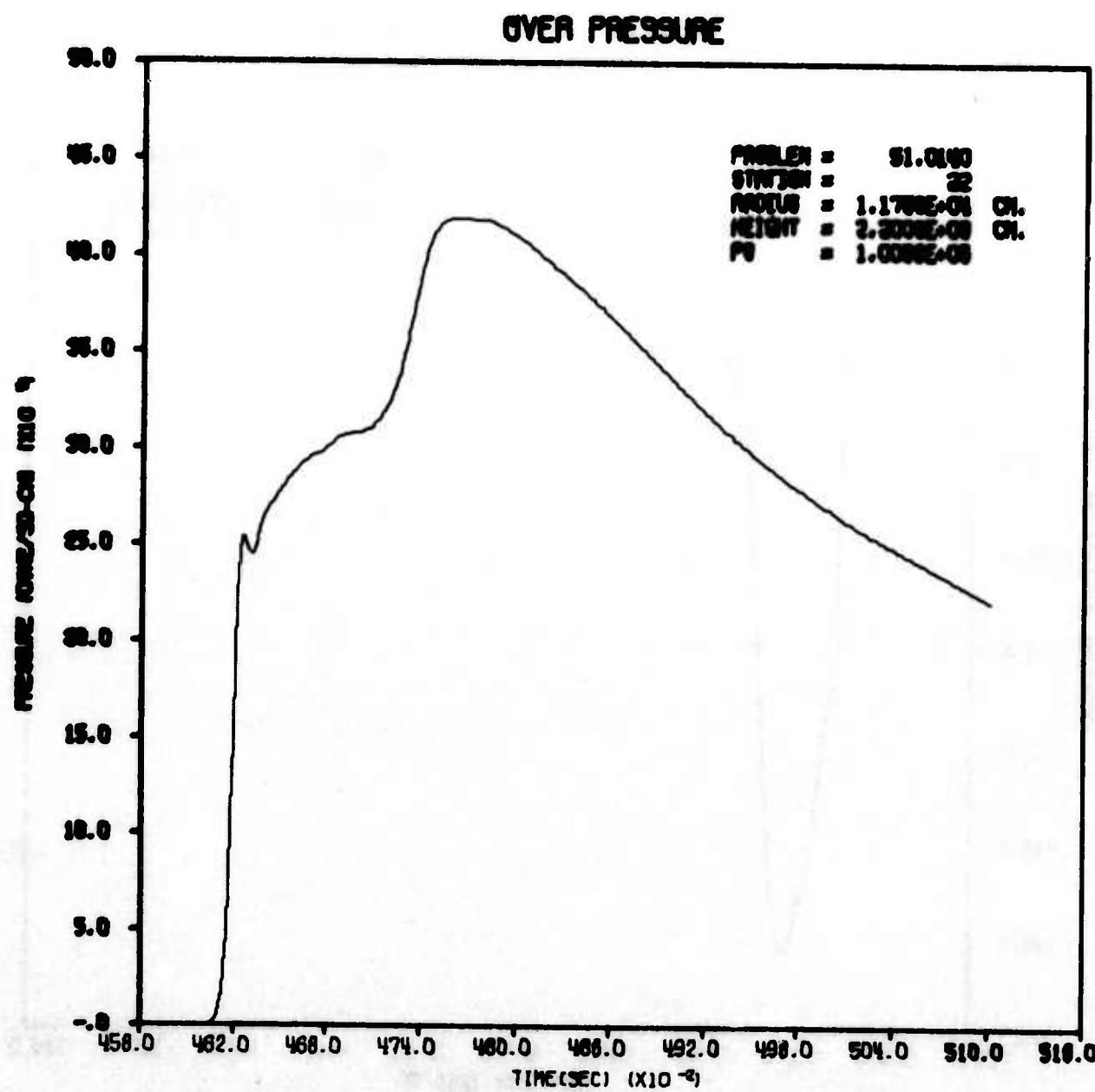
AFWL HULL CAL OF 1MT EFFECT ON DAM AT 10PSI RANGE



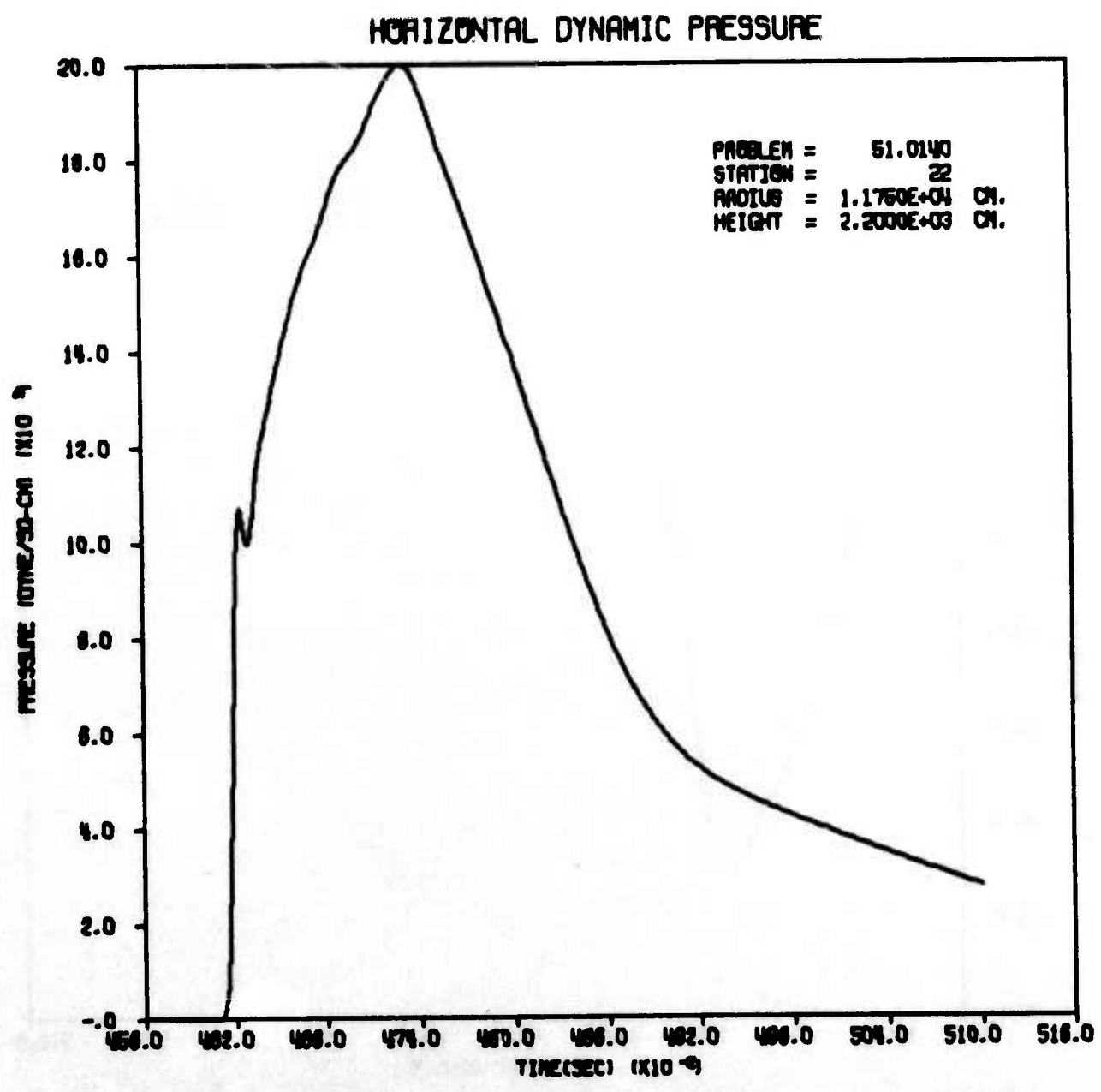
AFWL HULL CAL OF IMT EFFECT ON DAM AT 10PSI RANGE





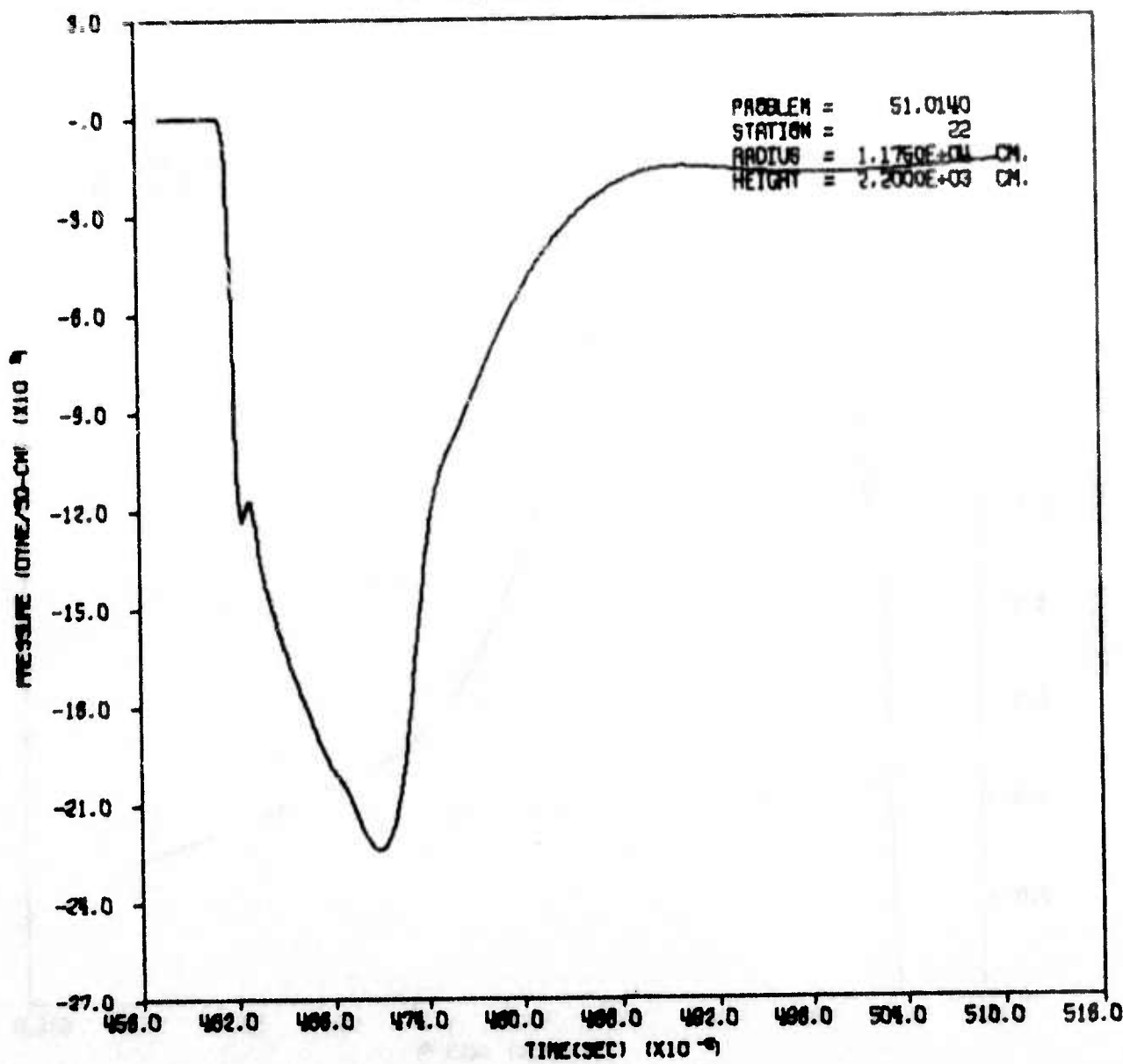


AFWL HULL CAL OF 1MT EFFECT ON DAM AT 10PSI RANGE

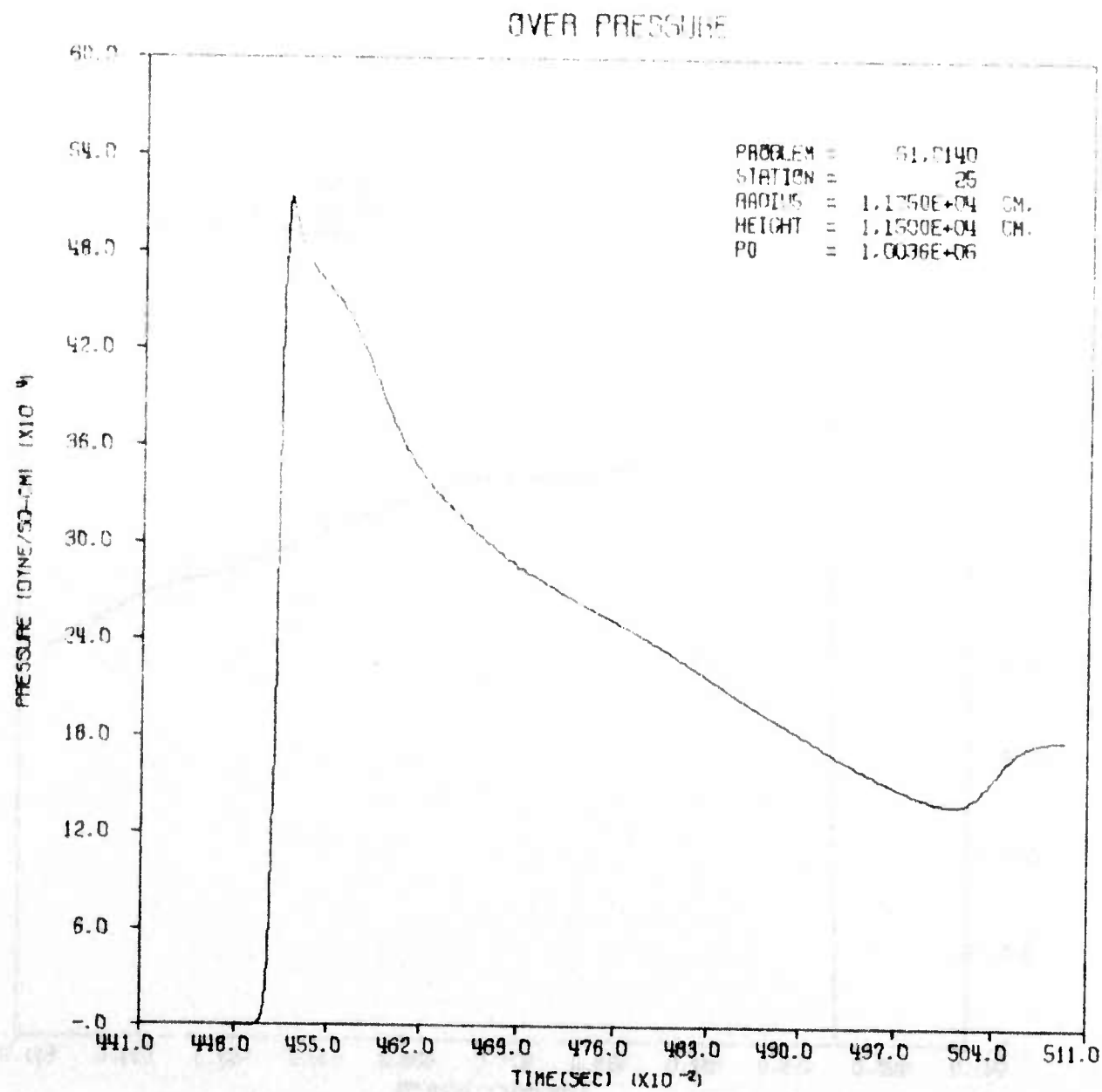


AFWL HULL CAL OF 1MT EFFECT ON DAM AT 10PSI RANGE

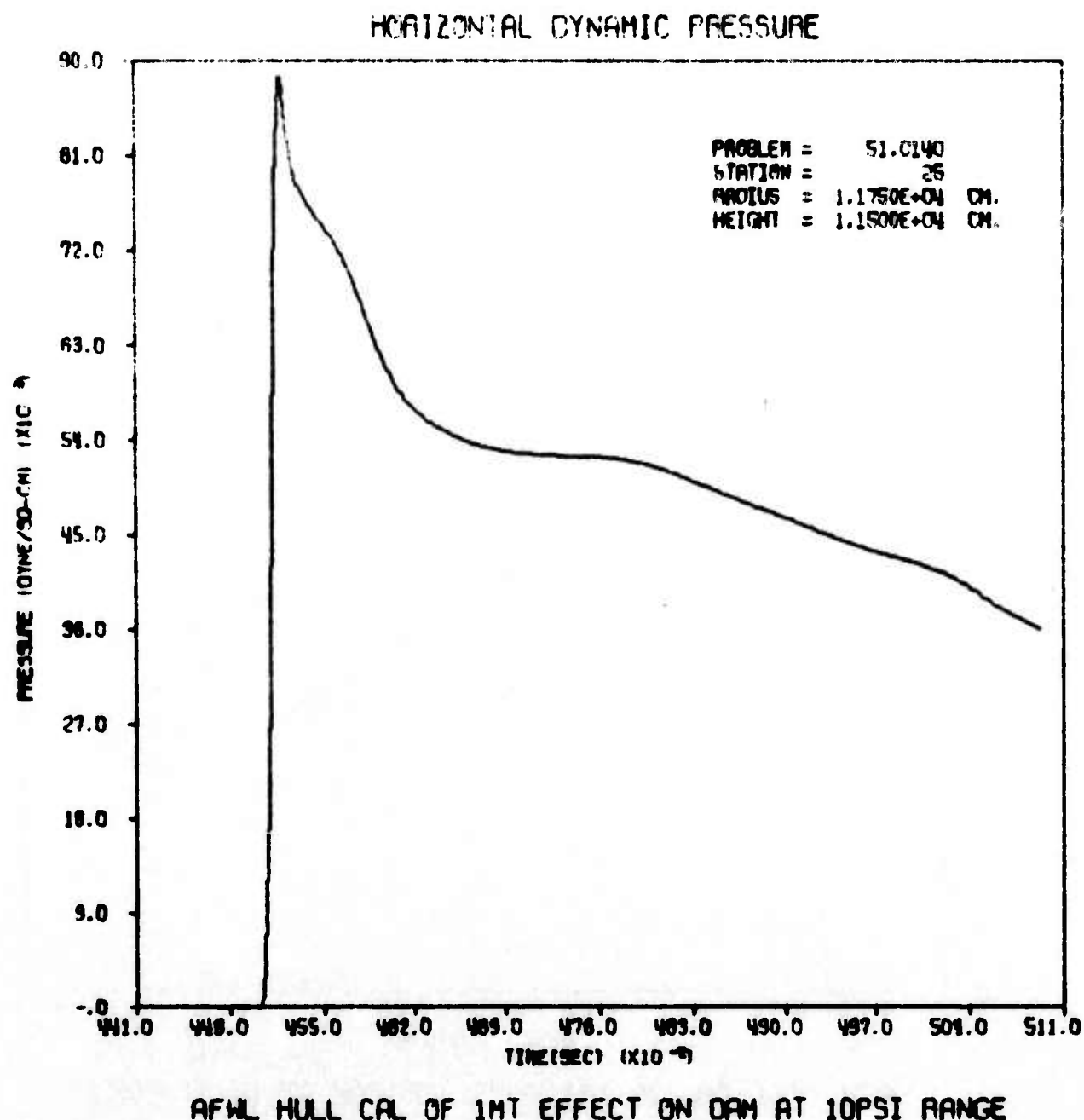
VERTICAL DYNAMIC PRESSURE

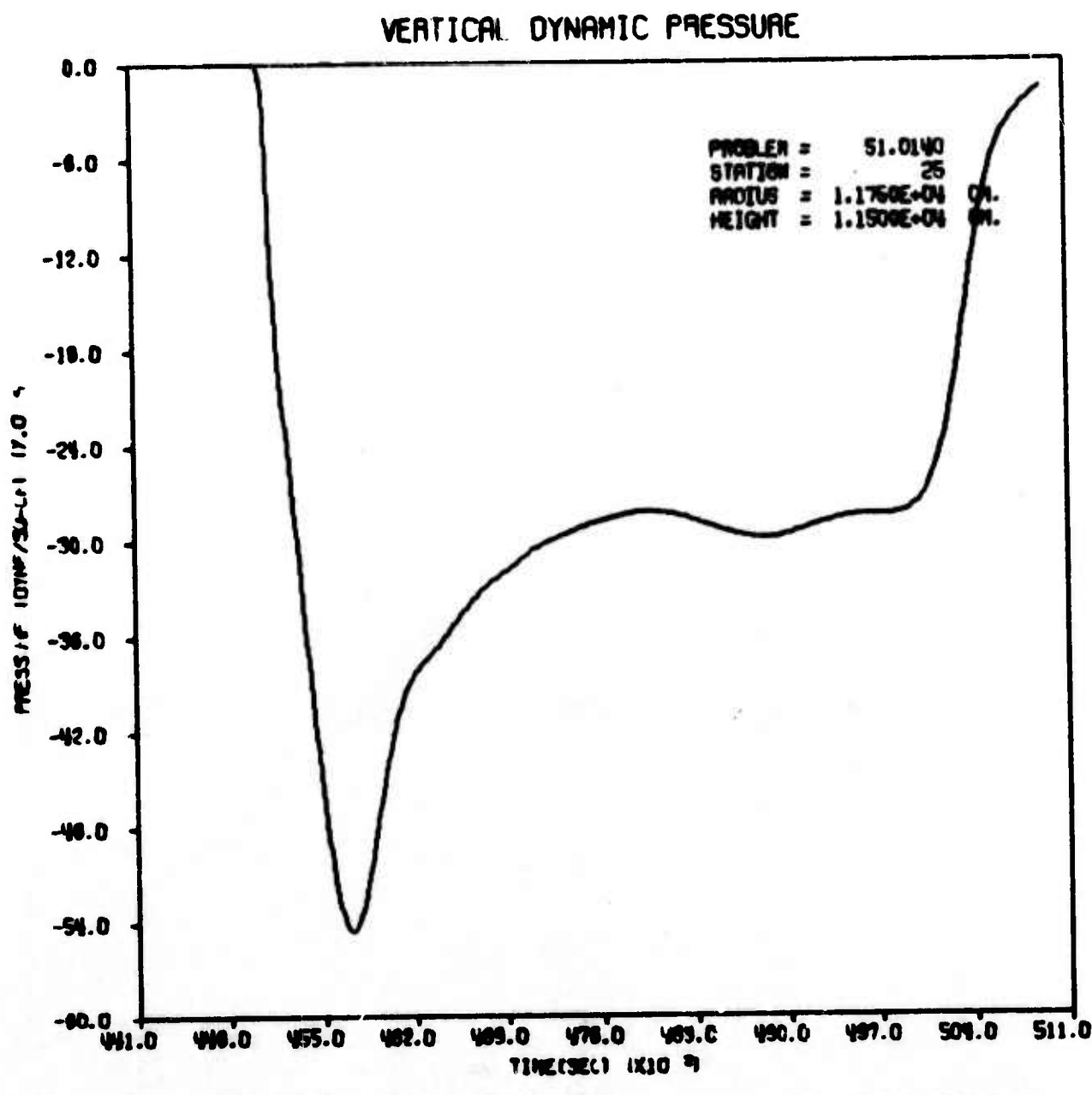


AFWL HULL CAL OF 1MT EFFECT ON DAM AT 10PSI RANGE



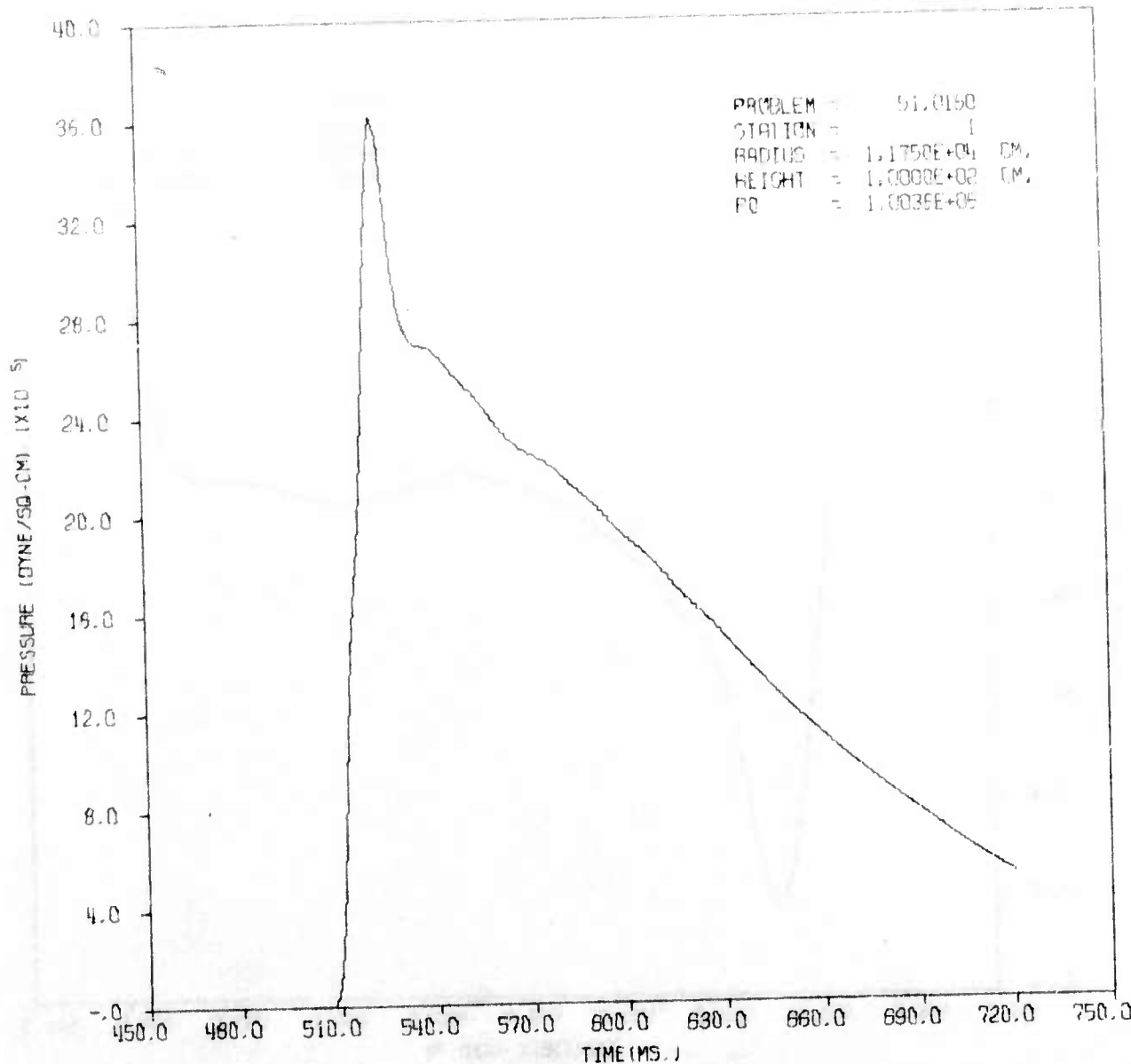
AFWL HULL CAL OF 1MT EFFECT ON DAM AT 10PSI RANGE



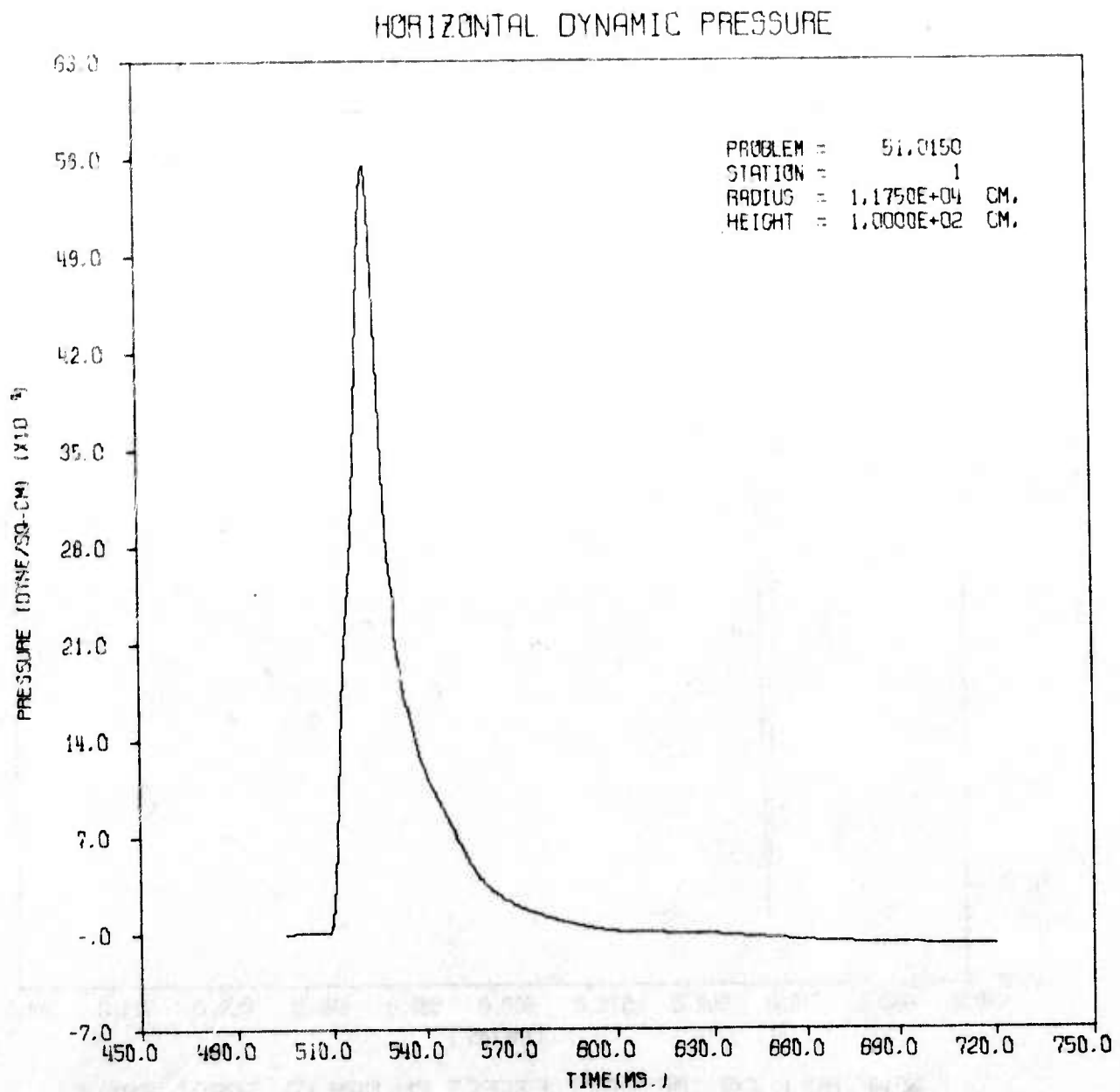


AFWL HULL CAL OF 1MT EFFECT ON DAM AT 10PSI RANGE

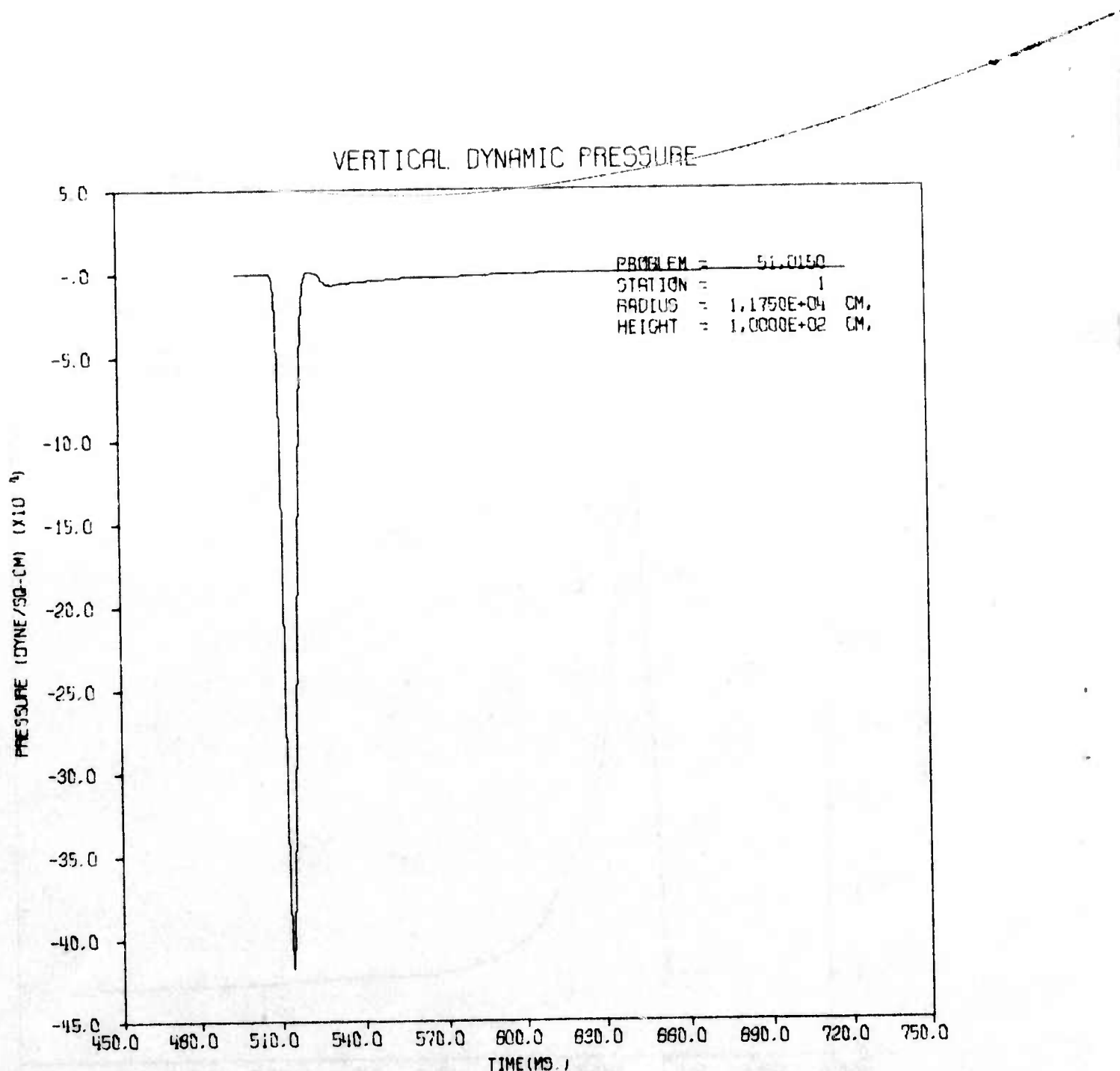
OVER PRESSURE



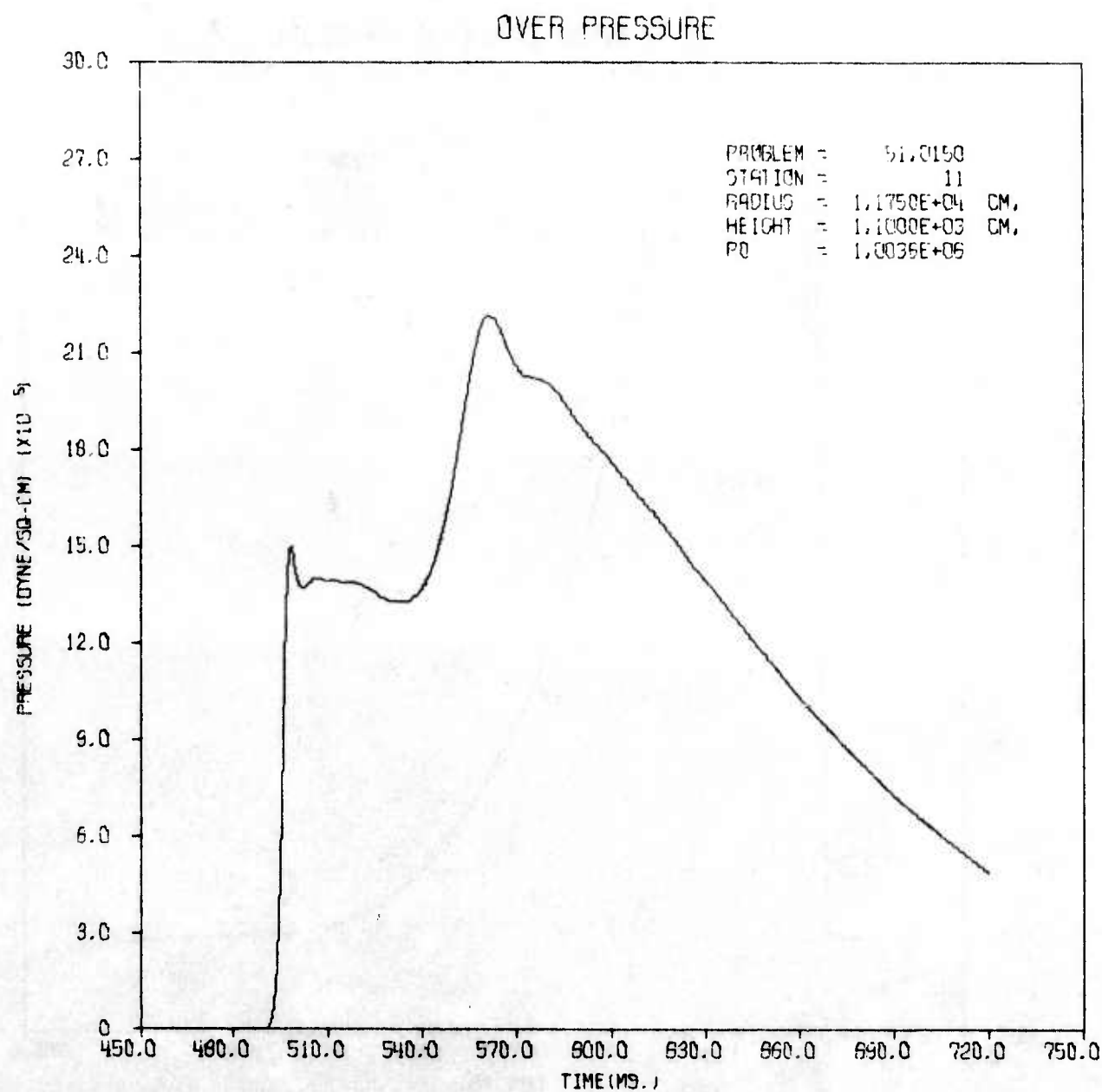
AFWL HULL CAL OF 50KT EFFECT ON DAM AT 50PSI RANGE



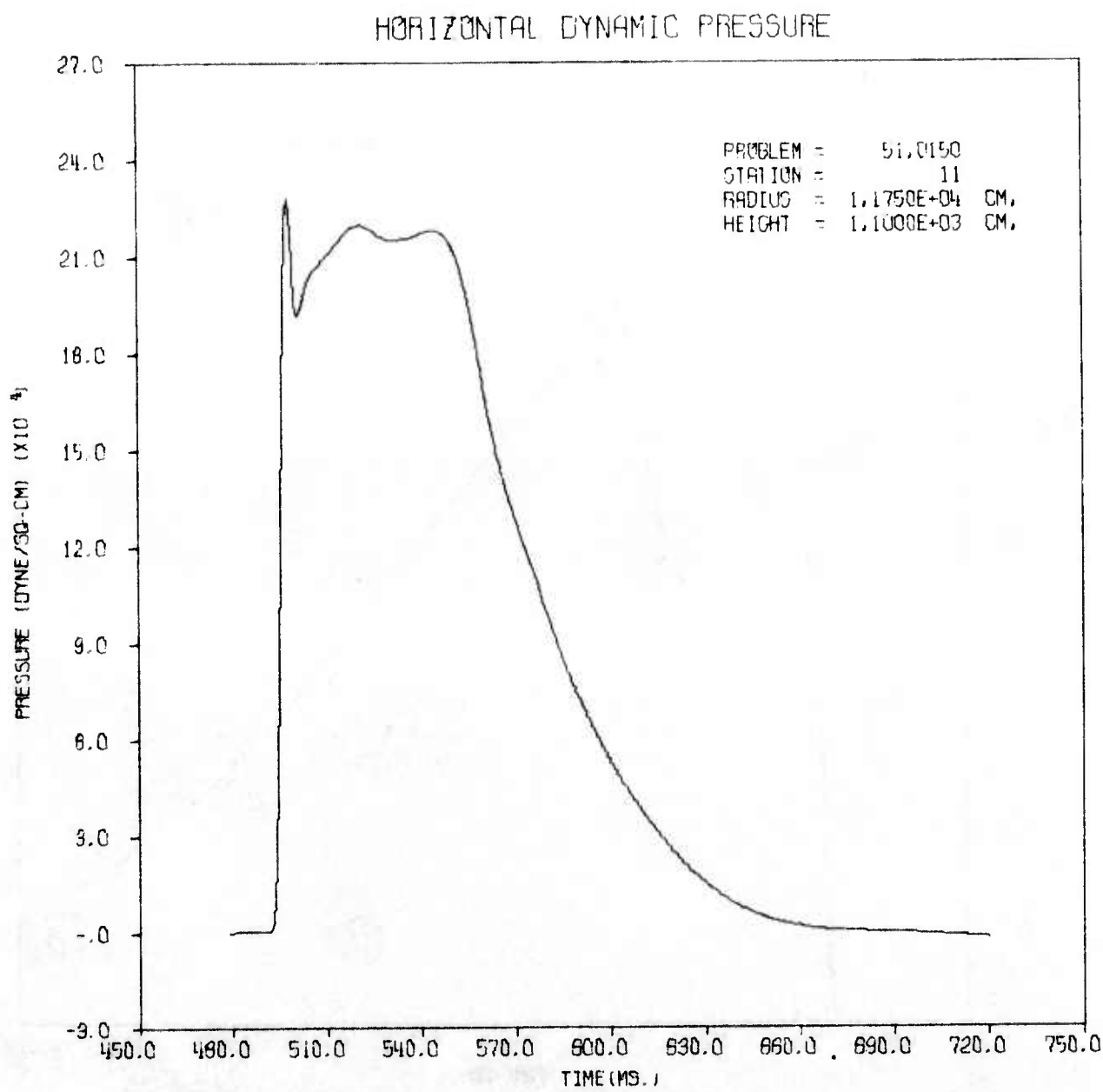
AFWL HULL CAL OF 50KT EFFECT ON DAM AT 50PSI RANGE



AFWL HULL CAL OF 50KT EFFECT ON DAM AT 50PSI RANGE

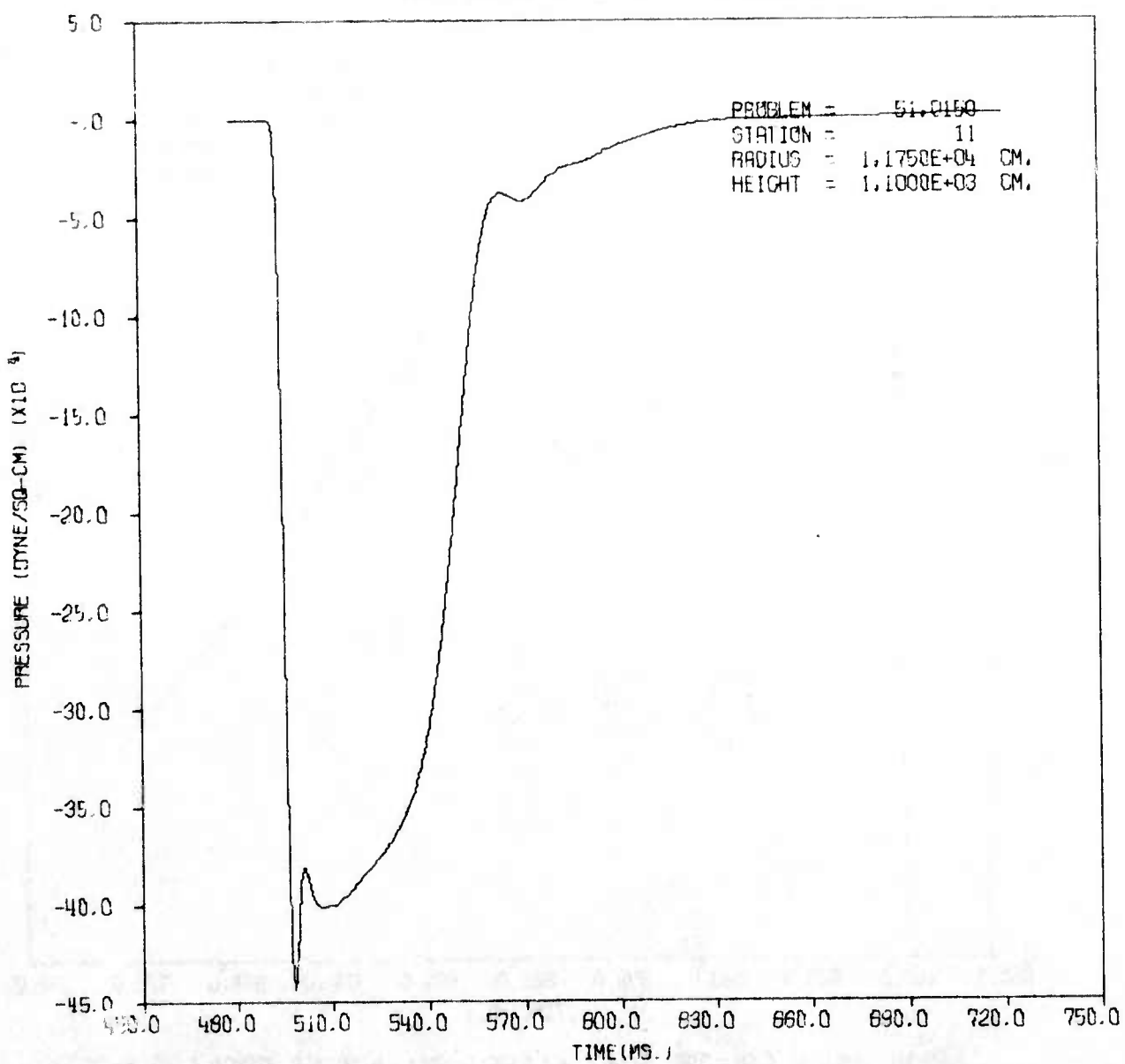


AFWL HULL CAL OF 50KT EFFECT ON DAM AT 50PSI RANGE

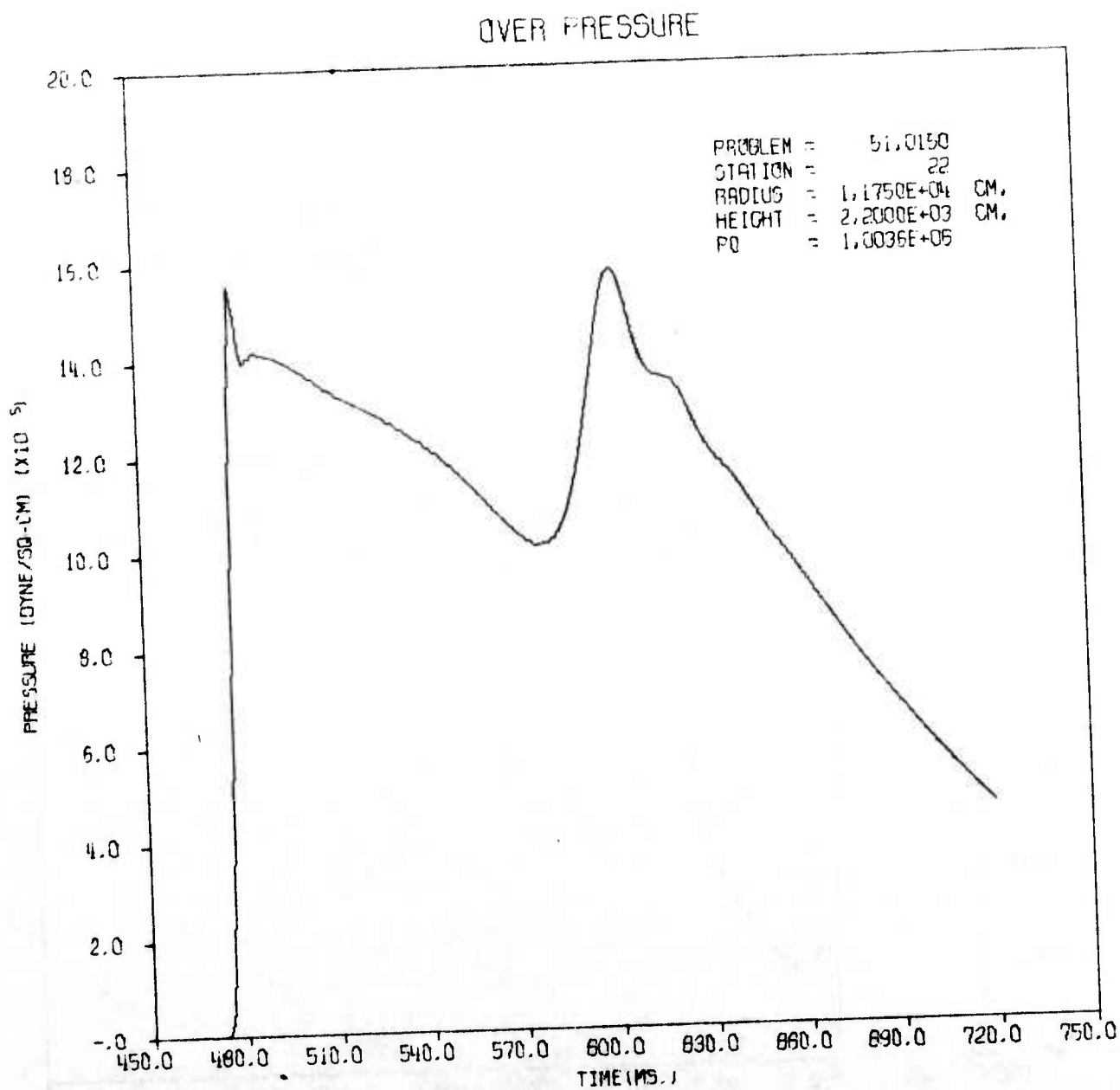


AFWL HULL CAL OF 50KT EFFECT ON DAM AT 50PSI RANGE

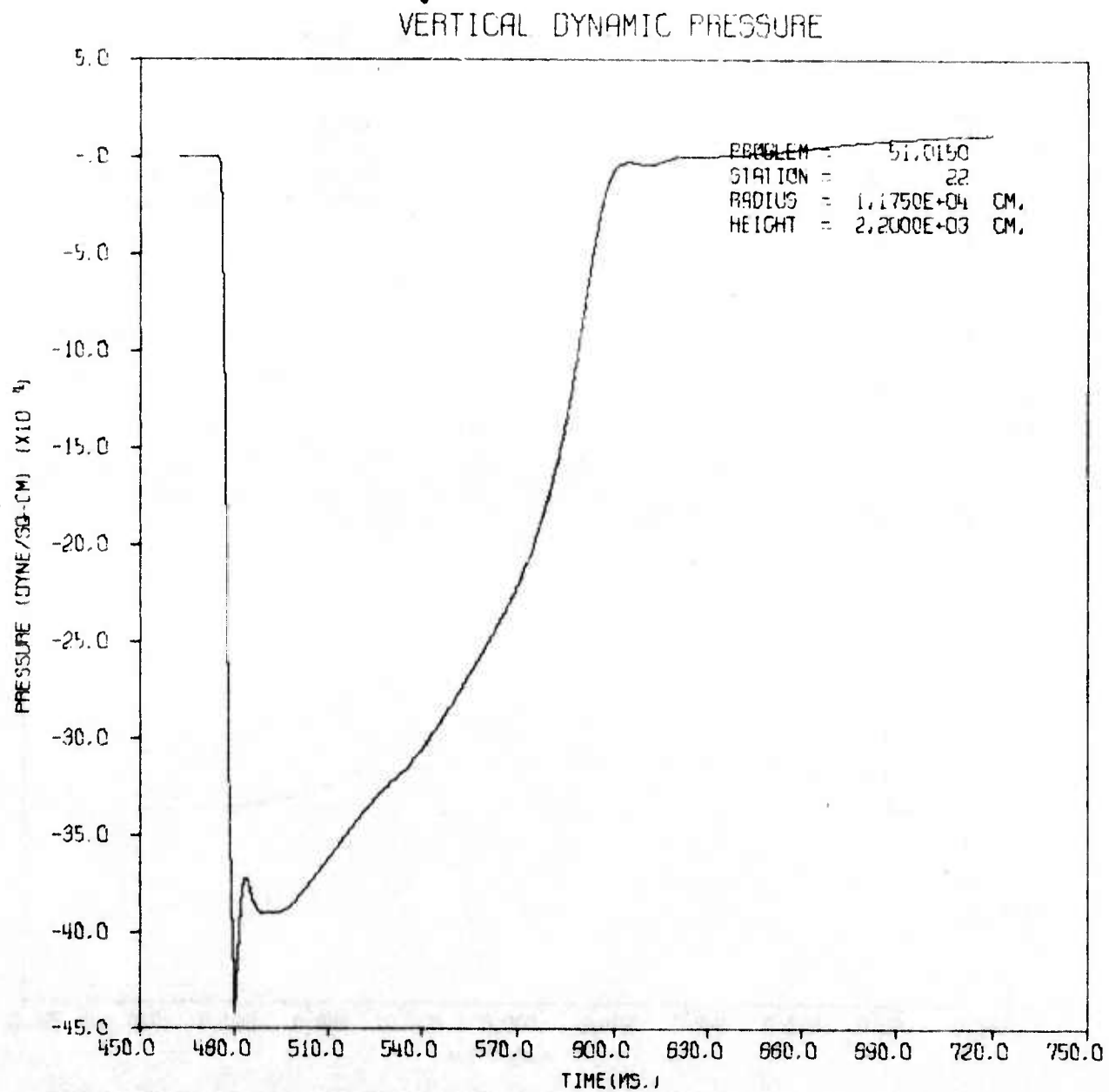
VERTICAL DYNAMIC PRESSURE



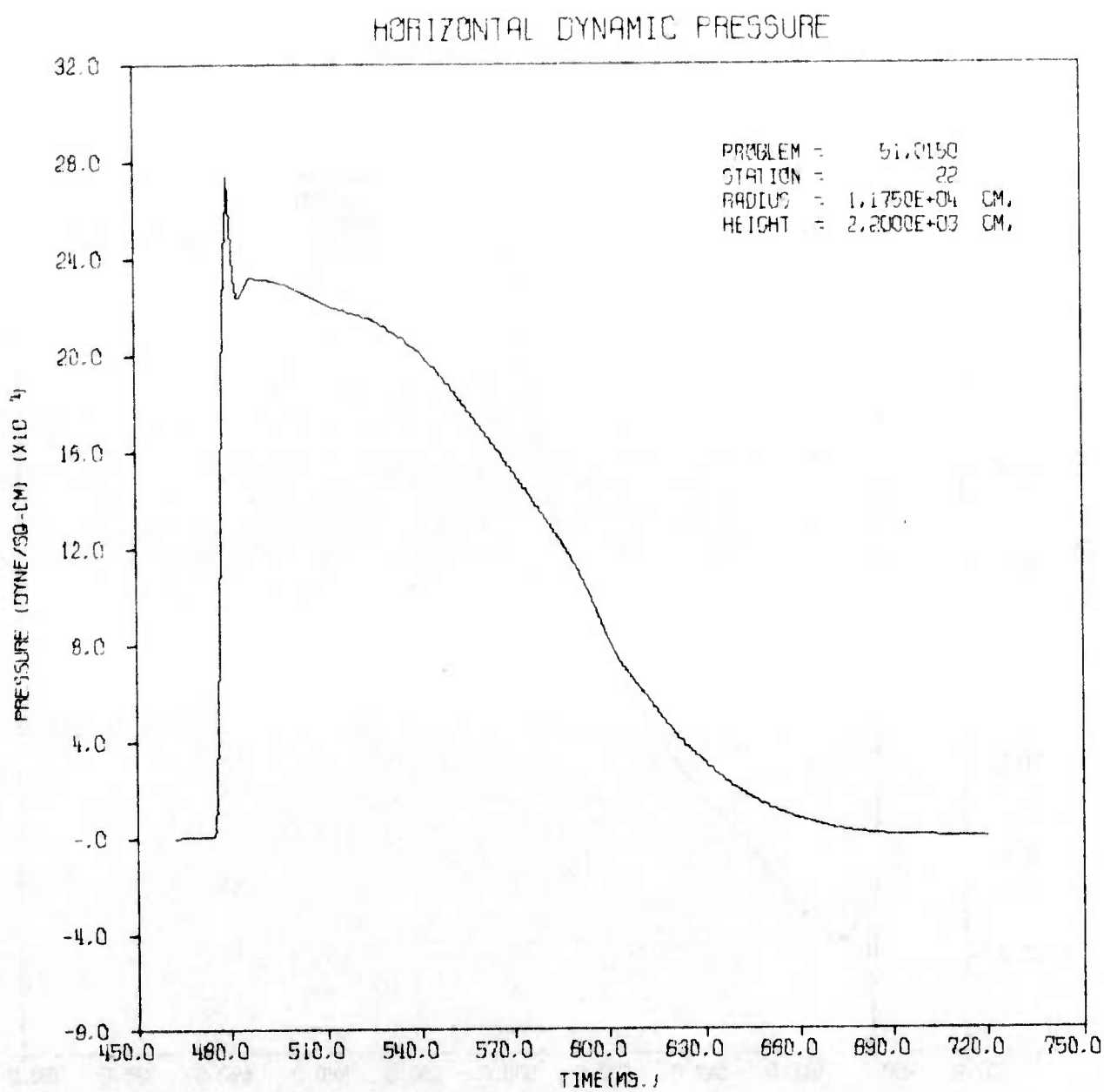
AFWL HULL CAL. OF 50KT EFFECT ON DAM AT 50PSI RANGE



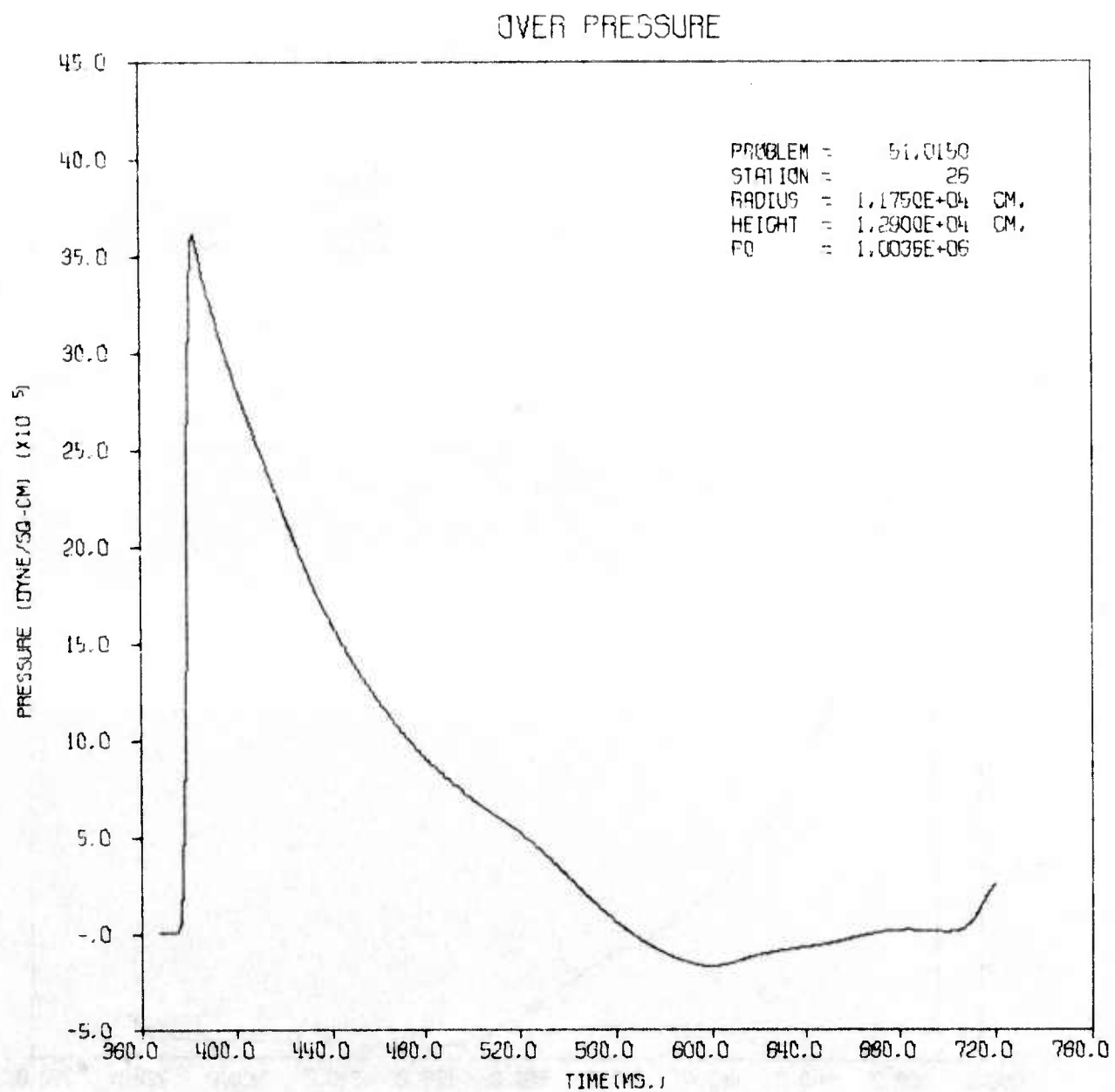
AFWL HULL CAL OF 50KT EFFECT ON DAM AT 50PSI RANGE



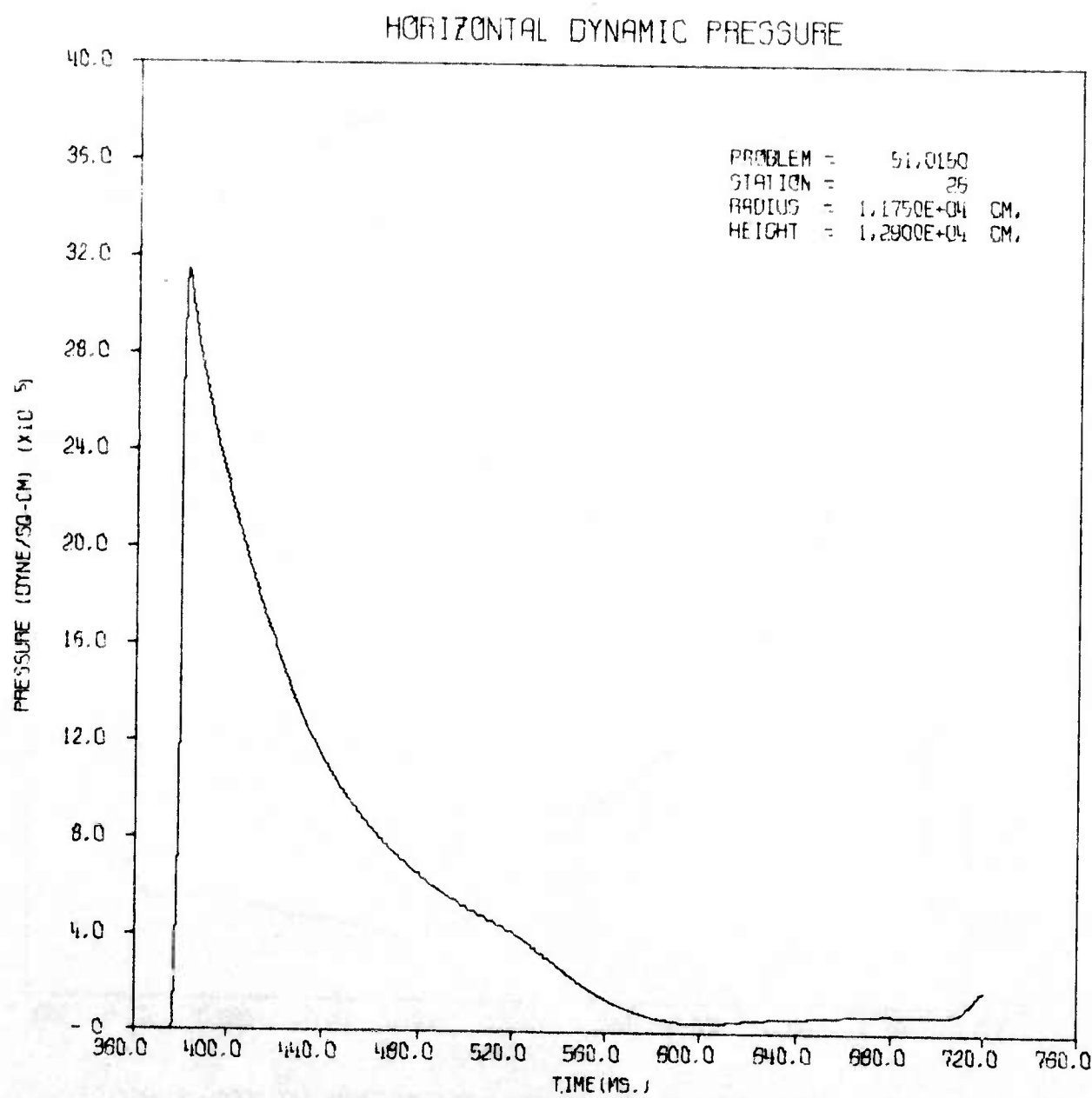
AFWL HULL CAL OF 50KT EFFECT ON DAM AT 50PSI RANGE



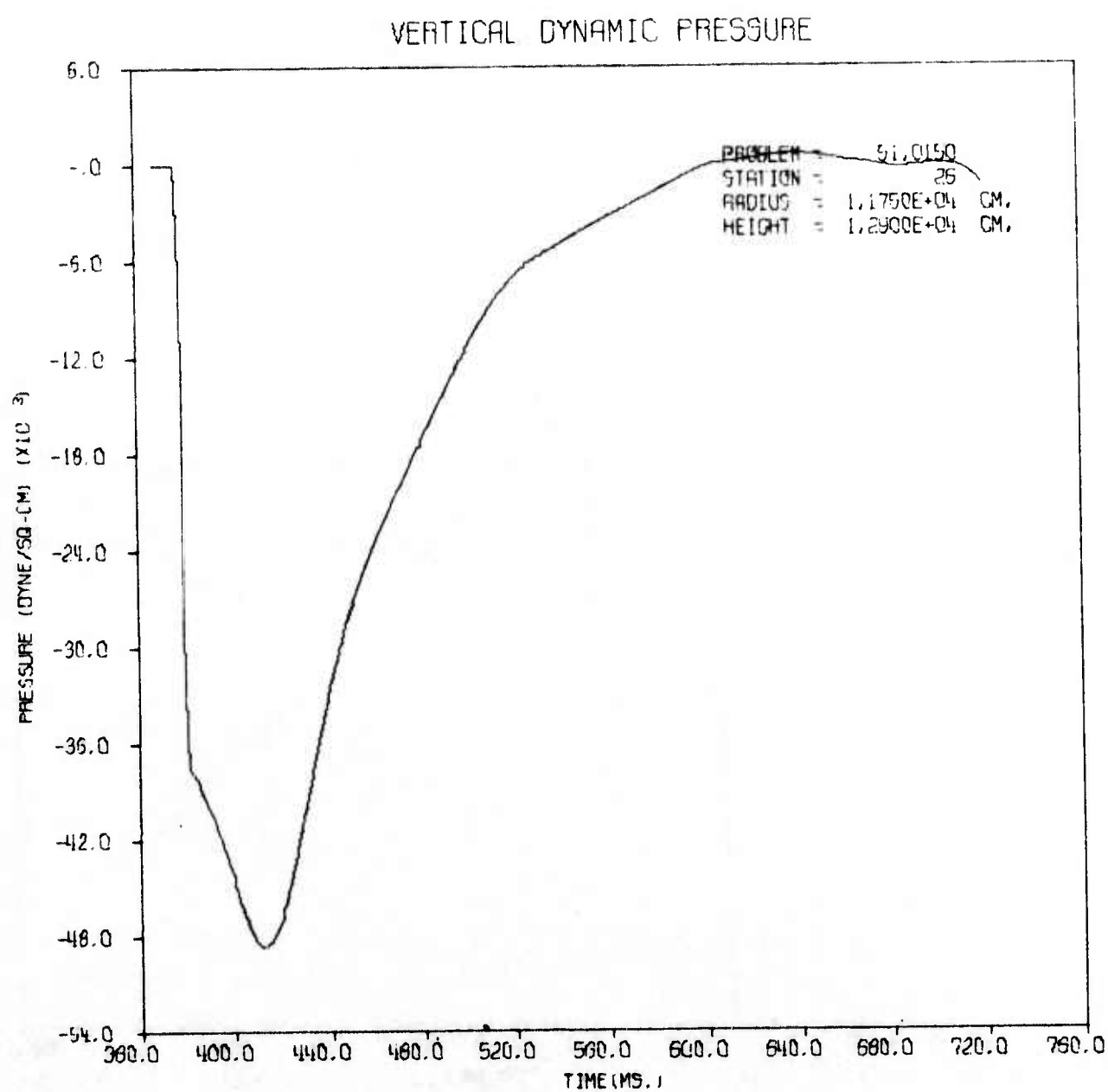
AFWL HULL CAL OF SOFT EFFECT ON DAM AT 50PSI RANGE



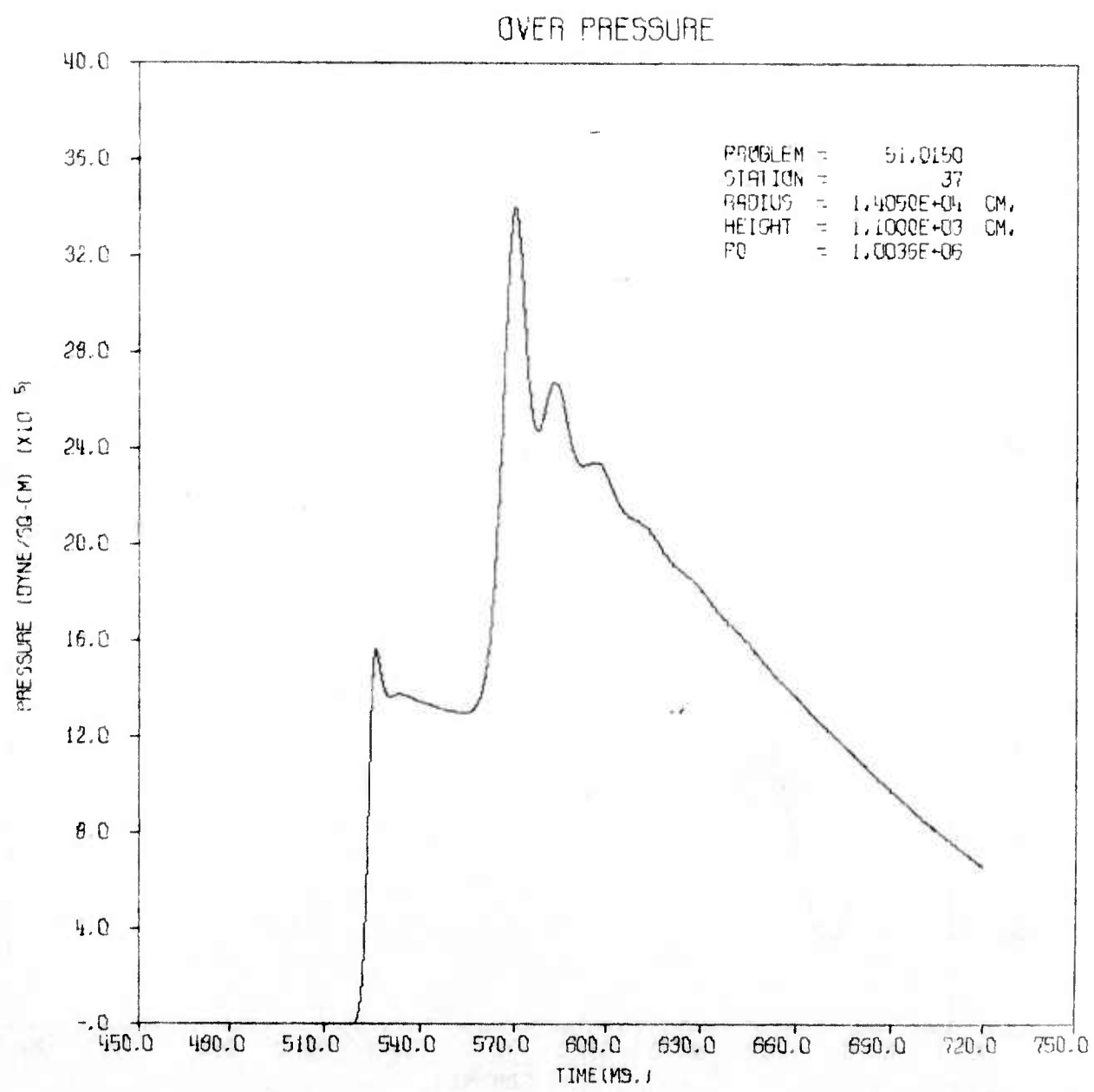
AFWL HULL CAL OF 50KT EFFECT ON DAM AT 50PSI RANGE



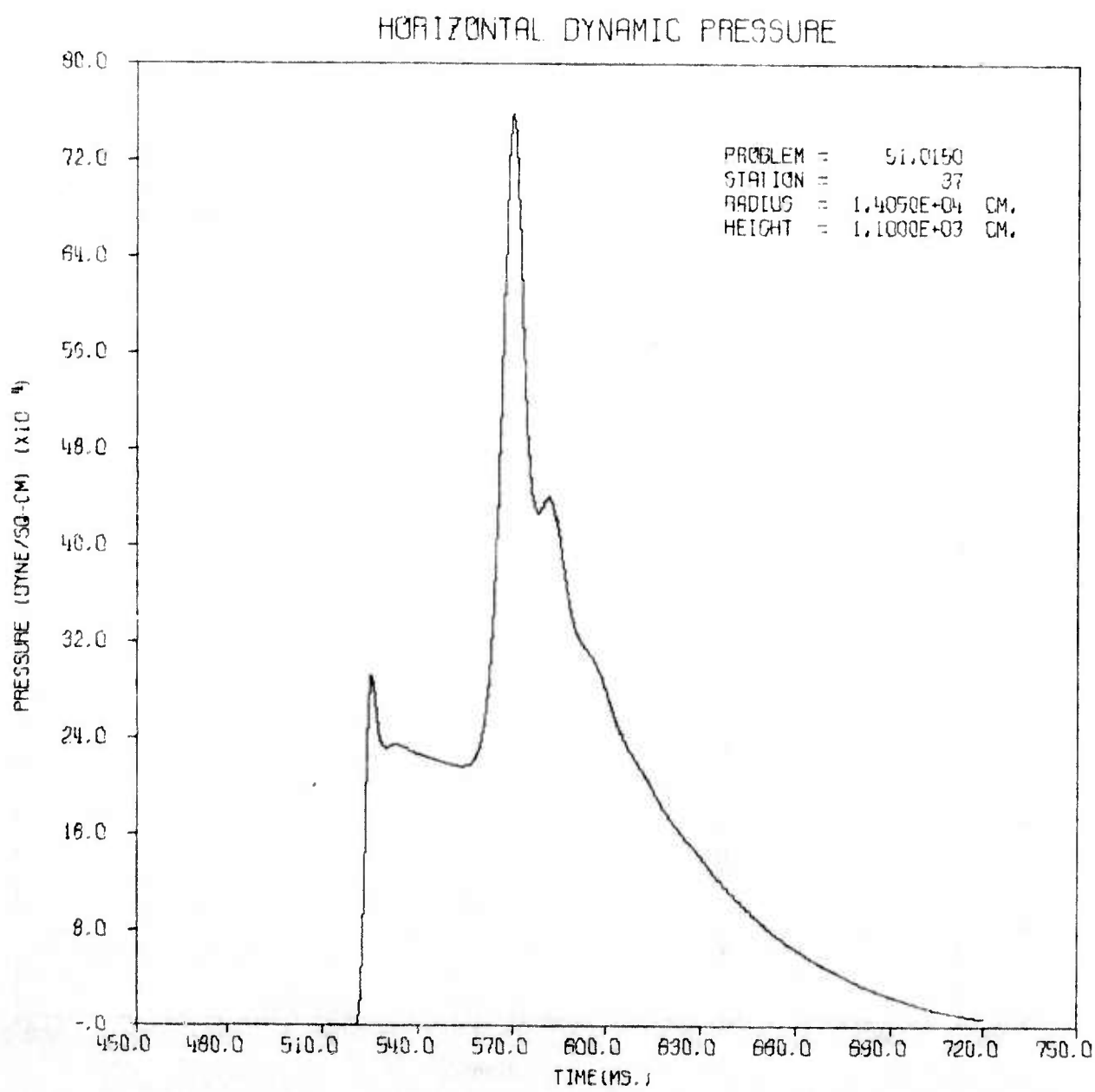
AFWL HULL CAL OF 50KT EFFECT ON DAM AT 50PSI RANGE



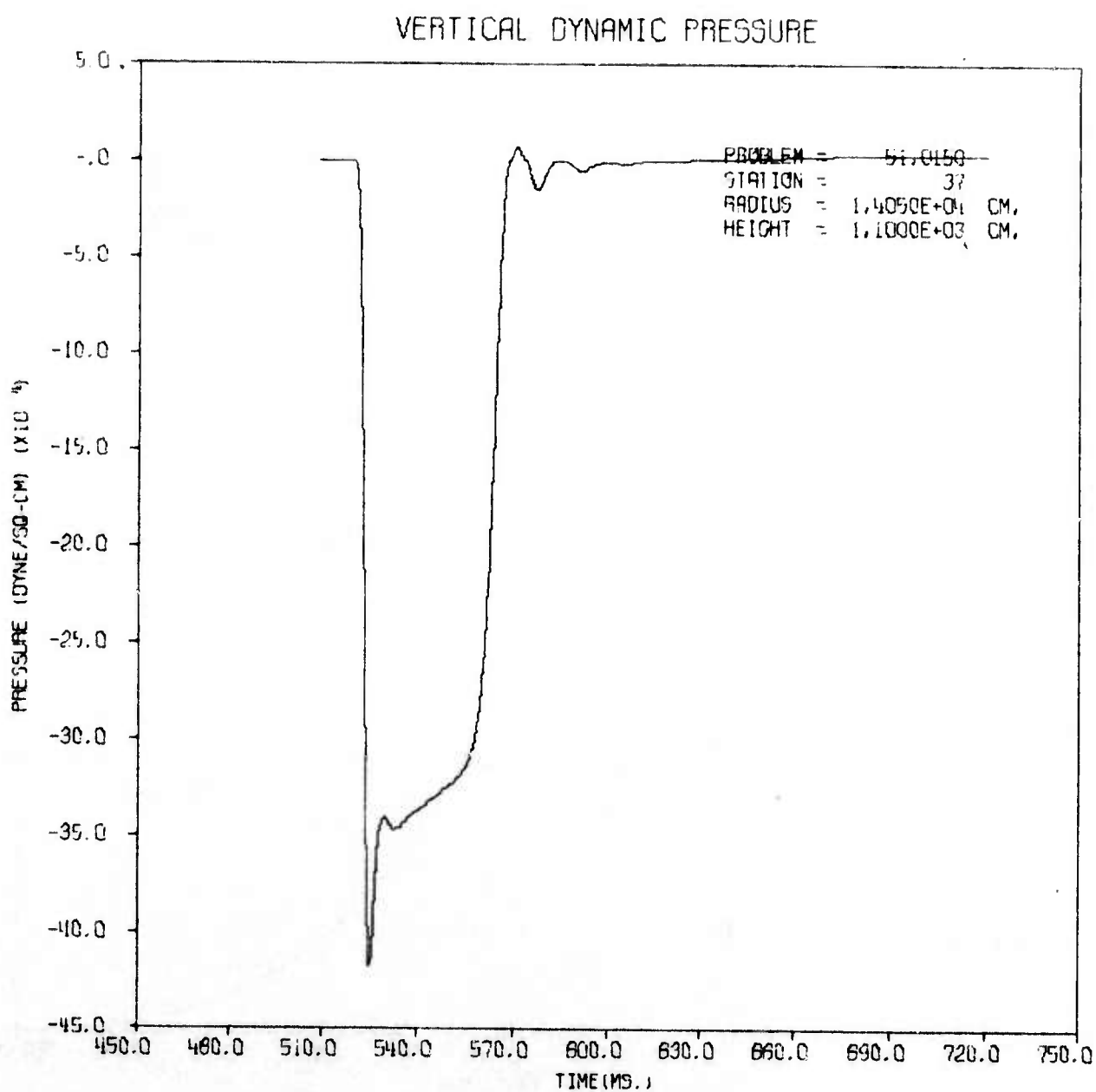
AFWL HULL CAL OF SOFT EFFECT ON DAM AT 50PSI RANGE



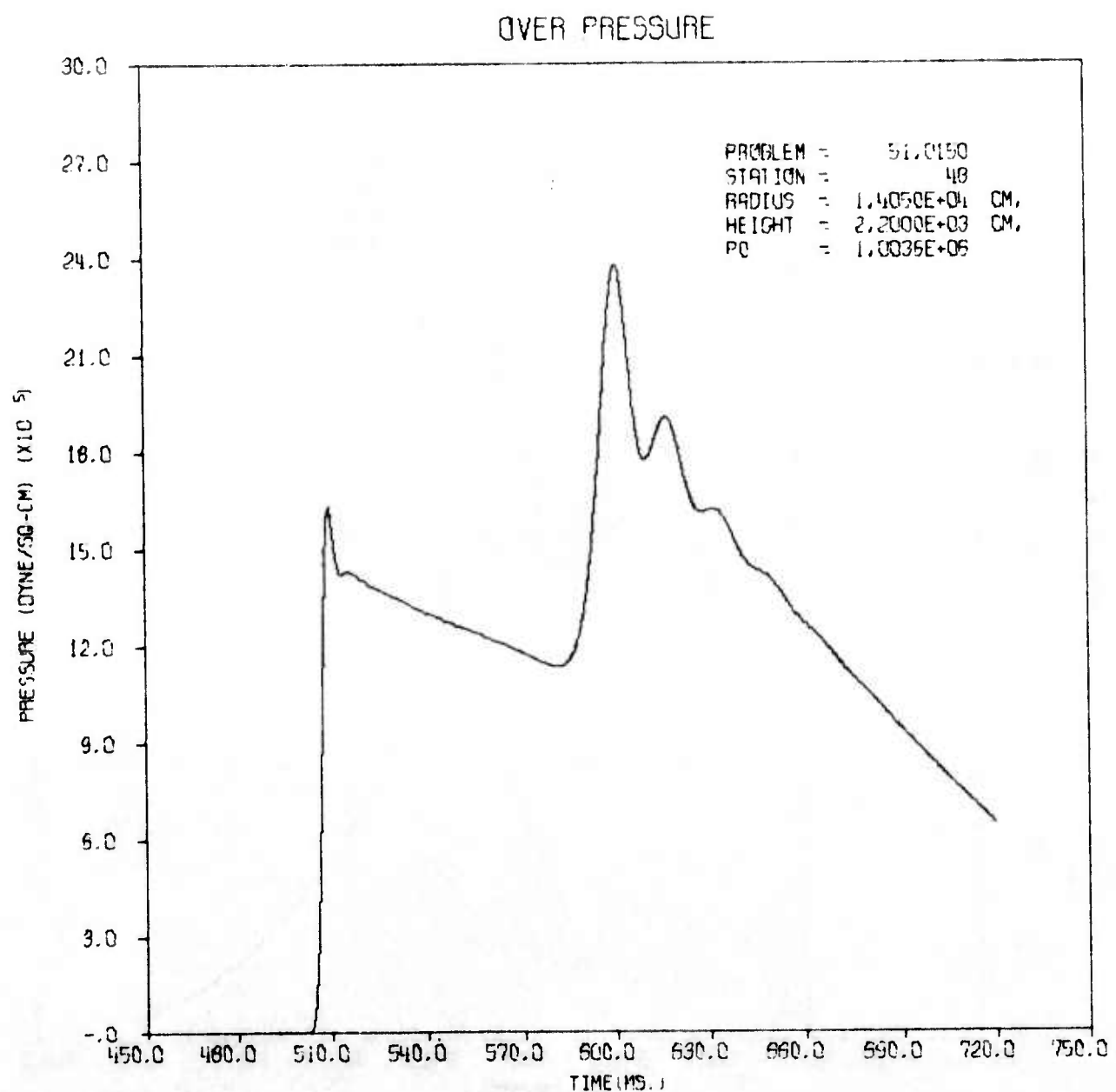
AFWL HULL CAL OF 50KT EFFECT ON DAM AT 50PSI RANGE



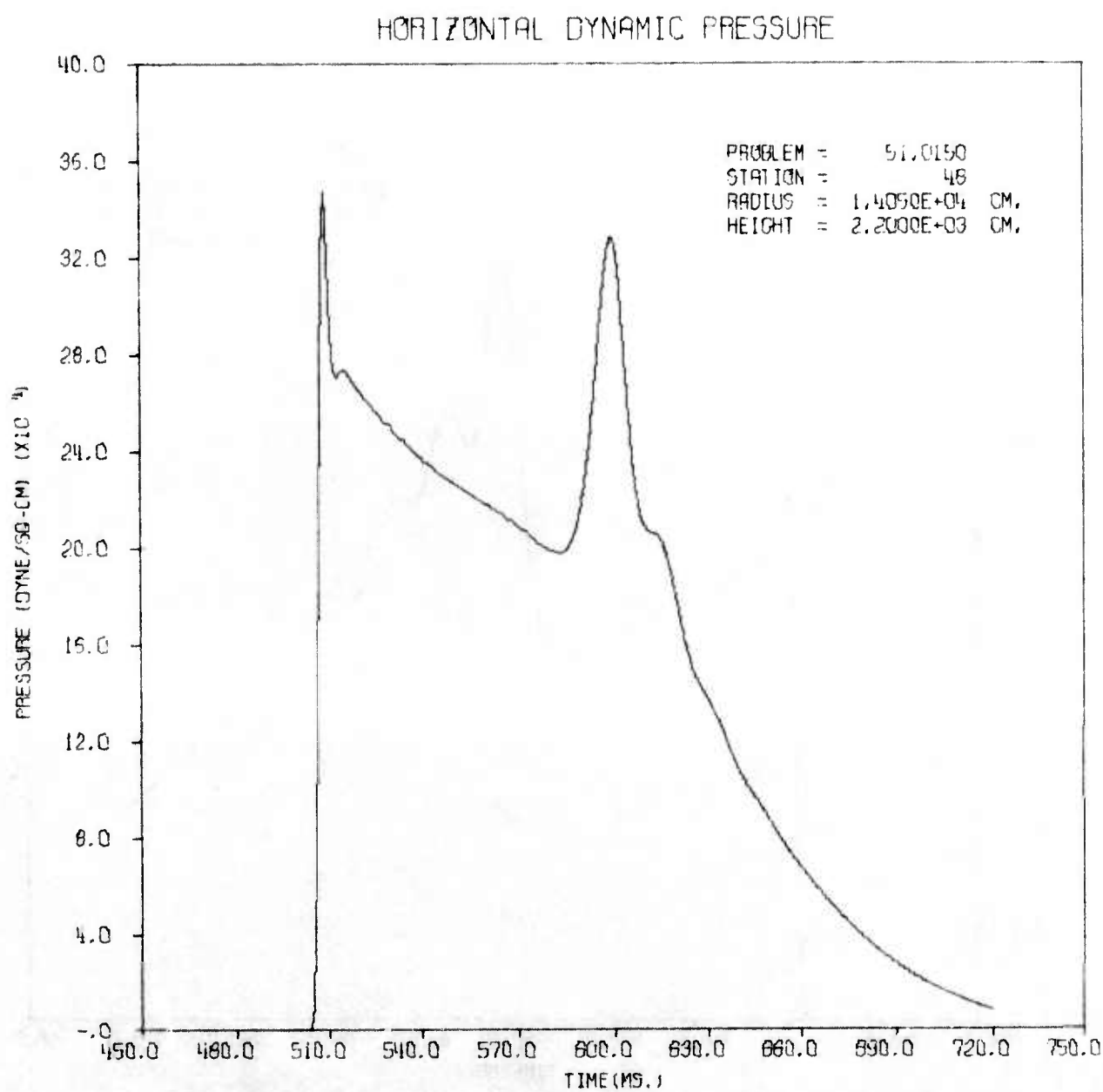
AFWL HULL CAL OF SOFT EFFECT ON DAM AT 50PSI RANGE



AFWL HULL CAL OF 50KT EFFECT ON DAM AT 50PSI RANGE



AFWL HULL CAL OF 50KT EFFECT ON DAM AT 50PSI RANGE

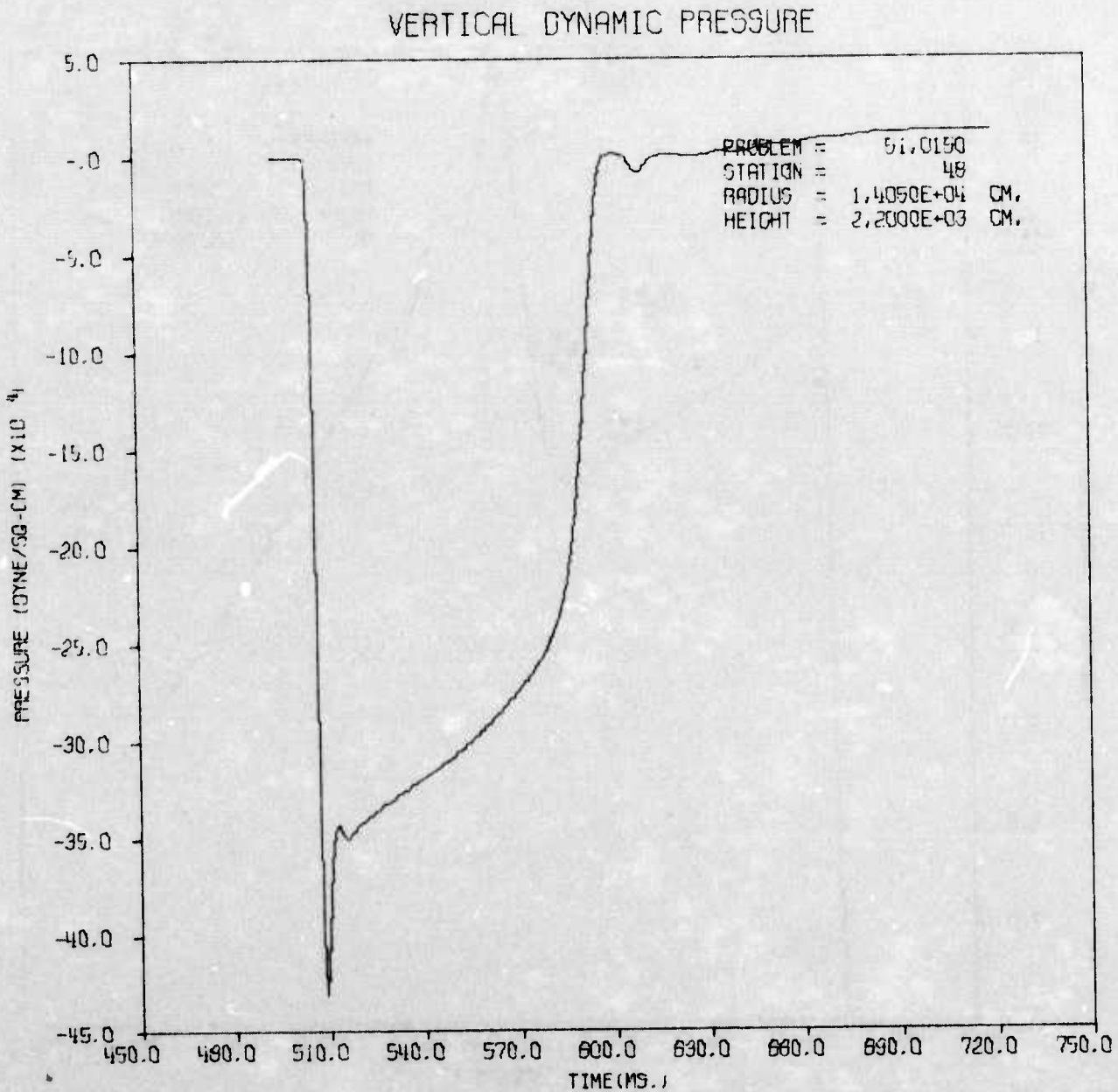


AFWL HULL CAL OF 50KT EFFECT ON DAM AT 50PSI RANGE

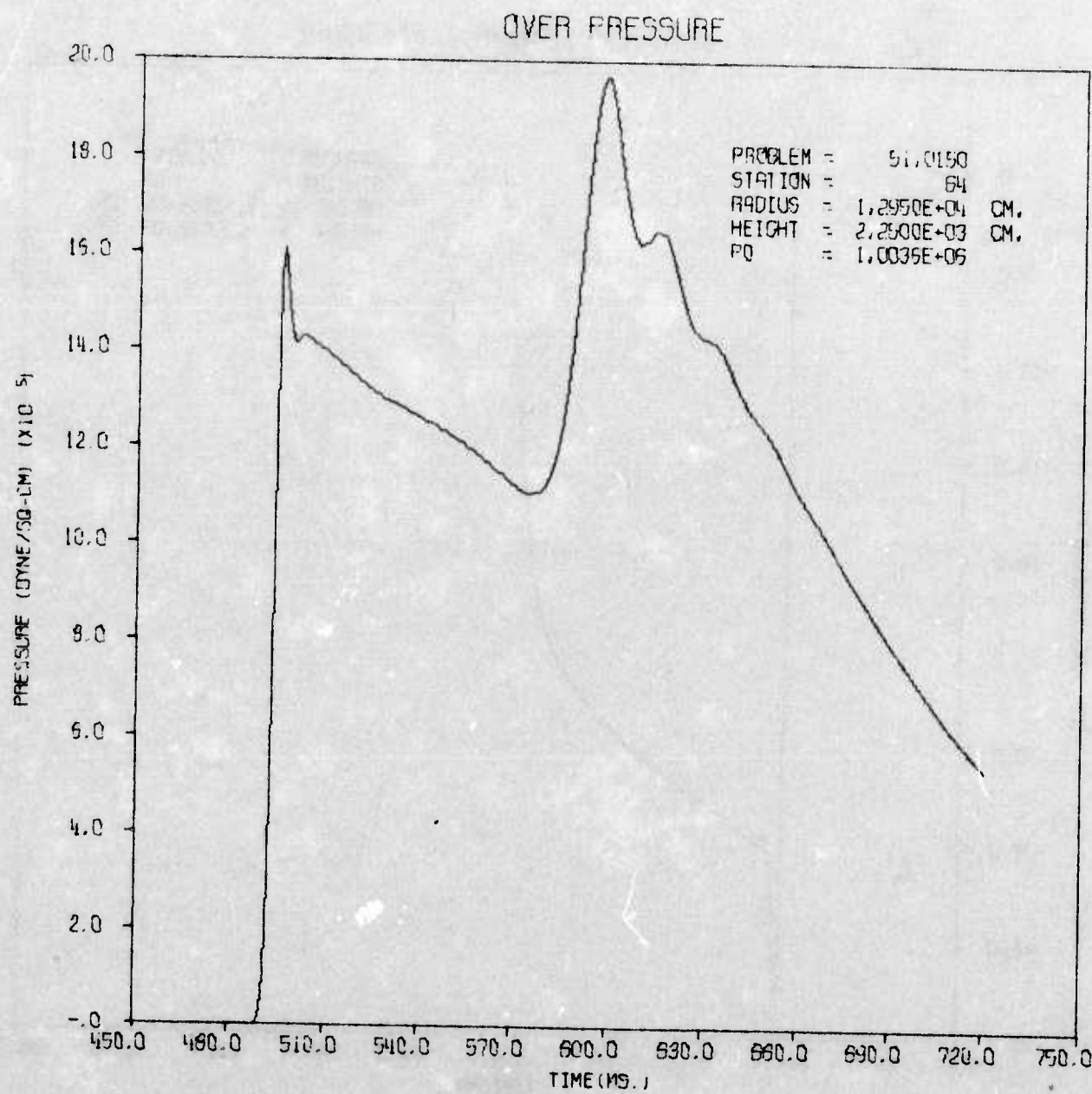
THIS REPORT HAS BEEN DELIMITED
AND CLEARED FOR PUBLIC RELEASE
UNDER DOD DIRECTIVE 5200.20 AND
NO RESTRICTIONS ARE IMPOSED UPON
ITS USE AND DISCLOSURE.

DISTRIBUTION STATEMENT A

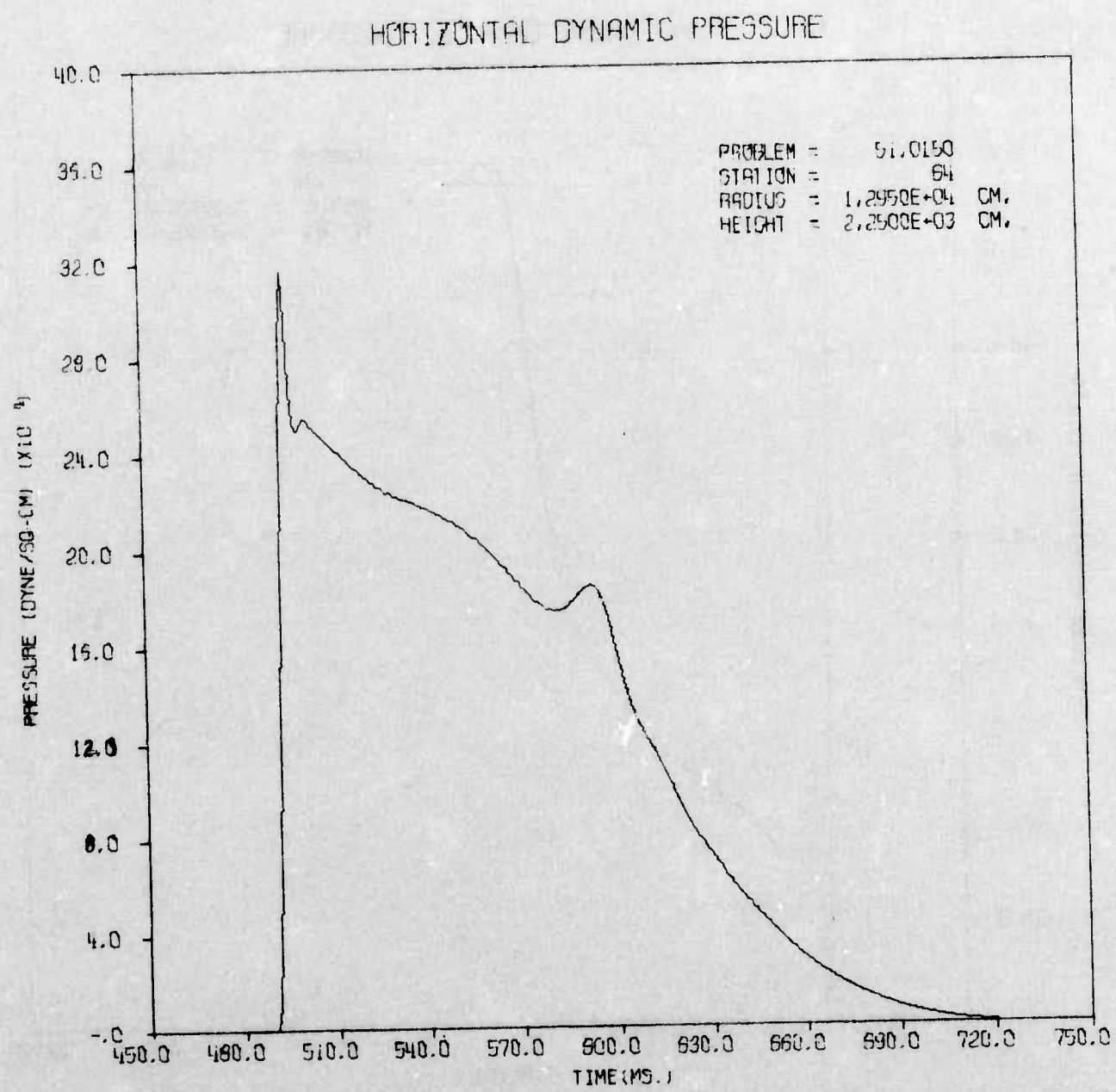
APPROVED FOR PUBLIC RELEASE,
DISTRIBUTION UNLIMITED.



AFWL HULL CAL OF 50KT EFFECT ON DAM AT 50PSI RANGE

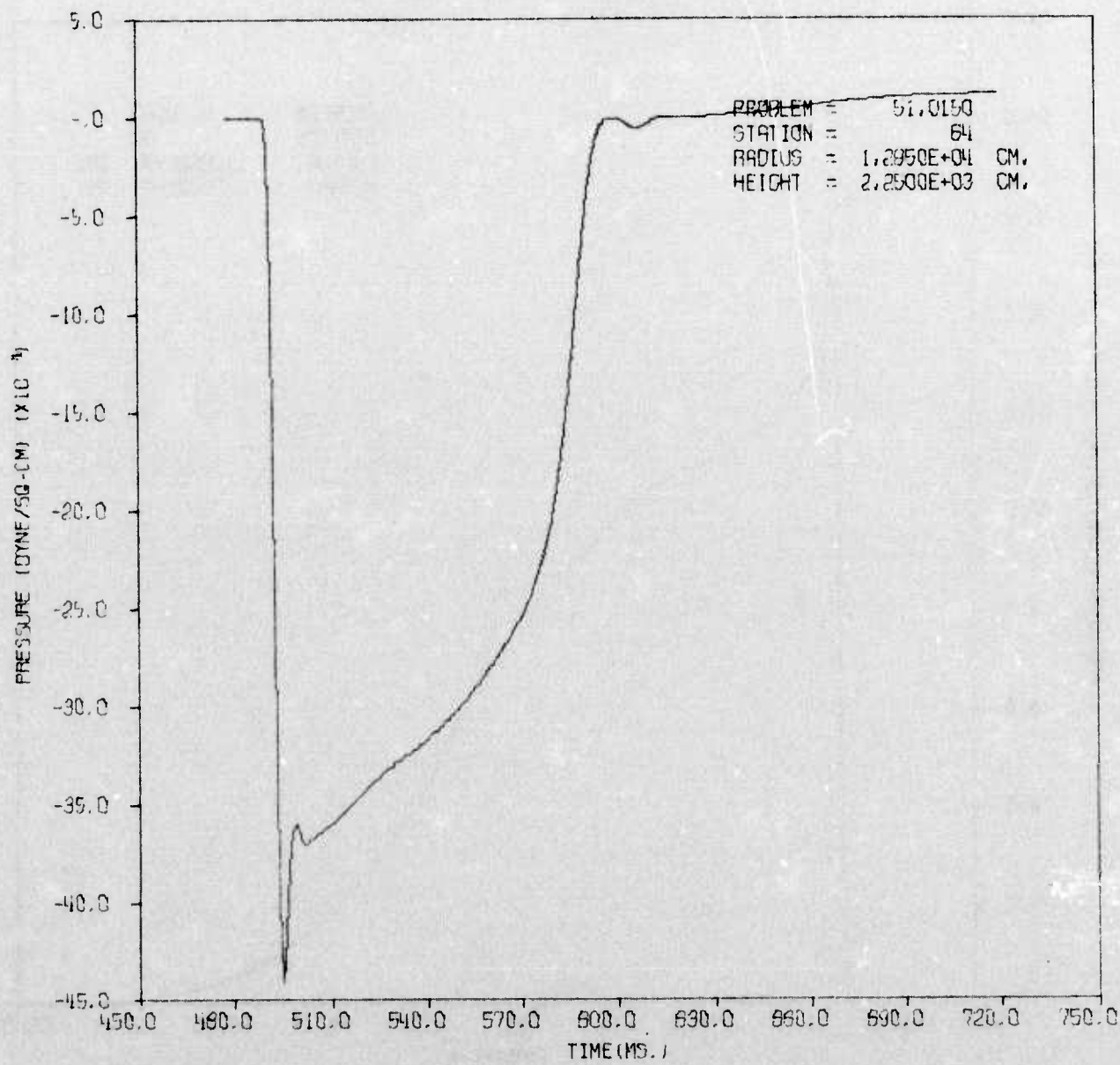


AFWL HULL CAL OF 50KT EFFECT ON DAM AT 50PSI RANGE

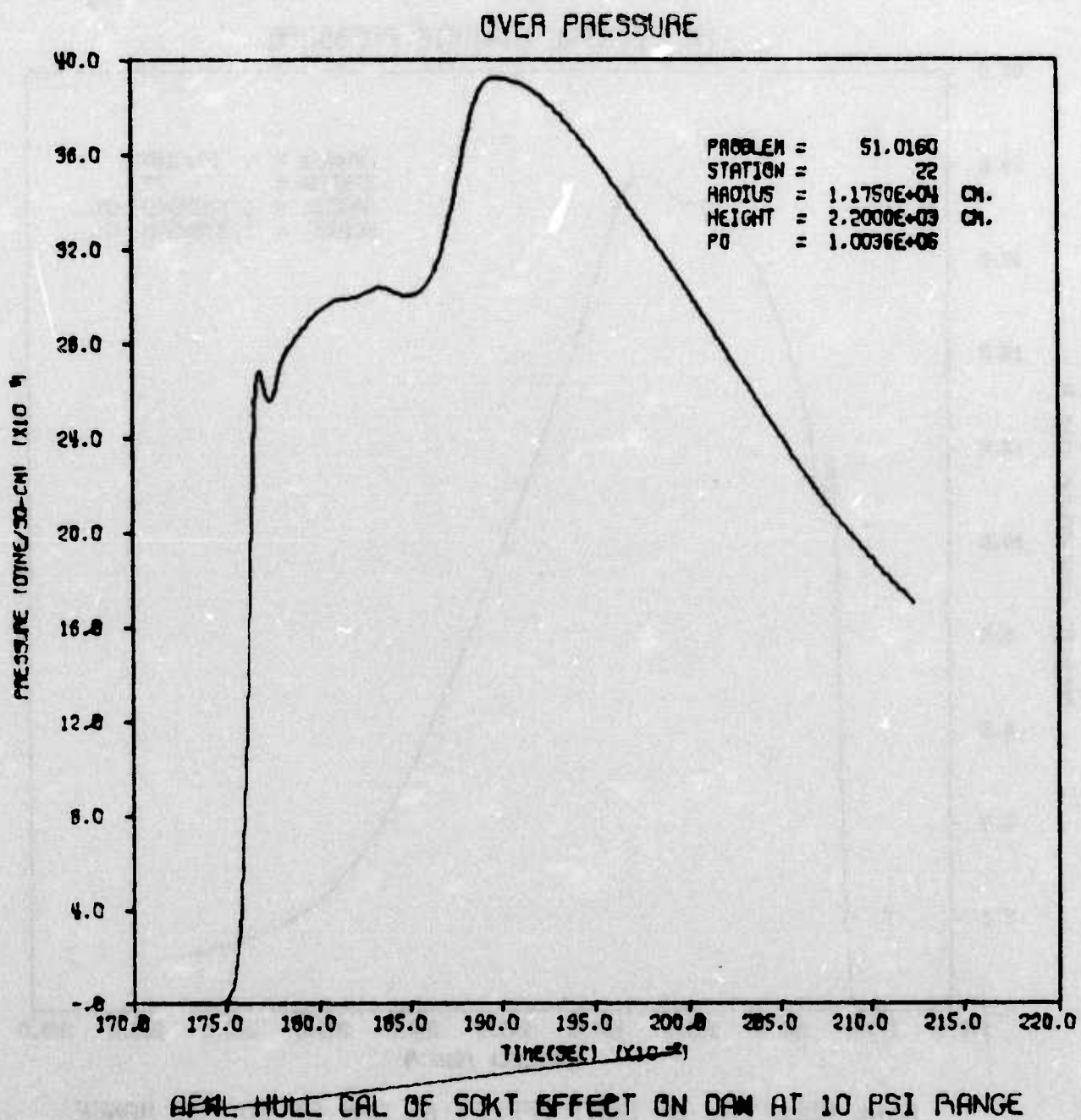


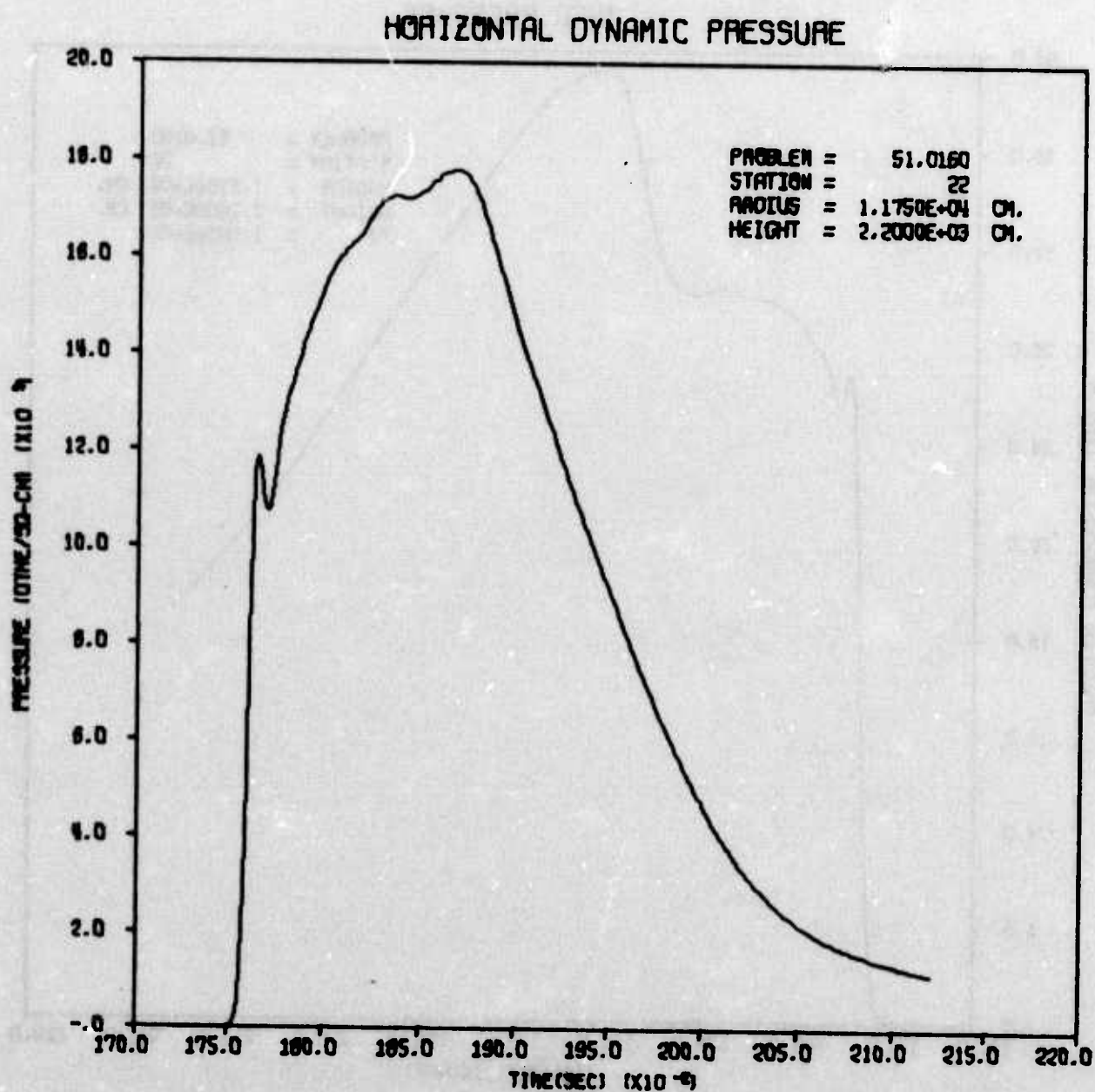
AFWL HULL CAL OF 50KT EFFECT ON DAM AT 50PSI RANGE

VERTICAL DYNAMIC PRESSURE



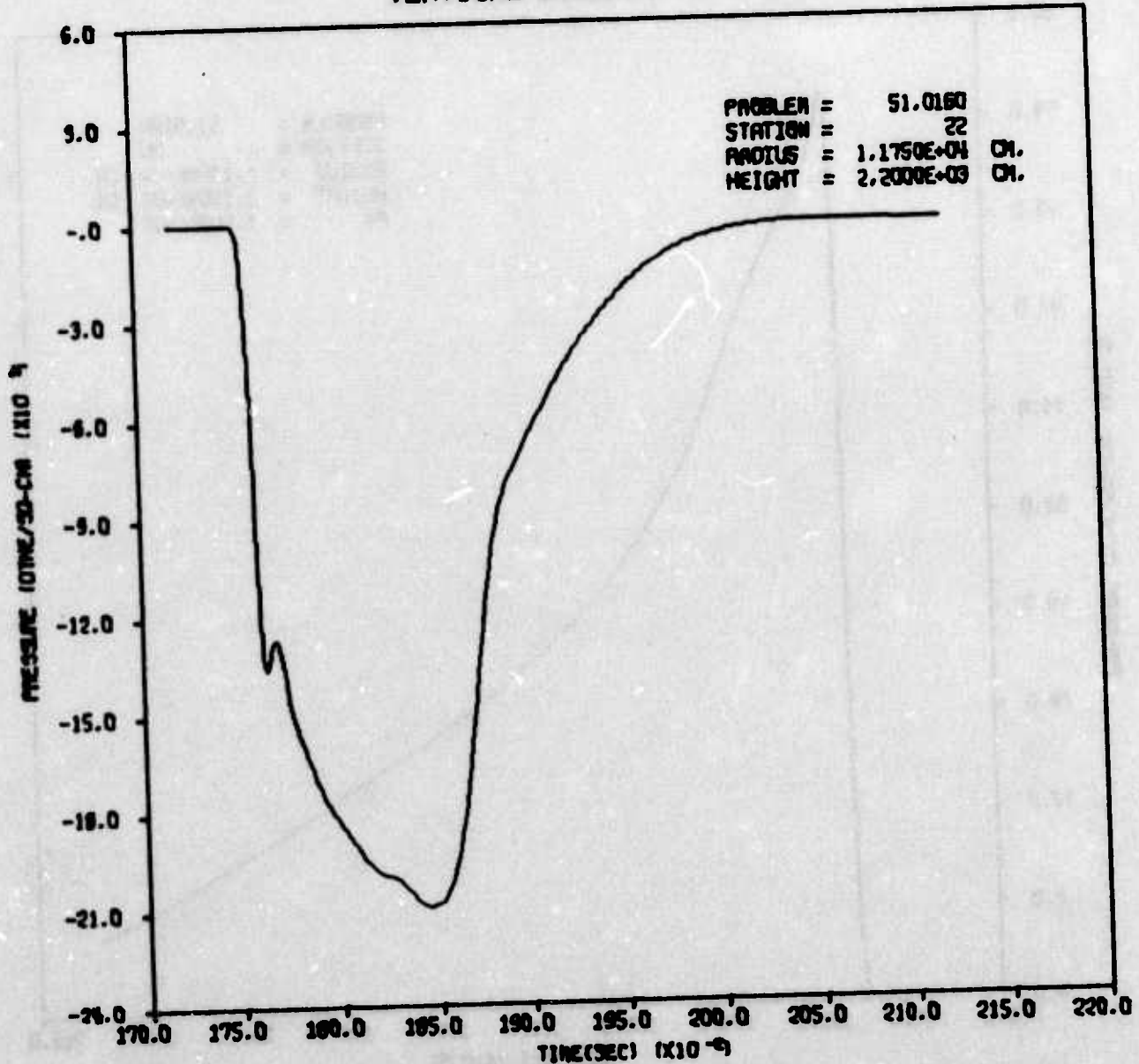
AFWL HULL CAL OF 50KT EFFECT ON DAM AT 50PSI RANGE



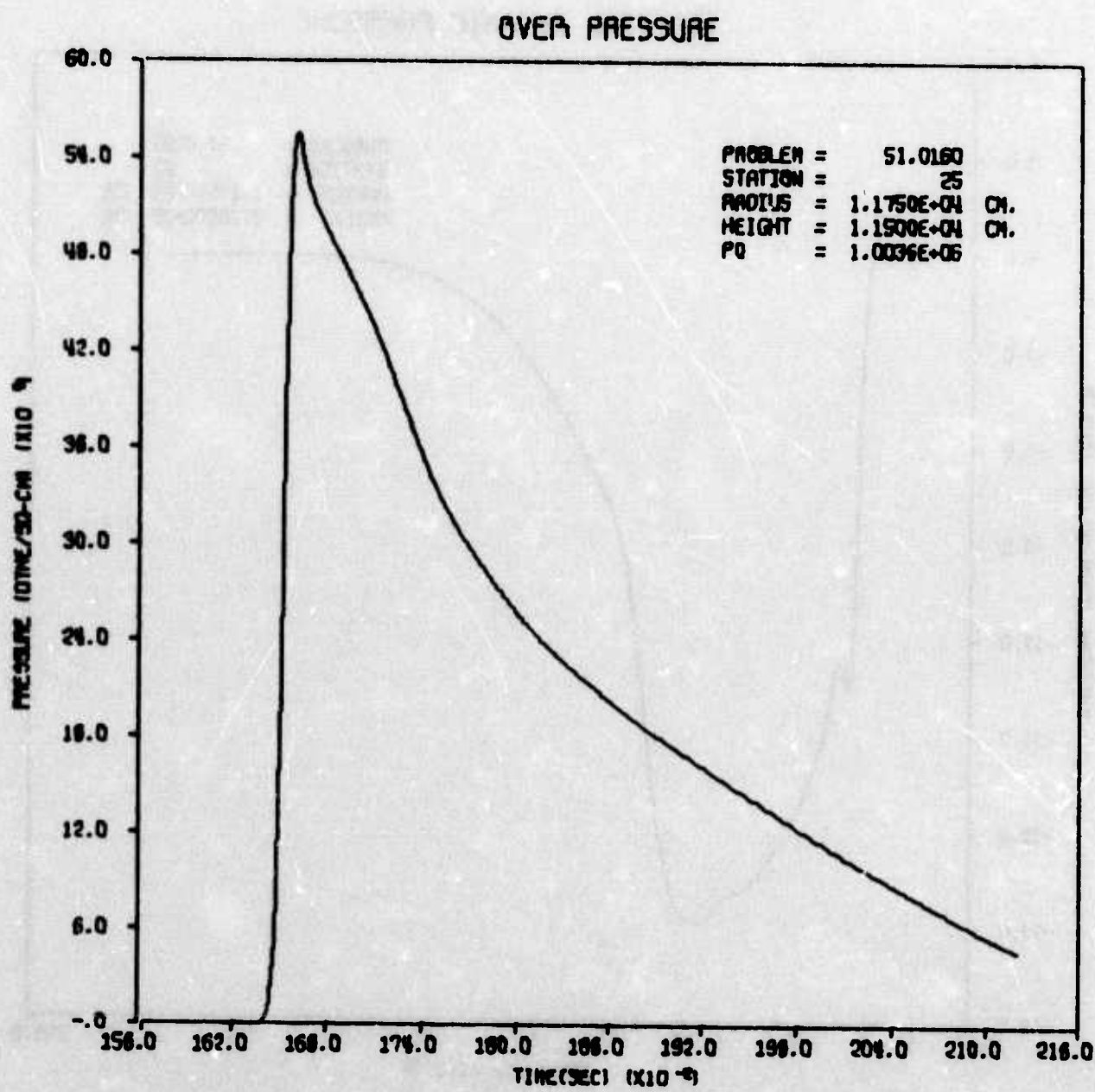


AFWL HULL CAL OF SOFT EFFECT ON DAM AT 10 PSI RANGE

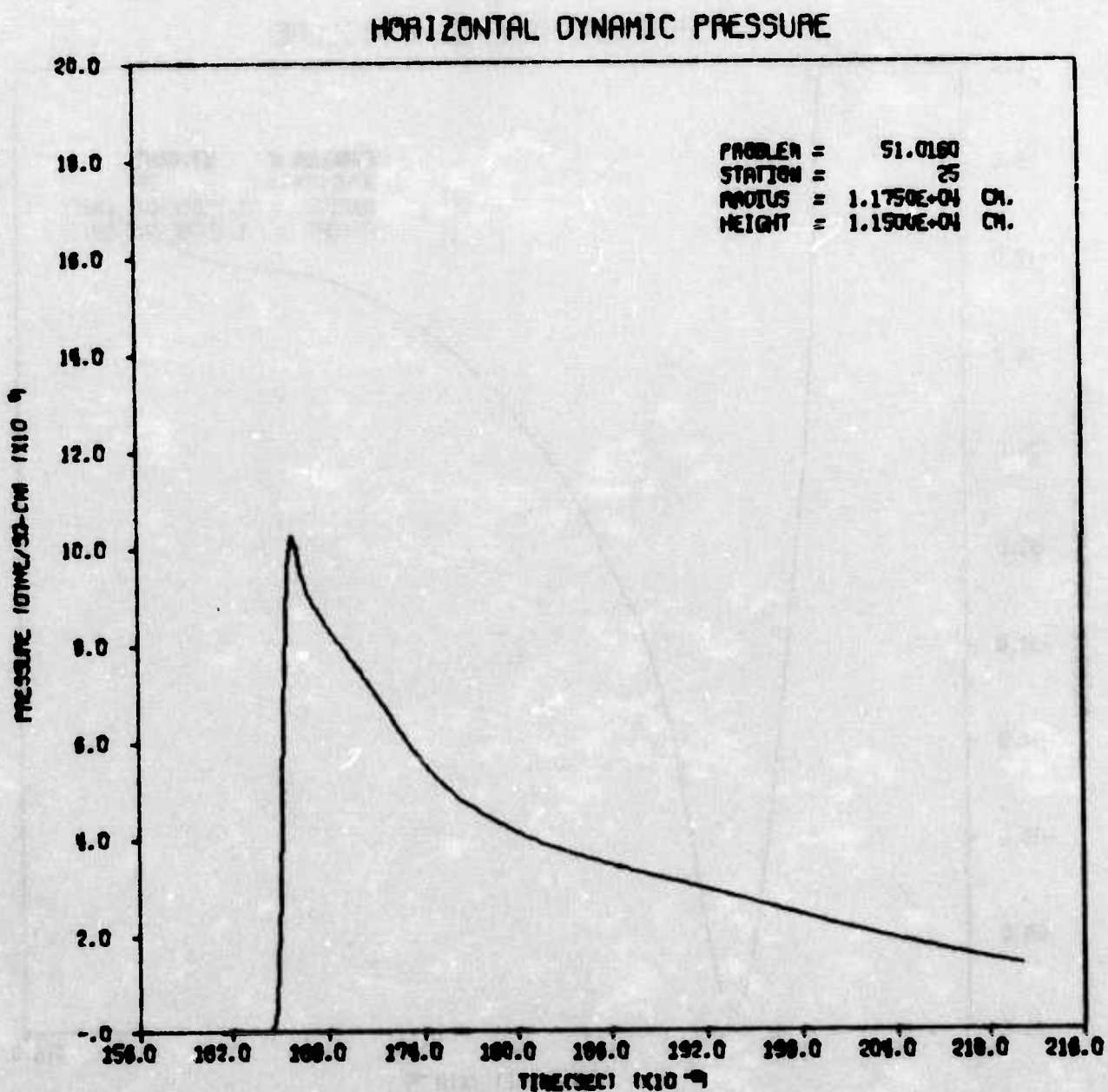
VERTICAL DYNAMIC PRESSURE



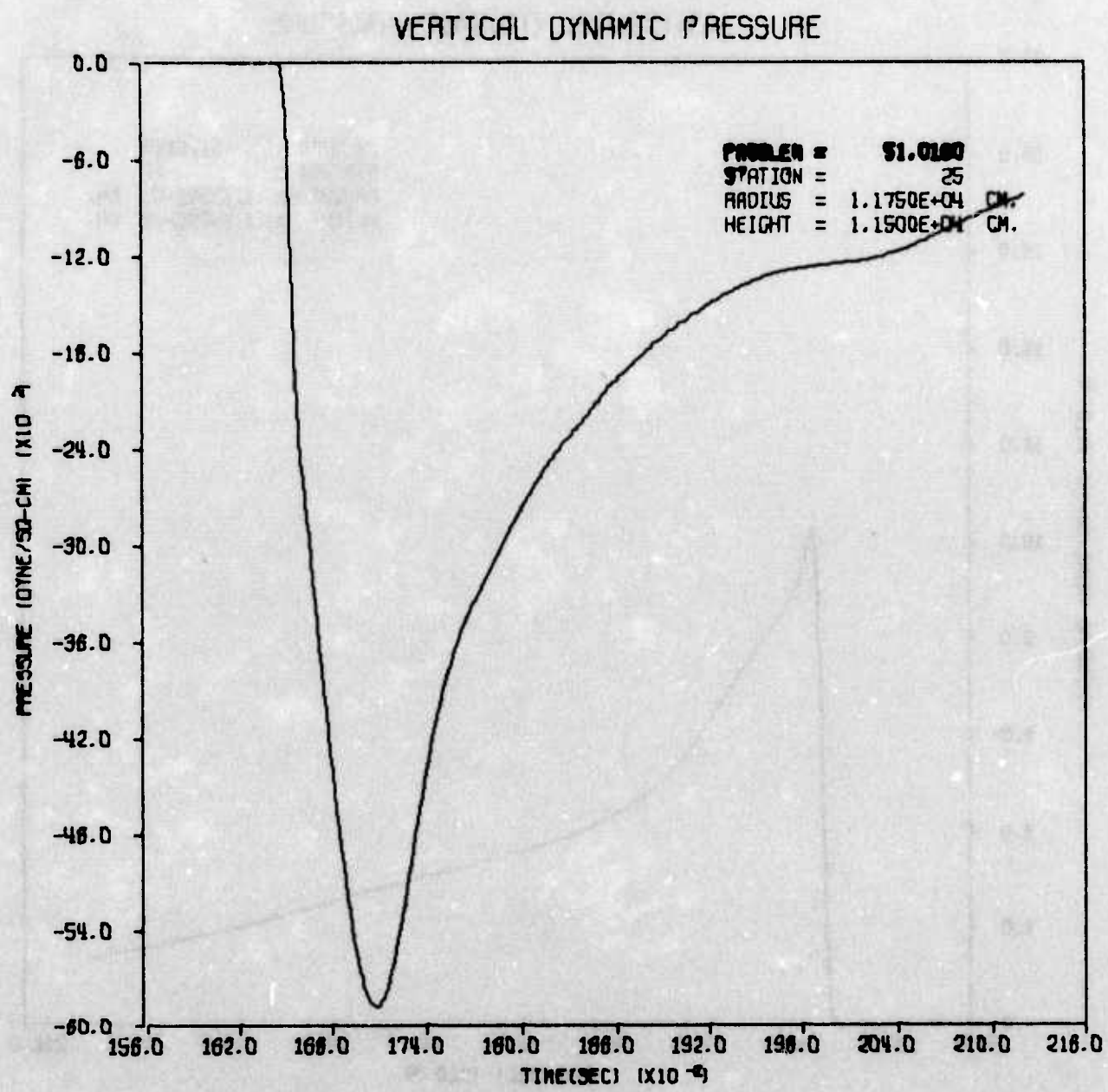
AFWL HULL CAL OF SOKT EFFECT ON DAM AT 10 PSI RANGE

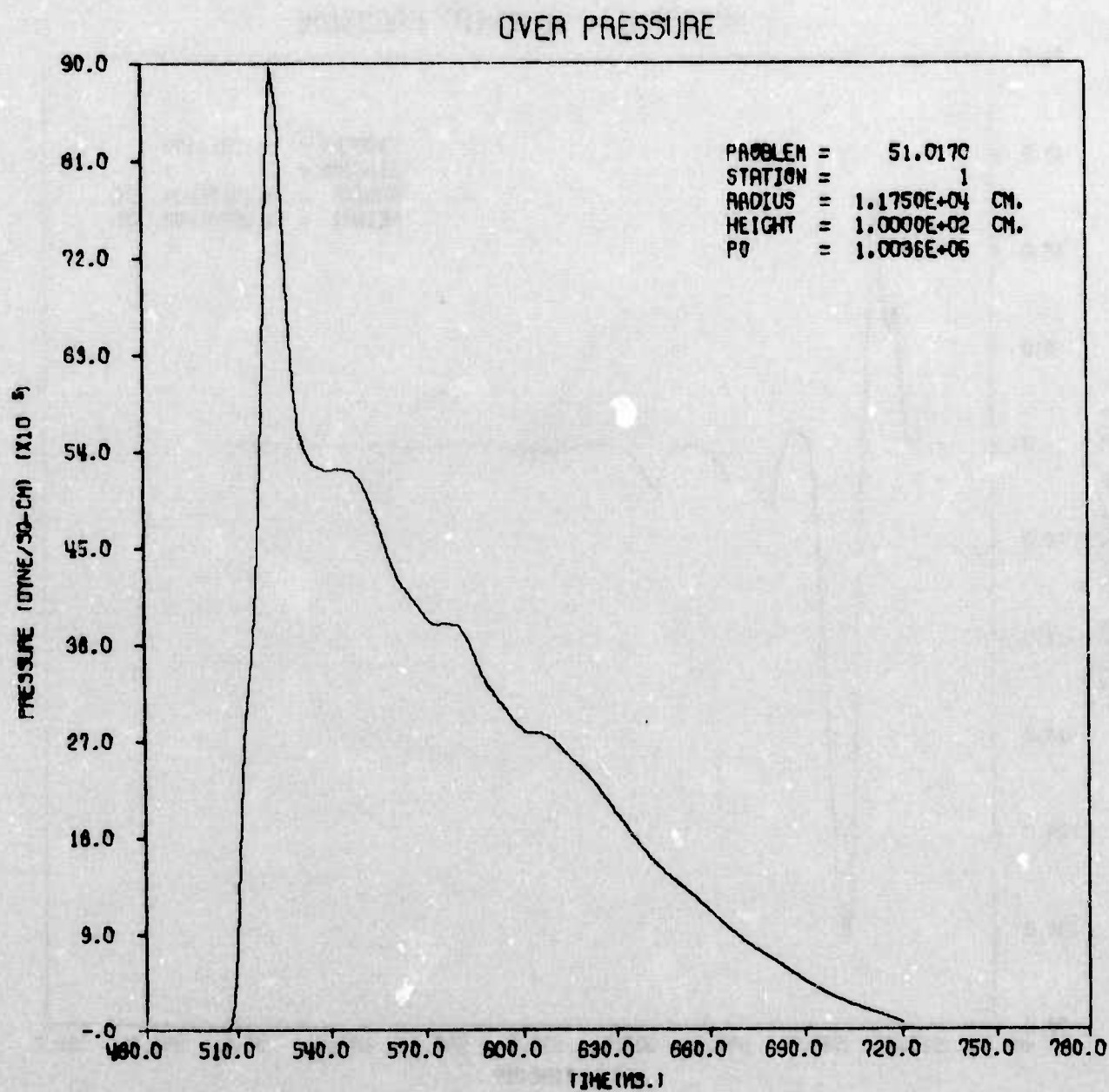


AFWL HULL CAL OF SOFT EFFECT ON DAM AT 10 PSI RANGE



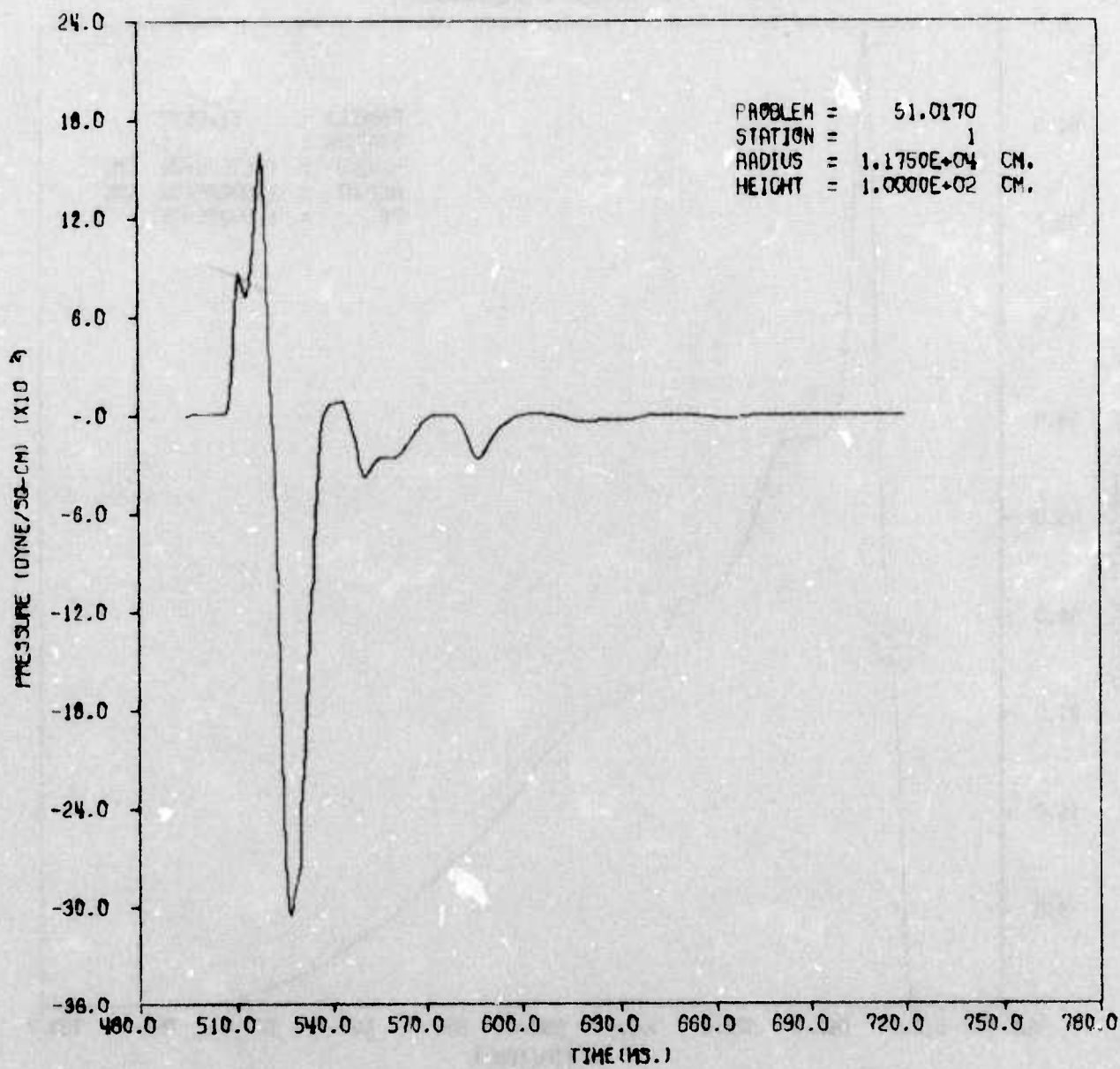
AFWL HULL CAL OF SOFT EFFECT ON DAM AT 10 PSI RANGE





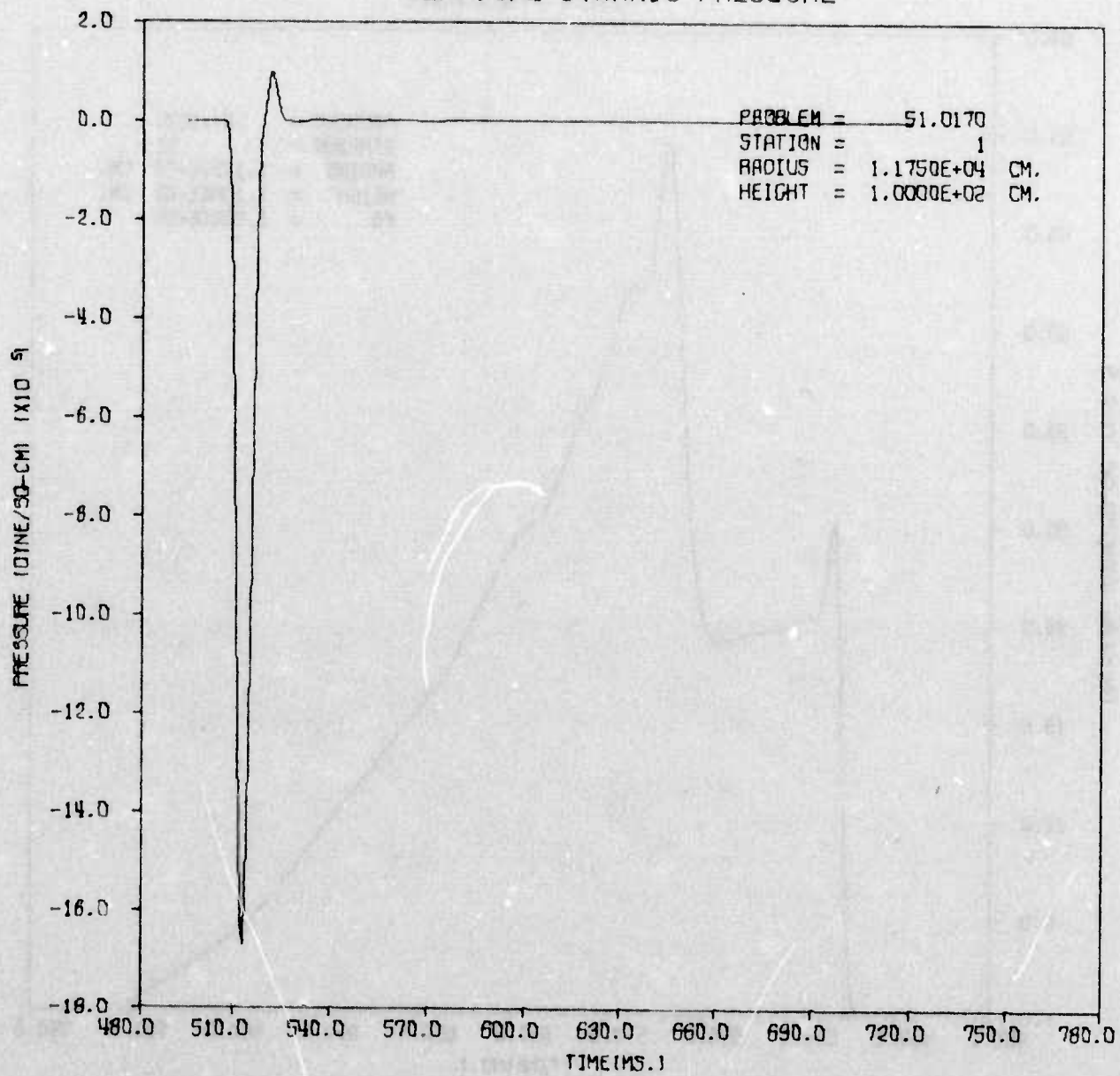
AFWL HULL CAL OF 50KT EFFECT ON DAM AND STRUCTURE AT 50PSI RANGE

HORIZONTAL DYNAMIC PRESSURE

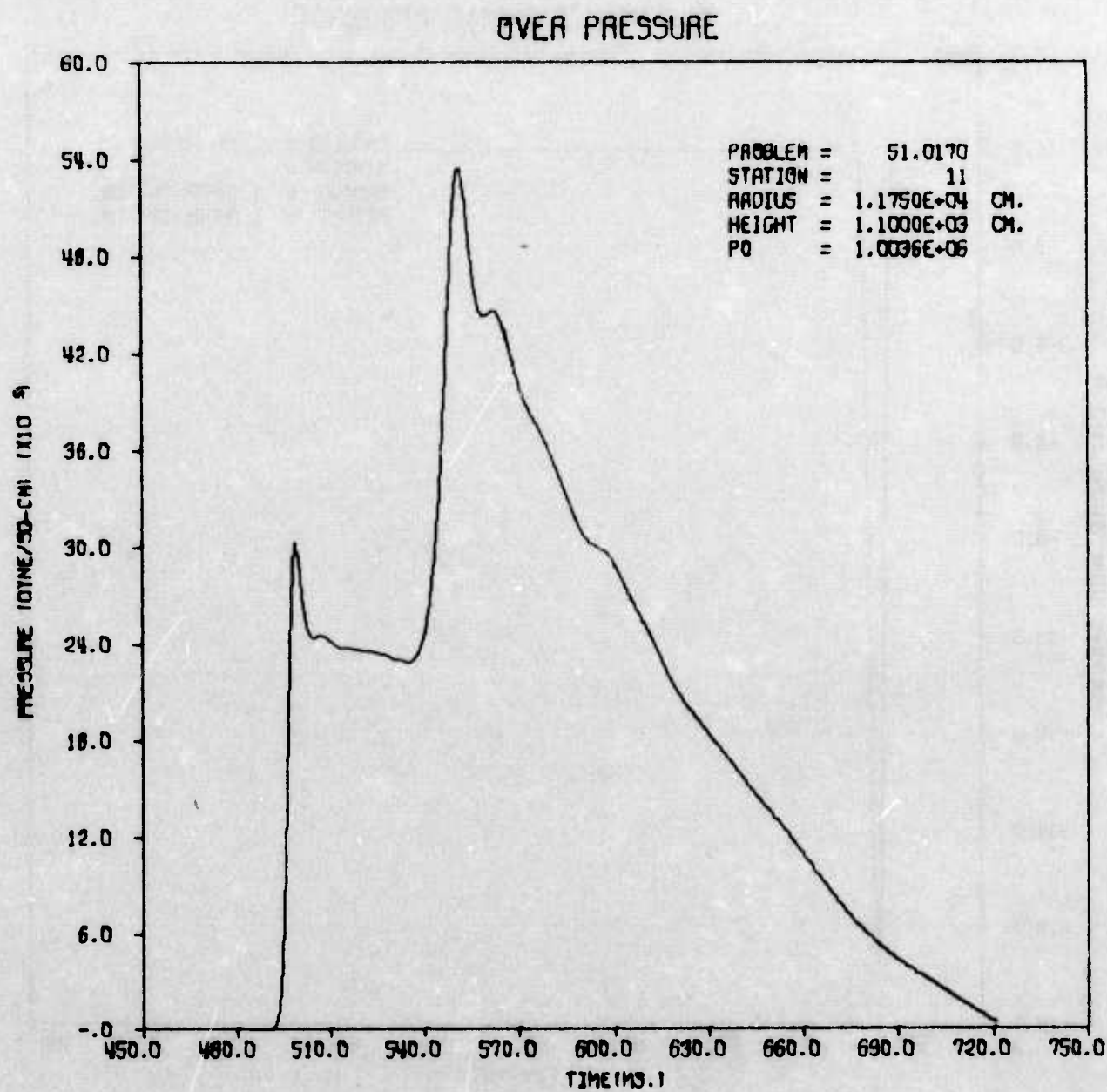


AFWL HULL CAL OF 50KT EFFECT ON DAM AND STRUCTURE AT 50PSI RANGE

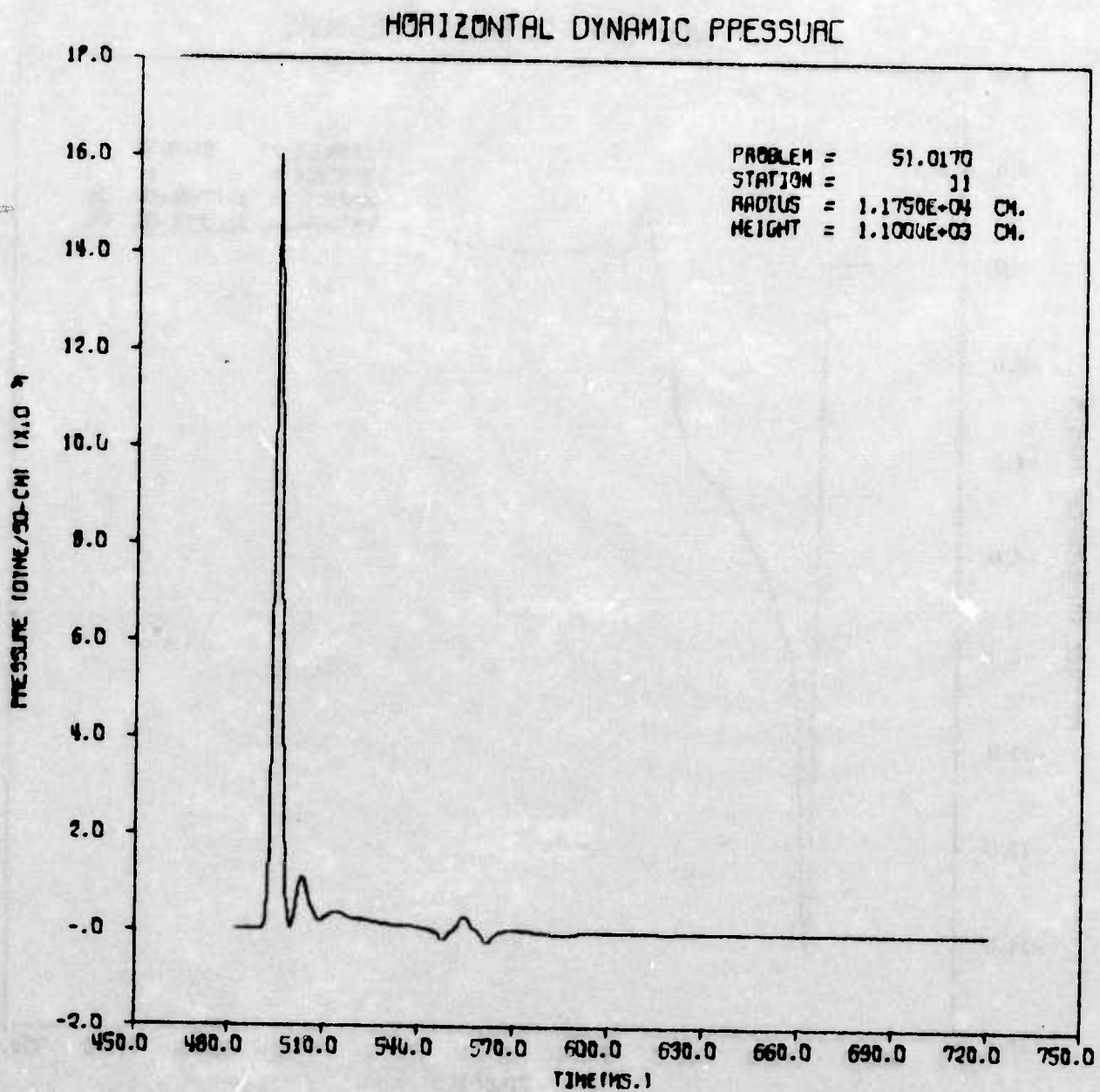
VERTICAL DYNAMIC PRESSURE



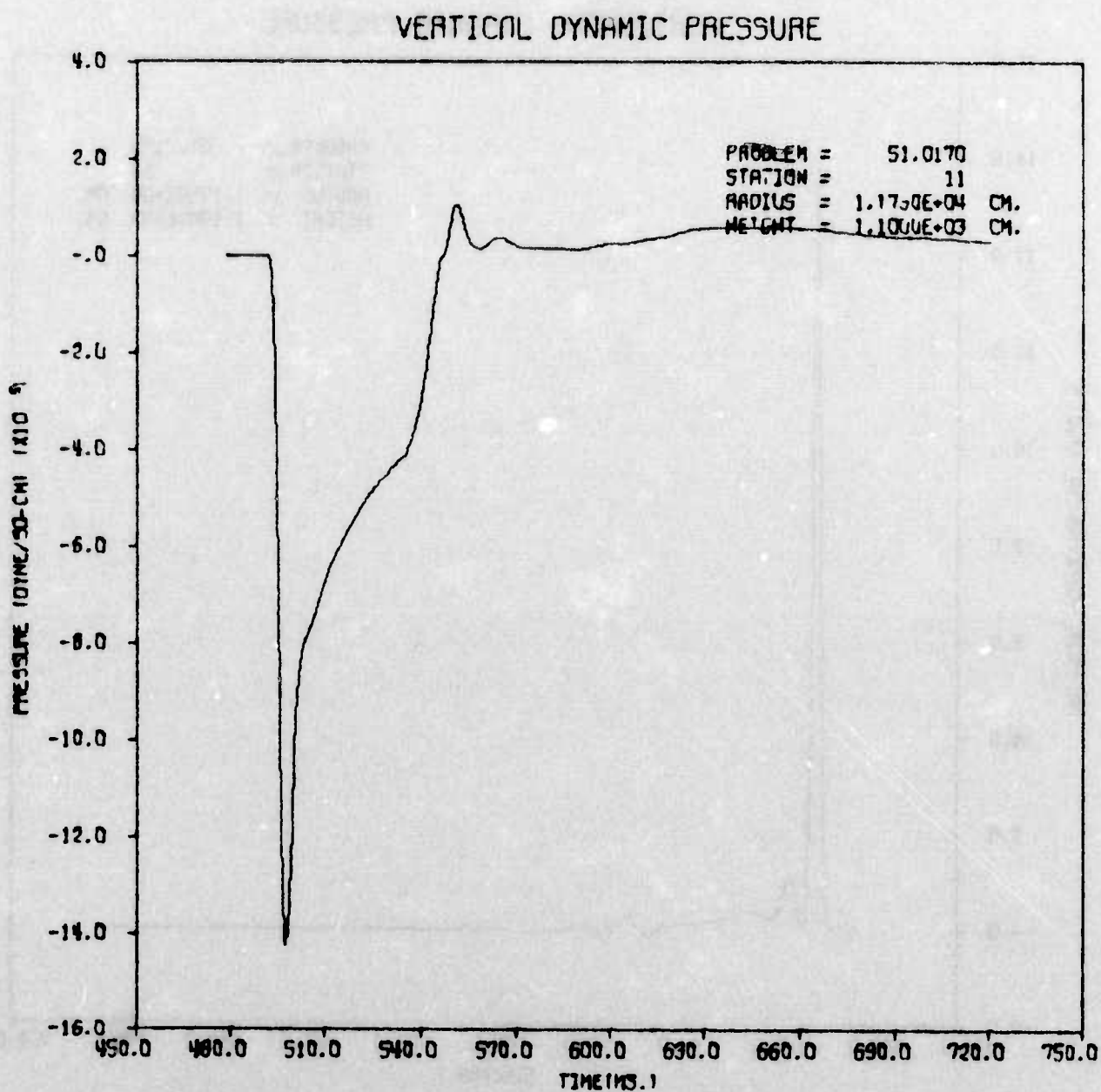
AFWL HULL CAL OF 50KT EFFECT ON DAM AND STRUCTURE AT 50PSI RANGE



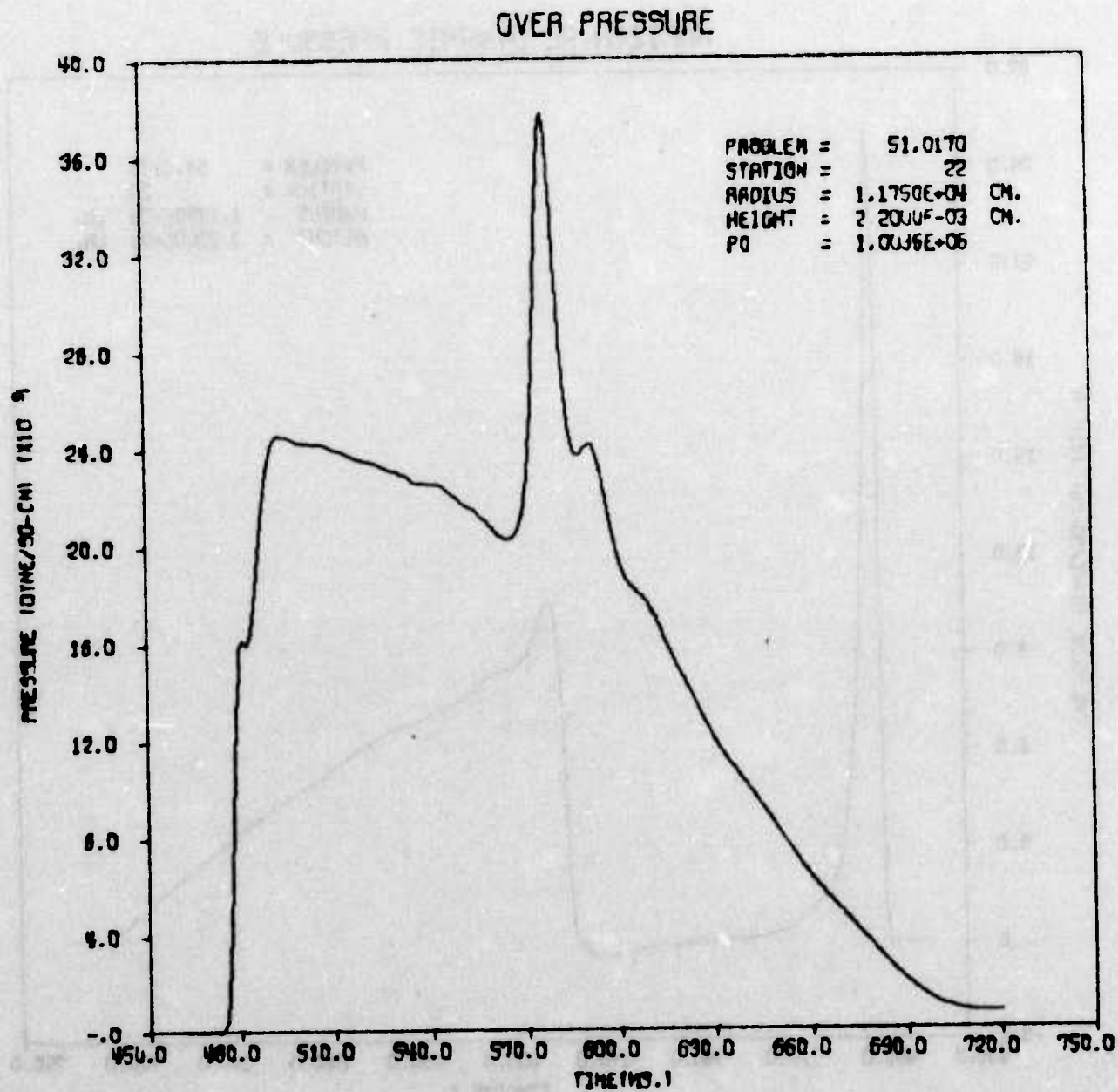
AFWL HULL CAL OF SOKT EFFECT ON DAM AND STRUCTURE AT 50PSI RANGE



AFWL HULL CAL OF SOFT EFFECT ON DAM AND STRUCTURE AT 50PSI RANGE

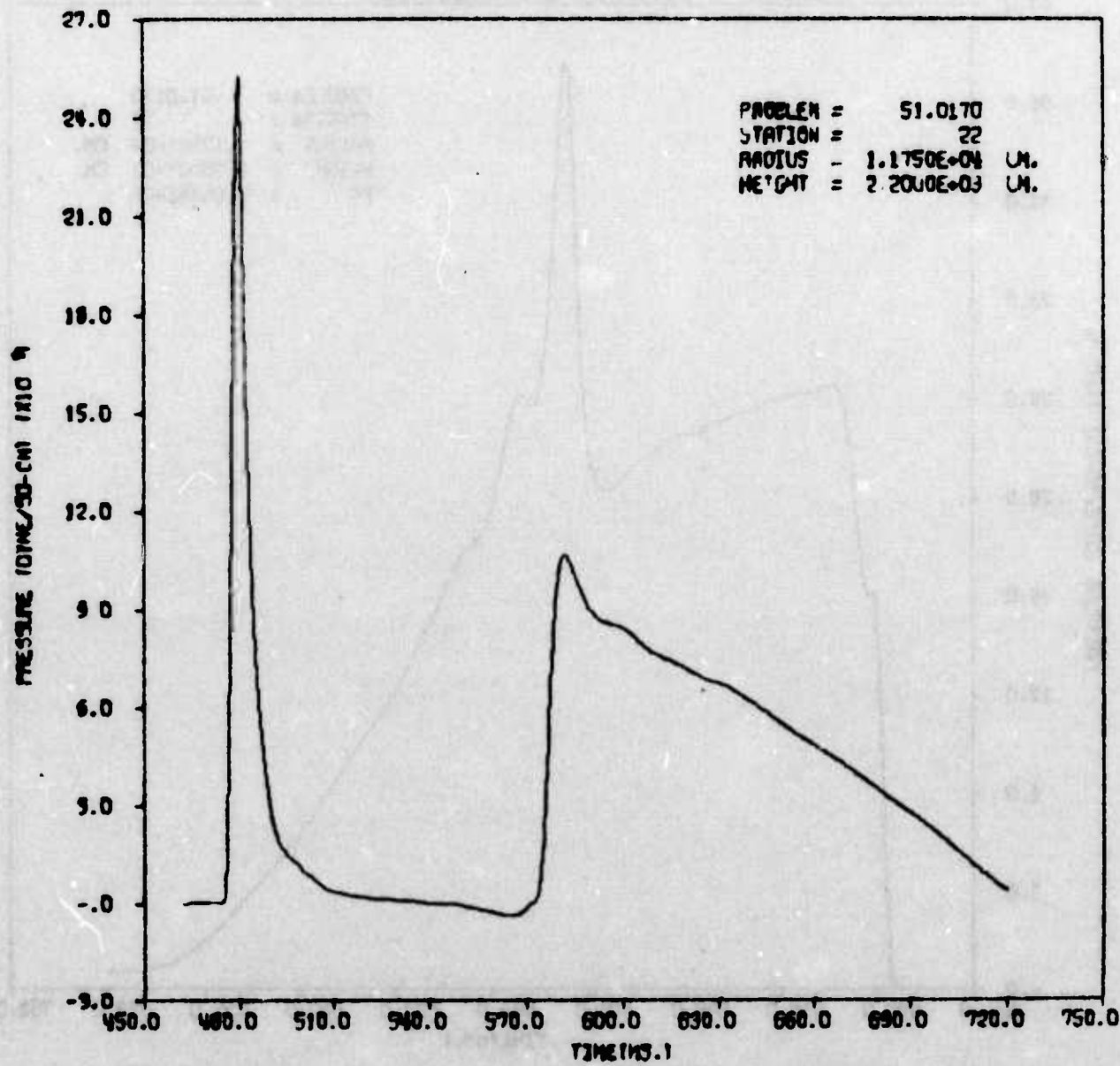


AFWL HULL CAL OF 50KT EFFECT ON DAM AND STRUCTURE AT 50PSI RANGE



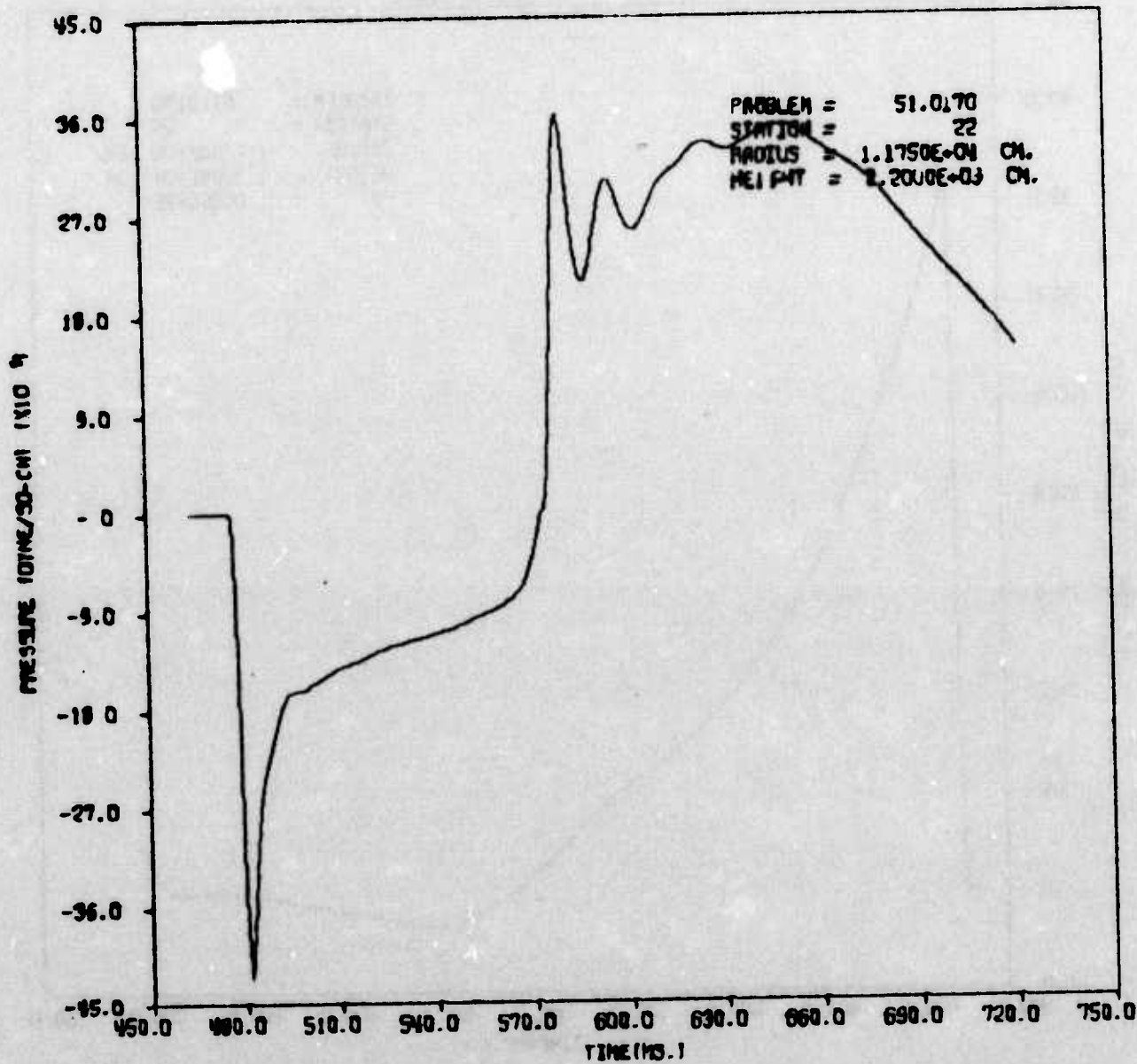
AFWL HULL CAL OF 50KT EFFECT ON DAM AND STRUCTURE AT 50PSI RANGE

HORIZONTAL DYNAMIC PRESSURE

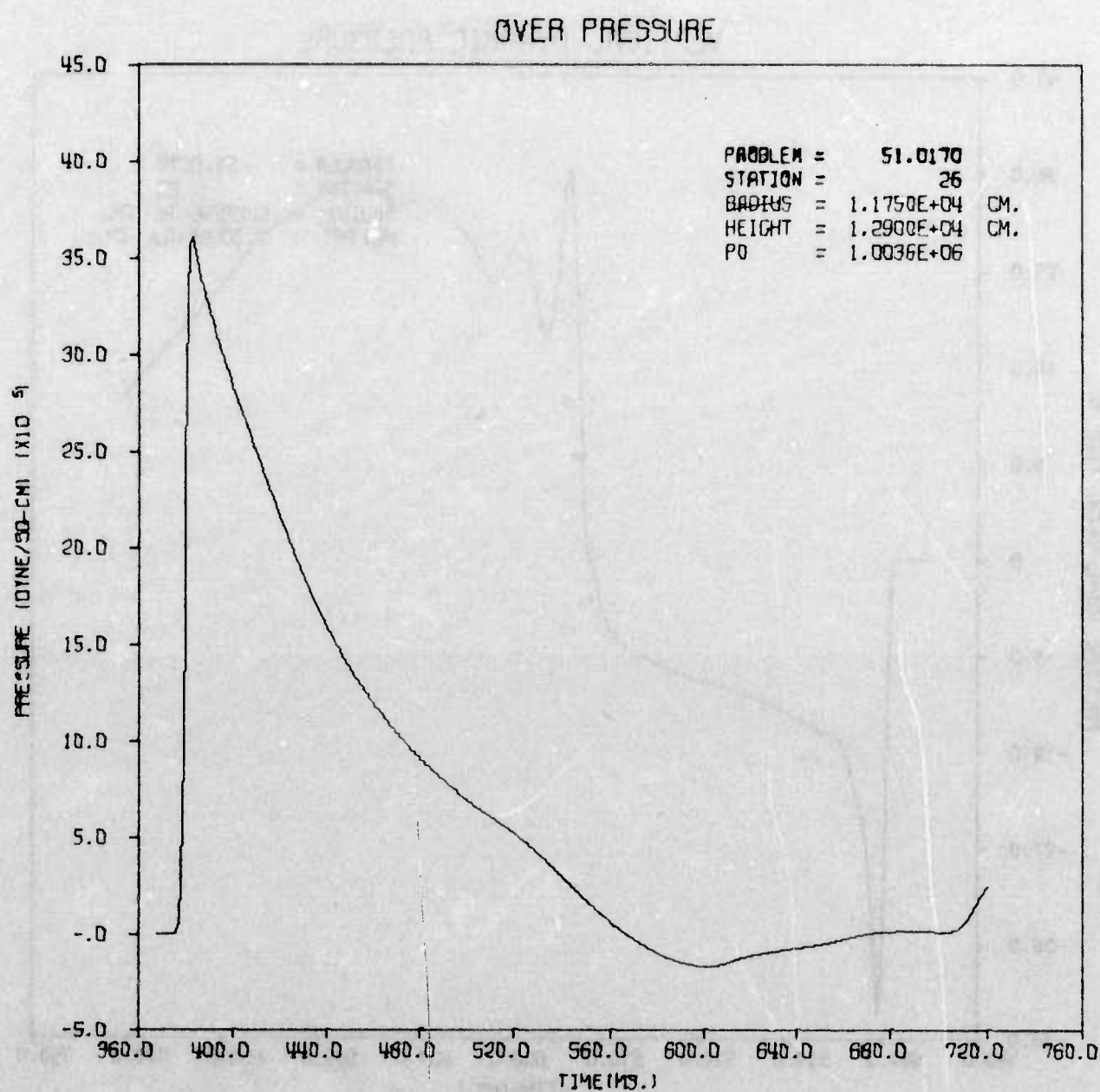


AFWL HULL CAL OF 50KT EFFECT ON DAM AND STRUCTURE AT 50PSI RANGE

VERTICAL DYNAMIC PRESSURE

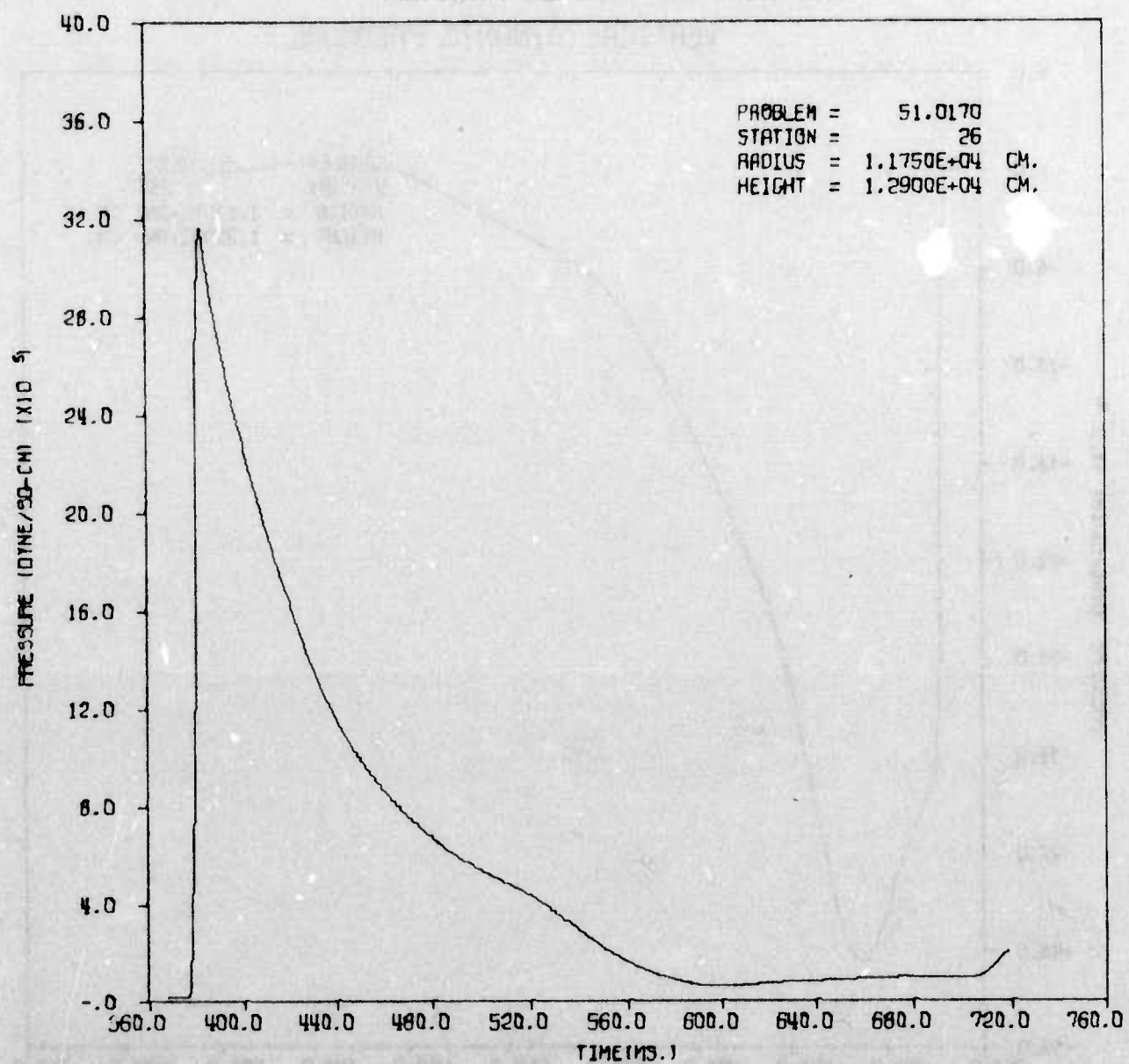


AFWL HULL CAL OF 50KT EFFECT ON DAM AND STRUCTURE AT 50PSI RANGE

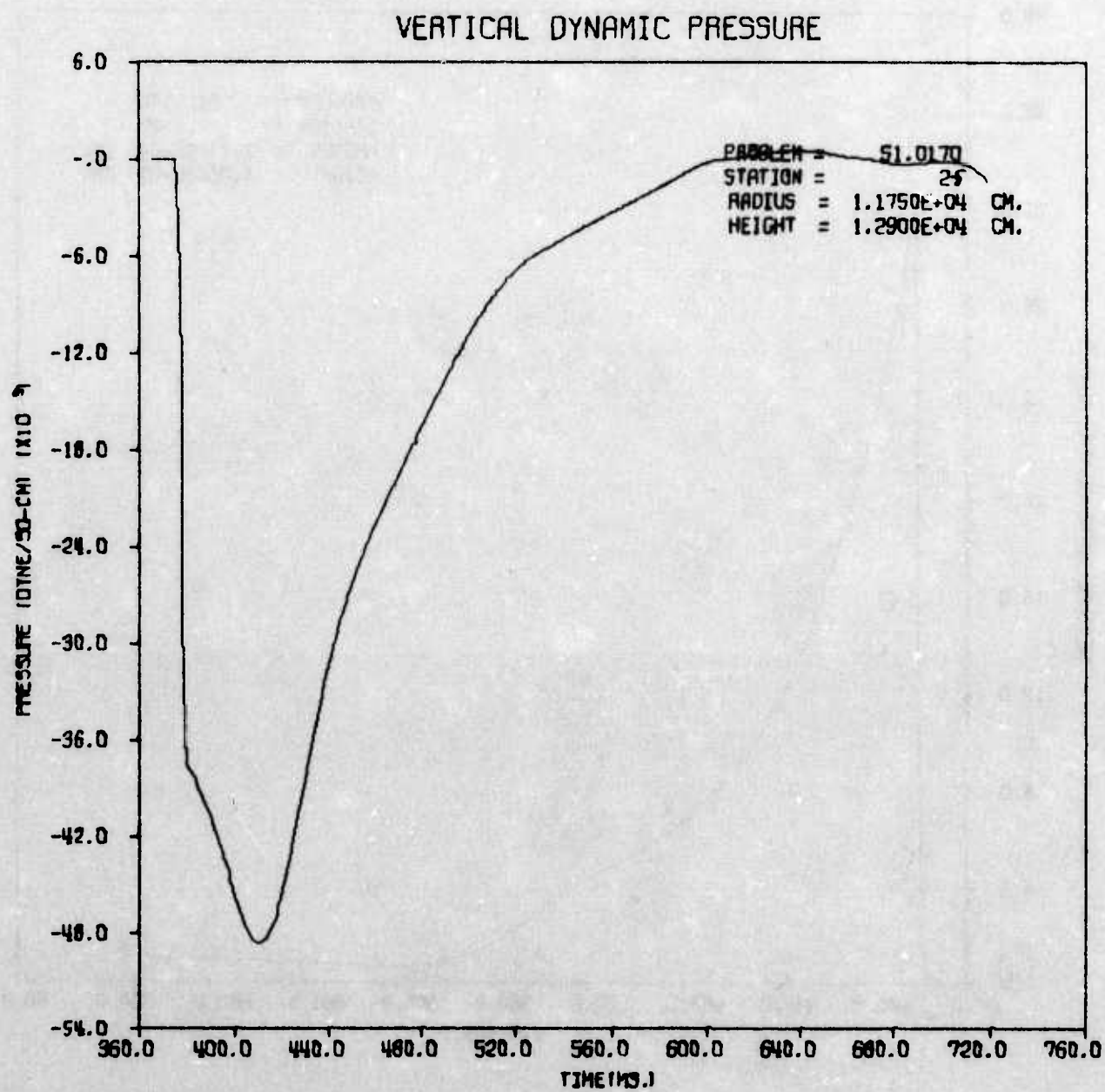


AFWL HULL CAL OF 50KT EFFECT ON DAM AND STRUCTURE AT 50PSI RANGE

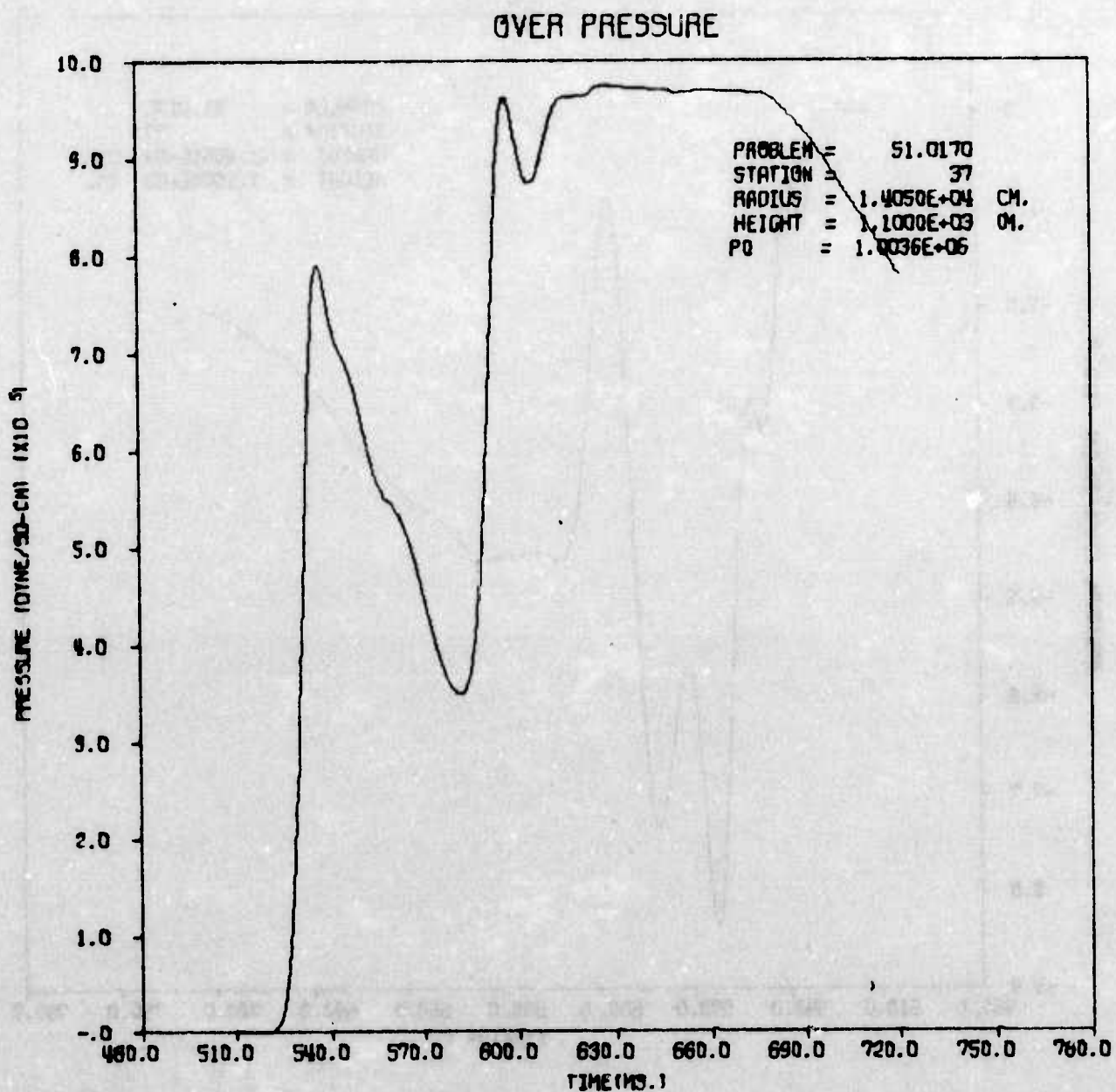
HORIZONTAL DYNAMIC PRESSURE



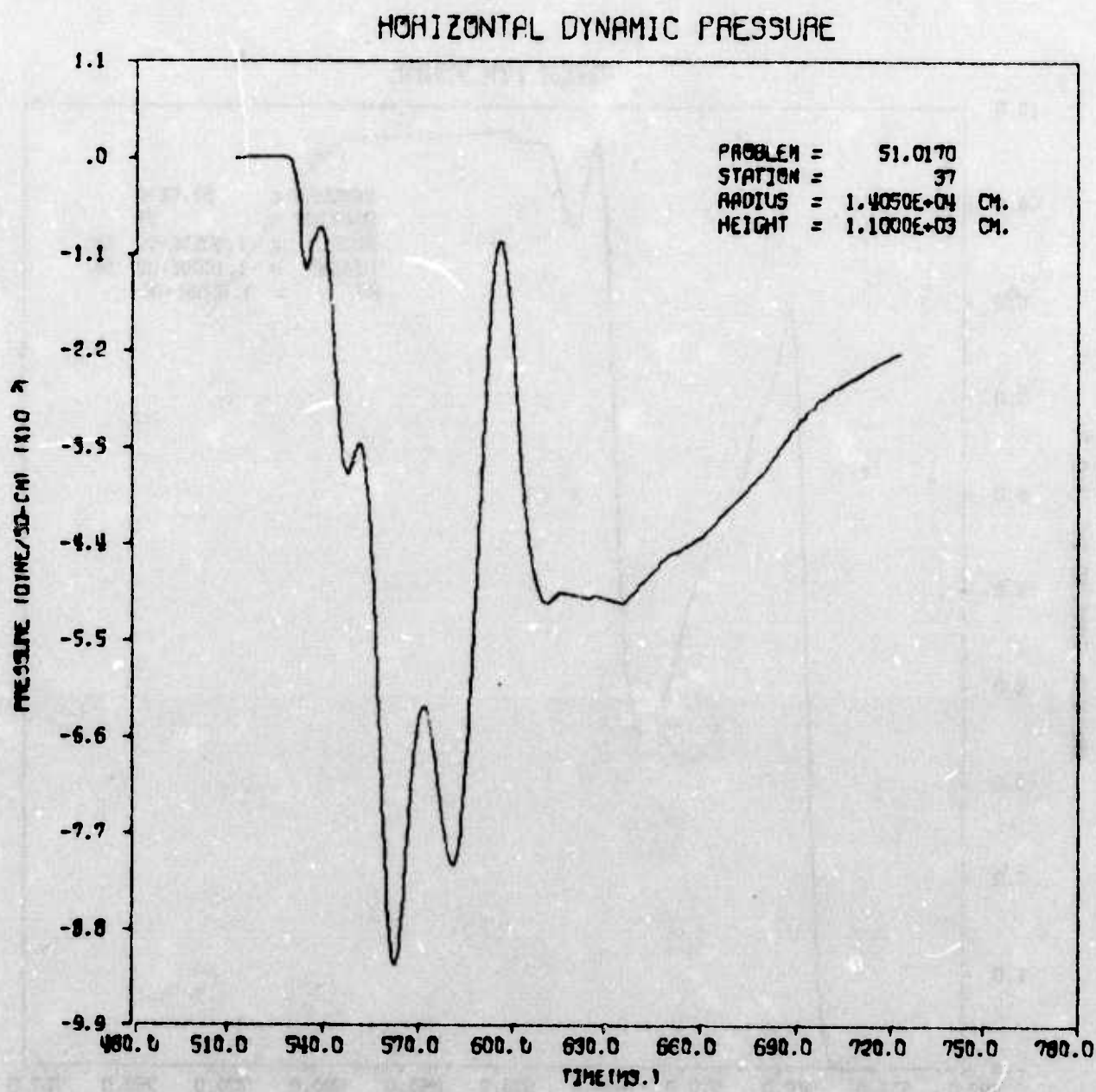
AFWL HULL CAL OF SOFT EFFECT ON DAM AND STRUCTURE AT 50PSI RANGE



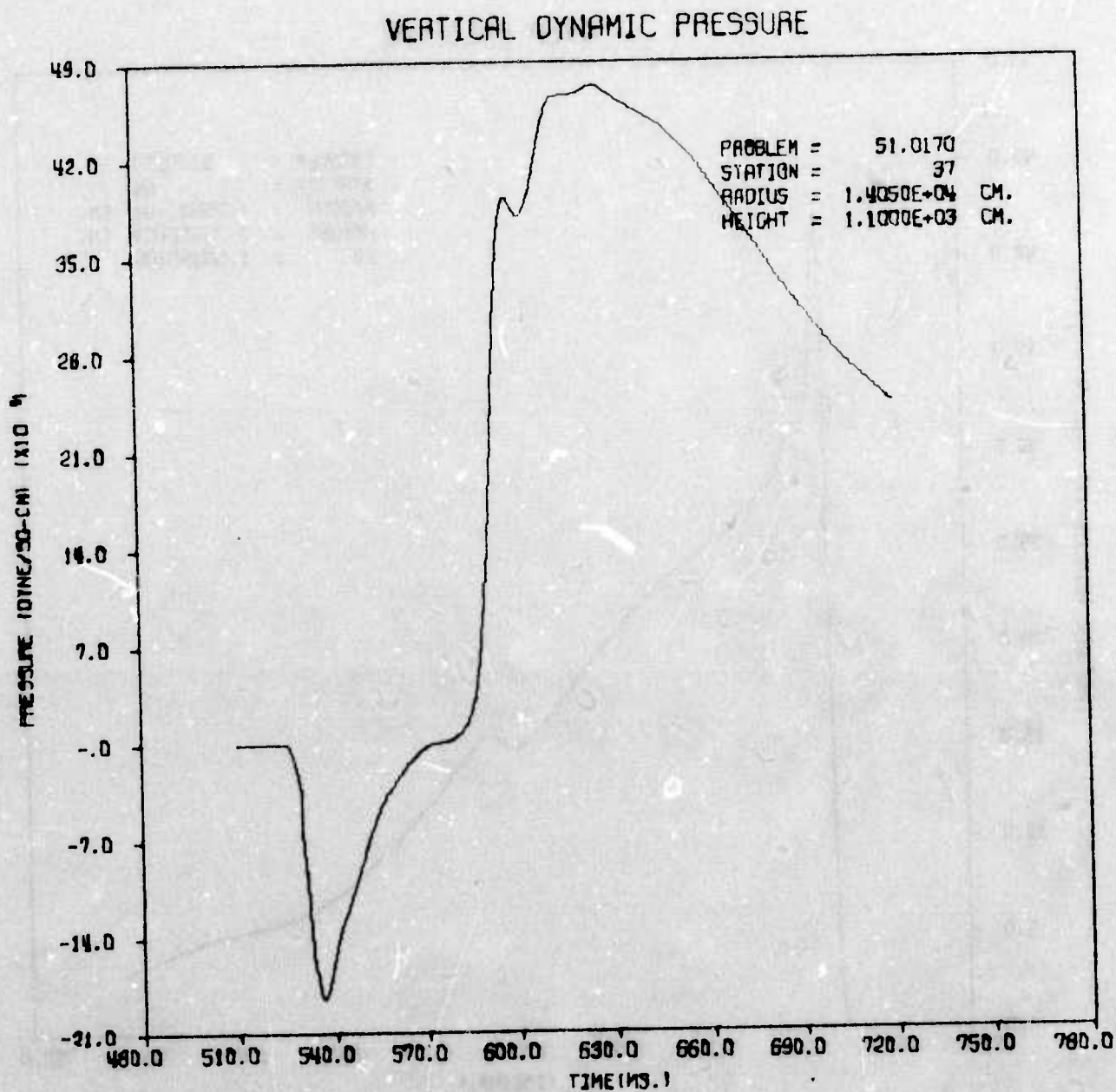
AFWL HULL CAL OF 50KT EFFECT ON DAM AND STRUCTURE AT 50PSI RANGE



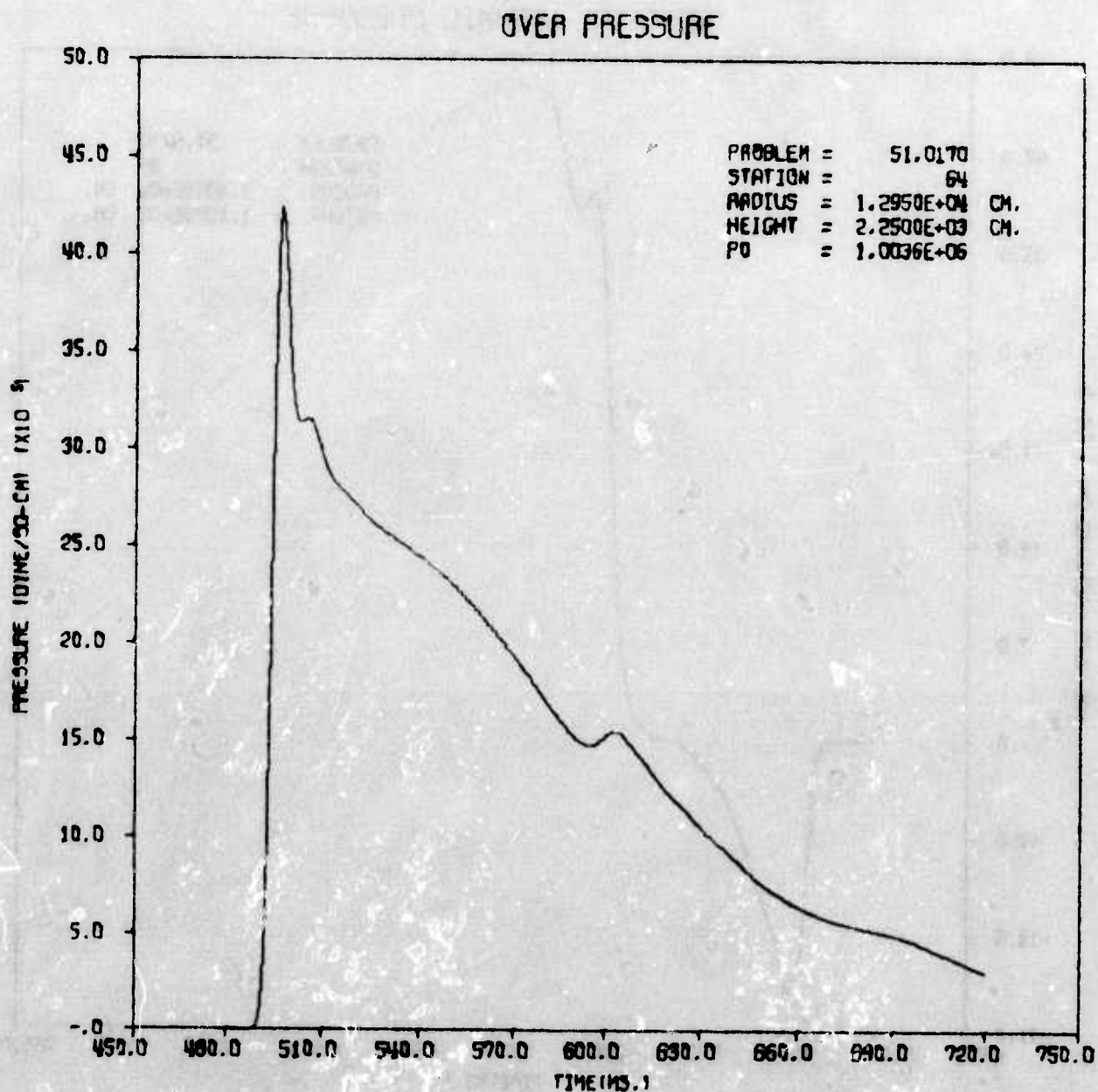
AFWL HULL CAL OF SOFT EFFECT ON DAM AND STRUCTURE AT 50PSI RANGE



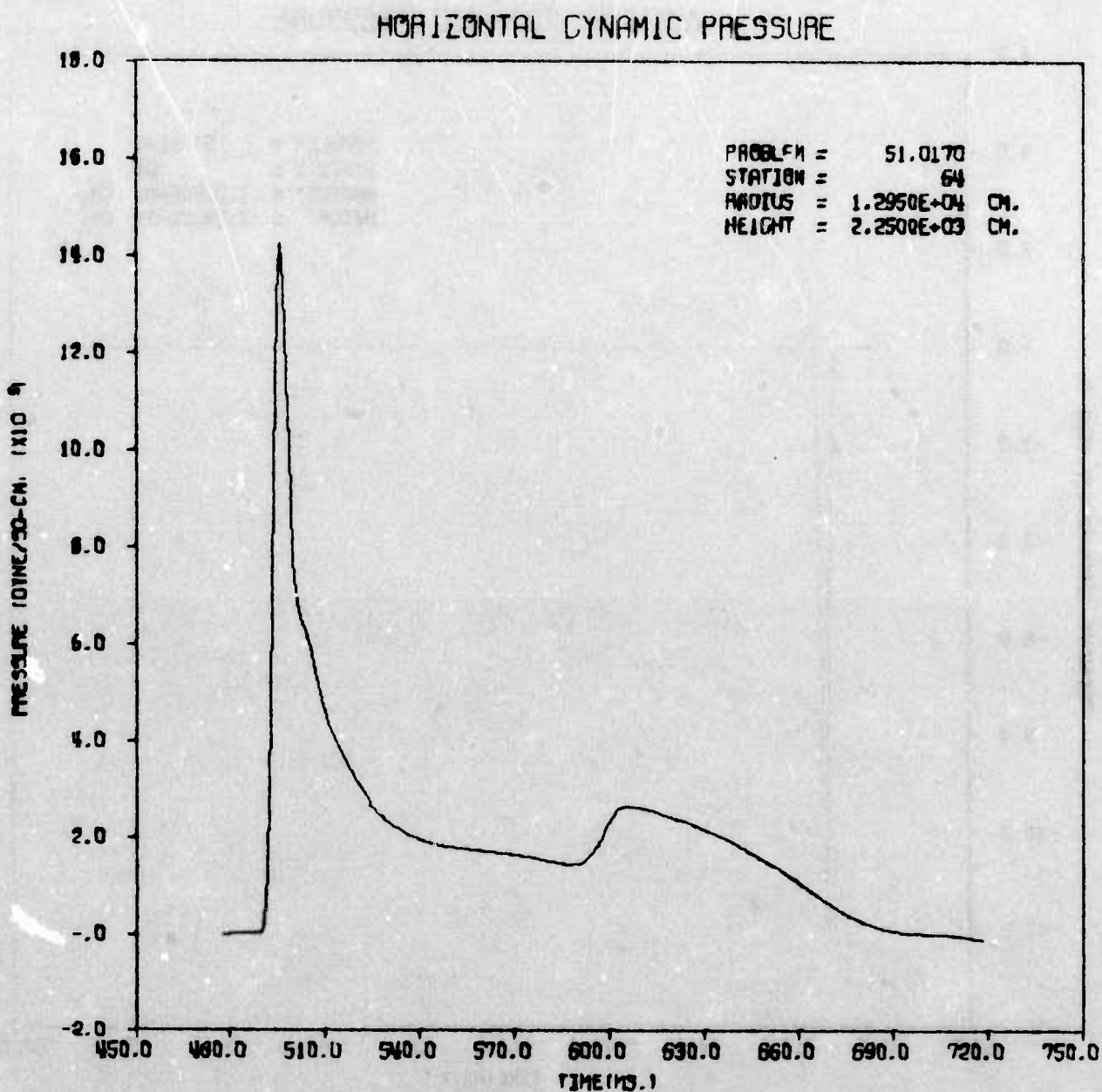
AFWL HULL CAL OF 50KT EFFECT ON DAM AND STRUCTURE AT 50PSI RANGE



AFWL HULL CAL OF 50KT EFFECT ON DAM AND STRUCTURE AT 50PSI RANGE

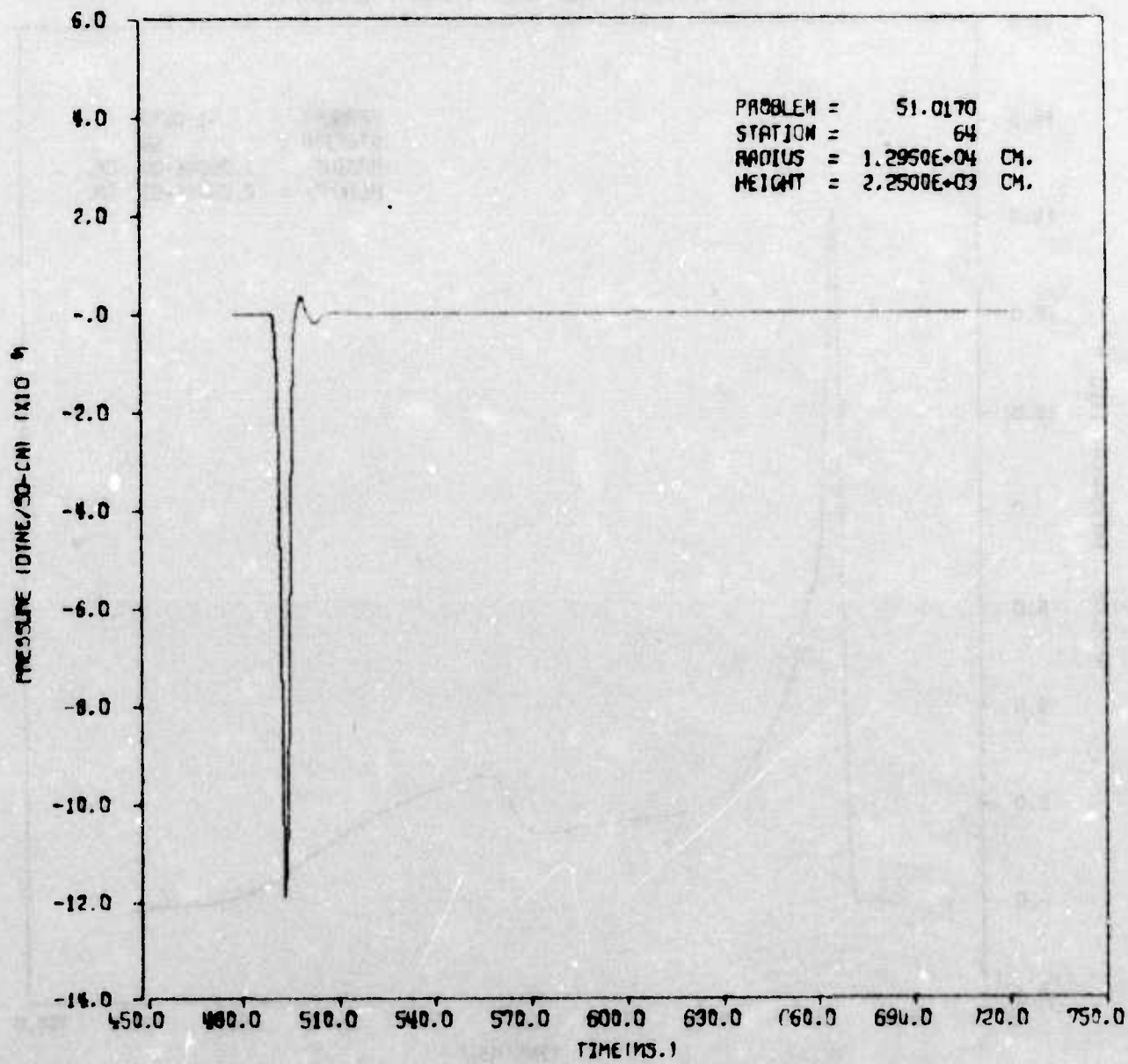


AFWL HULL CAL OF 50KT EFFECT ON DAM AND STRUCTURE AT 50PSI RANGE



AFWL HULL CAL OF 50KT EFFECT ON DAM AND STRUCTURE AT 50PSI RANGE

VERTICAL DYNAMIC PRESSURE



AFWL HULL CAL OF SOKT EFFECT ON DAM AND STRUCTURE AT 50PSI RANGE

DISTRIBUTION LIST

DISTRIBUTION

AFATL
 ATTN: Maj D. Matuska
 ATTN: R. Durrett

Stanford Research Institute
 ATTN: Dr. W. Chestnut
 ATTN: Dr. Allan Burns
 ATTN: Dr. Georgellen Smith

JSTPS/JPS
 ATTN: Capt D. Goetz

Euclid Research Group
 ATTN: Ian O. Huebsch

HDSAC/XOBM
 ATTN: Lt Col Kelley

SAMSO/MN
 ATTN: MNHI

Hq USAF
 ATTN: SA
 ATTN: SAMI
 ATTN: PREE
 ATTN: PREPB
 ATTN: RDQSM

Hq USAF
AFTAC
 ATTN: TAP

AFCEC
 ATTN: PREC

AFISCC
 ATTN: PQAL
 ATTN: SE

AFSC
 ATTN: DOB
 ATTN: DLSP
 ATTN: XRP
 ATTN: T & E

TAC
 ATTN: DEE
 ATTN: DERP
 ATTN: LGMD

CINCSAC
 ATTN: DEE
 ATTN: DOXS
 ATTN: XPPC

ADC
 ATTN: DOA
 ATTN: XPQDQ
 ATTN: XPQY

AUL
 ATTN: LDE

AU
 ATTN: ED, Dir., Civ. Eng.

DISTRIBUTION (Continued)

AFIT
 ATTN: Tech. Lib., Bldg. 640, Area B
 ATTN: CES

CINCUSAFE
 ATTN: DOA

USAFA, SCLO
 ATTN: Maj Pierson, Ch, LO

USAFA
 ATTN: DFSLB
 ATTN: FJSRL, CC
 ATTN: DFCE

AFML
 ATTN: Tech. Lib.

AFAL
 ATTN: TE

AFFDL
 ATTN: DOO/Lib.

AFAPL
 ATTN: Tech. Lib.

ASD
 ATTN: Tech. Lib.
 ATTN: DEE

SAMSO/DE
 ATTN: DEE

AFGL

AFATL
 ATTN: DLOSSL
 ATTN: DEE

RADC
 ATTN: Doc. Lib.
 ATTN: TUGF

AFRPL
 ATTN: DYSN

AFOSR

TAC
 ATTN: DEE

823 CES
 ATTN: IIR

CO
 Diamond Lab.
 ATTN: Lib.

CO
 USACDC

USAMC, RSIC
 ATTN: Chief, Doc. Sec.
 ATTN: SENSC-DB

DISTRIBUTION (Continued)

CO
BRL
ATTN: AMXBR-TB
ATTN: AMXBR-BL
ATTN: AMXBR-RL

CO
Picatinny Arsenal
ATTN: SMUPA-TN

CO
USARO
Ch. Eng.
Dept. of the Army
ATTN: DAEN-RDM

Dir.
USA Eng. WWES
ATTN: WESRL
ATTN: WESSS, Joe Zelasko

Dir.
NRL
ATTN: 2027

Dir.
NRL/EOTPO
ATTN: 5503

CO/Dir.
NEL
ATTN: 4223

CDR
NWC
ATTN: 753

OSC
Dept. of the Navy

CO
NWEF
ATTN: ADS

DDR&E
ATTN: Asst. Dir., Strat. Wpns.

Dir.
DIA
ATTN: DI-7D
ATTN: DI-3

Dir. OSD, ARPA
ATTN: NMR

CDR
FC DNA
ATTN: FCPR

ESD
ATTN: DEE

Dir.
WSEGp
ATTN: Doc. Con.

JSTPS
ATTN: JLTW

DISTRIBUTION (Continued)

ERDA
ATTN: Lib.

LLL
ATTN: Lib.

DDC
2 cy ATTN: TC

GE TEMPO
ATTN: T. Barret

NRL
ATTN: Code 2070
ATTN: J. Boris

NSWC
ATTN: Code 730
ATTN: J. Peters
ATTN: Exp. Eff. Div., Mr. Hornig

DNA
2 cy ATTN: DDST, Dr. Atkins, Mr. P. Haas
3 cy ATTN: STTL
6 cy ATTN: SPSS, E. Sevin, Captain J. Stockton,
Major T. Strong, K. Goering & Dr. Ulrich
4 cy ATTN: SPAS, J. Moulton, M. Rubenstein,
Captain Garrison & Major Anderson
ATTN: STAP
3 cy ATTN: RAAE, P. Fleming, Captain Mueller &
Major Bigoni
ATTN: RATN, CDR Alderson

ARPA
ATTN: Lieutenant Colonel Whitaker

JSTPS
ATTN: Maj Greene

DIA
ATTN: Mr. Castlebury

Sandia Lab.
ATTN: Org. 3141
ATTN: Div. 1111
ATTN: Org. 1723, C. E. Barr
ATTN: Div. 5644, J. Reed
3 cy ATTN: M. Merrit, L. Vortman & D. Dahlgren

Sandia Lab.
ATTN: Org. 8000, Dr. Cook
ATTN: R. Scholer
ATTN: T. Gold
ATTN: J. Mansfield

LLL
ATTN: L-51, M. Hanson
ATTN: TID
ATTN: Jeff Thompson

LASL
ATTN: Rpt. Lib.
2 cy ATTN: J-10, E. Jones & R. Gentry

Aerospace Corp.
ATTN: Lib.
ATTN: R. L. Beck

DISTRIBUTION (Continued)

Bmn. Eng. Co.
ATTN: V. Kenner, MS-44
ATTN: C. Wayne
ATTN: J. Dobkins

McDon. Doug.
8 cy ATTN: K. Stone, P. Lewis, D. Dean, T. Thomas,
D. Hildebrand, J. Logan, R. Zach, &
H. Herdman

Kaman Sci.
ATTN: D. Pirio
ATTN: D. Sachs

Kaman Av.
ATTN: J. Reutenik

MartMar
4 cy ATTN: R. Heffner, C. Washburn, H. Suguichi &
D. Cooke

MRC
2 cy ATTN: R. Christian & D. Sowle

SAI
2 cy ATTN: C. Busch & R. Lowen

SAI
ATTN: D. Hove

SAI
ATTN: R. Hiliendahl

SAI
ATTN: M. Tobrinen

SAI
ATTN: R. Clemens

BTL
ATTN: W. Troutman

Calspan
ATTN: R. Deliberis

ISI
ATTN: W. Dudziak

Lockheed

MITRE
2 cy ATTN: S. Morin & J. Brown

CRT
ATTN: M. Rosenblatt

R & D Assoc.
4 cy ATTN: H. Brode, C. Knowles, J. Carpenter &
R. Lelevler

MARA
ATTN: S. Kalasas

TRW Sys. Gp.
ATTN: Lib.
2 cy ATTN: A. Kuhl
ATTN: J. Peterson

AVCO
ATTN: G. Grant

DISTRIBUTION (Continued)

IDA

ASD
ATTN: I&L

ARM for Stf. Col.
ATTN: Lib.

Ind. Col. Arm. For.

Nat. War Col.
ATTN: Lib.

USAMC
ATTN: AMCRD-RP-B

USAEC
ATTN: AMSEL-RD

USNCEL
ATTN: Code L31
ATTN: CEC Ofcr.

MIT
ATTN: Dr. Hansen

Princeton U.
ATTN: PPL, Dr. Bleakney

Un. MI
ATTN: Rsch. Soe. Ofc.
ATTN: IS&T, G. Frantti

St. Louis Un.
ATTN: Dr. Kisslinger

Boeing
ATTN: R. Carlson

GATC
ATTN: MRD Div. Lab.

H&N Sp. Pro. Div.
ATTN: S. Smith

URS

SWRI
ATTN: M. Whitfield

Un. IL
ATTN: Dr. Newmark, Tal. Lab.

HTRI

RAC
ATTN: Lib.

ADC
ATTN: ADSWO

SACLO

TACLOS

DISTRIBUTION (Continued)

AFWL

ATTN: IIO, Dr. Minge
2 cy ATTN: SUL
ATTN: DE
ATTN: DEV
ATTN: DEX
ATTN: DY
ATTN: DYS
ATTN: DYV
10 cy ATTN: DYT
ATTN: DYX
20 cy ATTN: DYT, Capt M. Stucker
20 cy ATTN: DYT, Capt M. Fry
ATTN: SA
ATTN: SAB
ATTN: SAS
2 cy ATTN: SAT, Mr. Sharp & Mr. Murphy
ATTN: SAW
ATTN: Charles E. Needham
ATTN: Burton S. Chambers, III
ATTN: Maj Gary P. Ganong

Official Record Copy, Capt Mark Fry/DYT